Neural and Behavioral Mechanisms of Interval Timing in the Striatum

Gustavo Borges Moreno e Mello

Dissertation presented to obtain the Ph.D degree in Biology | Neuroscience

Instituto de Tecnologia Química e Biológica António Xavier | Universidade Nova de Lisboa

Oeiras,
March, 2016

Neural and Behavioral Mechanisms of Interval Timing in the Striatum

Gustavo Borges Moreno e Mello

Dissertation presented to obtain the Ph.D degree in Biology | Neuroscience

Instituto de Tecnologia Química e Biológica António Xavier | Universidade Nova de Lisboa

Research work coordinated by:

Oeiras, March, 2016

Neural and Behavioral Mechanisms of Interval Timing in the Striatum

Gustavo Borges Moreno e Mello

Dissertation presented to obtain the Ph.D degree in Biology | Neuroscience

Instituto de Tecnologia Química e Biológica António Xavier | Universidade Nova de Lisboa

Research work coordinated by:

FUNDAÇÃO CALOUSTE GULBENKIAN
Instituto Gulbenkian de Ciência

Champalimaud Foundation

Oeiras, December, 2015

INSTITUTO
DE TECNOLOGIA
QUÍMICA E BIOLÓGICA
ANTÓNIO XAVIER /UNL

Knowledge Creation

Neural and Behavioral Mechanisms of Interval Timing in the Striatum.

Gustavo Borges Moreno e Mello

Dissertation presented to obtain the Ph.D degree in Biology | Neuroscience

Instituto de Tecnologia Química e Biológica António Xavier | Universidade Nova de Lisboa

The work presented in this dissertation was carried out under the International Neuroscience Doctoral Programme (INDP, at the Champalimaud Neuroscience Programme, Champalimaud Centre for the Unknown, Lisbon, Portugal) under supervision of Dr. Joseph James Paton. Financial support was given by a doctoral fellowship from the Portuguese Science and Technology Foundation (FCT, Fundação para a Ciência e Tecnologia), with the reference SFRH/BD/51713/2011 attributed to Gustavo Borges Moreno e Mello.

Champalimaud Foundation

INSTITUTO GULBENKIAN DE CIÊNCIA

UNIVERSIDADE NOVA DE LISBOA

FCT Fundação para a Ciência e a Tecnologia

ITQB INSTITUTO DE TECNOLOGIA QUÍMICA E BIOLÓGICA ANTÓNIO XAVIER /UNL

TABLE OF CONTENT

ABBREVIATIONS

2D	Two dimensions or bi-dimensional
3D	Three dimensions or three-dimensional
AP	Anteroposterior
BeT	Behavioral theory of timing
BF	Beat frequency
BG	Basal Ganglia
ChAT	Choline acetyltransferase
CPu	Caudate-putamen
COM	Center of mass
CTX	Cortex
CV	Coefficient of variation
DA	Dopamine
D_n	Dopamine receptor of n type
DLPFC	Dorsolateral prefrontal cortex
DV	Dorsoventral
EP	Entopenducular nucleus
FI	Fixed interval
FS	Fast spiking interneurons
fMRI	Functional magnetic resonance imaging
GABA	γ - aminobutyric acid
GPe	Globus pallidus pars externa
GPi	Globus pallidus pars interna
LED	Light-emitting diode
LeT	Learning-to-time
LFP	Local field potential
LOFC	Lateral orbitofrontal cortex
LTS	Low-threshold spiking interneurons
M1	Primary motor cortex
MDpl	Thalamic mediodorsal nucleus (lateral part)
ML	Mediolateral
Ml	Maximum likelihood
MSN	Medium spiny neurons

Nac	Nucleus accumbens
OC	Operant conditioning
PBS	Phosphate-buffered-saline
PC	Principal component
PCA	Principal component analysis
PD	Parkinson's disease
PFC	Prefrontal cortex
PKP	Parkinsonian patients
PI	Peak interval
PPN	Pendunculopontine nucleus
PRP	Post reinforcement Pause
PST	Pressing start time
PSTH	Peri-stimulust time histogram
PV	Parvalbumine
RL	Reinforcement learning
SBF	Striatal beat frequency
SDF	Spike density function
SET	Scalar expectancy theory
SFI	Serial fixed interval
SN	Substantia nigra
SNc	Substantia nigra pars compacta
SNr	Substantia nigra pars reticulata
STN	Subthalamic nucleus
STR	Striatum
TAFC	Two-alternative forced choice task
TAN	Tonically active neuron
VApc	Thalamic ventral anterior nucleus (parvocelullar part)
VAmc	Thalamic ventral anterior nucleus (magnocellular part)
VLcr	Thalamic ventrolateral nucleus (rostral division of the caudal part)
VLm	Thalamic ventrolateral nucleus (medial part)
VLo	Thalamic ventrolateral nucleus (pars oralis)
VTA	Ventral tegmental area

ACKNOWLEDGEMENTS

To my mother Antonia Borges Moreno, who made all this possible by teaching me values and life lessons that have proven to be the best knowledge I ever acquired. She is a woman of restless perseverance, greater sense of purpose and kindness; a role model of character that I will carry dearly until my very last day on earth;

To my girlfriend Natalia Ziolkowska, for her support and comprehension, always making me feel loved and understood, especially during times when work was frustrating or required long hours of solitude;

To my colleague (a.k.a. Partner in crime) Sofia Soares, whose hard work and diligence were inspiring, for her support during the lab work, friendship and conversations;

To the Learning lab members, especially Tiago Monteiro, Thiago Gouvêa and Gonçalo Lopes whose great hearts and witty minds were always ready to help a colleague;

To Alfonso Renart, member of my thesis committee, for the support and critical comments that always allowed me to move forward;

To Masayoshi Murakami, Andreia Cruz, Rodrigo Oliveira, Nivaldo Vasconcelos, Ekaterina Vinnik, Guillaume Dugué, Fatuel Tecuapetla, Lauren McElvain, for sharing their knowledge, skills and opinions;

To the Champalimaud Neuroscience Programme, this outstanding group of people that managed in few years to create a magnificent place with outstanding science, and a culture that is warm and humane;

To Joseph James Paton (a.k.a. Joe), my thesis advisor, for being a mentor, a role model and a friend. Also for being able to see beyond what was the immediate situation, transforming every experience and experiment, good or bad, into a life lessons that allowed me to go through the most inspiring, enlightening and humbling experience of my life, my PhD project.

"What are we doing when we measure silence, and say that this silence has lasted as long as that voice lasts? Do we not project our thought to the measure of a sound, as if it were then sounding, so that we can say something concerning the intervals of silence in a given span of time? For, even when both the voice and the tongue are still, we review -- in thought -- poems and verses, and discourse of various kinds or various measures of motions, and we specify their time spans -- how long this is in relation to that. "

- Saint Augustine, Confessions XI, Chapter 27, 36

RESUMO

Para orientar o comportamento e aprender a partir de suas consequências, o cérebro precisa representar o tempo em múltiplas escalas, desde milissegundos a dias. Ainda não se conhece que sinal neuronal é usado para codificar o tempo na escala de segundos a minutos. O *corpus striatum* é a principal área de entrada de informação para os gânglios da base; ele desempenha um papel importante na aprendizagem, controle motor e é necessário para o comportamento normal de cronometragem na escala de segundos a minutos. Nós investigamos como a atividade de neurônios no corpo estriado pode codificar o tempo nesta escala. Para este fim, gravamos a atividade elétrica de neurônios do estriado de ratos enquanto estes resolviam uma tarefa temporal. Nesta tarefa os animais tiveram que estimar intervalos de tempos fixos para obter uma recompensa, e estes intervalos mudavam aleatoriamente ao longo da sessão em blocos de ensaios. Embora o tempo de início de resposta tenha sido proporcional ao intervalo, a precisão deste tempo não caiu linearmente com o tamanho do intervalo. O que sugere uma estratégia paralela para otimizar a adaptação à mudanças de contingências temporais e consequentemente melhorar a taxa de reforço ao longo da sessão. Quanto à atividade neuronal, observamos que neurônios dispararam em atrasos que se estenderam por dezenas de segundos e que este padrão de resposta refletiu uma interação entre tempo e o estado sensório-motor dos animais ao longo da sessão. Surpreendentemente, os neurônios re-escalaram suas repostas no tempo em conformidade com as mudanças de intervalo, o que indica que a população de neurônios do corpo estriado codifica tempo relativo. Ademais, estimativas de tempo descodificadas a partir da atividade predisseram ensaio-a-ensaio a estimativa temporal do animal a medida em estes animais ajustavam aos novos intervalos, e perturbações no funcionamento do corpo estriado, através de injeções locais de muscimol, causaram decréscimo na competência de adaptar o comportamento às demandas de tempo da tarefa. Diante da limitação prática em testar a suficiência de um fenômeno em sistemas biológicos, nós corremos uma simulação simples da tarefa. Nesta simulação, nós mostramos que respostas neuronais similares às que observamos são teoricamente suficientes para

produzir comportamentos adaptados no tempo. Finalmente, para testar a hipótese de que os animais poderiam usar sequência de ações para representar a passagem do tempo, nós geramos estimativas de tempo a partir de vídeos em alta velocidade dos animais desempenhando a tarefa temporal. Nós não conseguimos encontrar evidências que expliquem os processos temporais exclusivamente a partir do comportamento corrente. Em conjunto, estes resultados sugerem que a atividade dos neurônios no corpo estriado constitui um código escalonável para o tempo, sendo portanto uma provável fonte de informação temporal que animais podem usar para organizar suas ações.

ABSTRACT

To guide behavior and learn from its consequences, the brain must represent time over many scales. Yet, the neural signals used to encode time in the seconds to minute range are not known. The striatum is the major input area of the basal ganglia; it plays important roles in learning, motor function and normal timing behavior in the range of seconds to minutes. We investigated how striatal population activity might encode time. To do so, we recorded the electrical activity from striatal neurons in rats performing the serial fixed interval task, a dynamic version of the fixed Interval schedule of reinforcement. The animals performed in conformity with proportional timing, but did not strictly conform to scalar timing predictions, which might reflect a parallel strategy to optimize the adaptation to changes in temporal contingencies and consequently to improve reward rate over the session. Regarding the neural activity, we found that neurons fired at delays spanning tens of seconds and that this pattern of responding reflected the interaction between time and the animals' ongoing sensorimotor state. Surprisingly, cells rescaled responses in time when intervals changed, indicating that striatal populations encoded relative time. Moreover, time estimates decoded from activity predicted trial-by-trial timing behavior as animals adjusted to new intervals, and disrupting striatal function with local infusion of muscimol led to a decrease in timing performance. Because of practical limitations in testing for sufficiency a biological system, we ran a simple simulation of the task; we have shown that neural responses similar to those we observe are conceptually sufficient to produce temporally adaptive behavior. Furthermore, we attempted to explain temporal processes on the basis of ongoing behavior by decoding temporal estimates from high-speed videos of the animals performing the task; we could not explain the temporal report solely on basis of ongoing behavior. These results suggest that striatal activity forms a scalable population firing rate code for time, providing timing signals that animals use to guide their actions.

Key-words: Basal Ganglia, Striatum, Interval Timing, Fixed Interval, Embodied Cognition, Bayesian Decoder

CHAPTER 1: Introduction

Animals live in an ever-changing and complex environment. To survive, they must not only learn which actions to take, but also the spatial and the temporal context in which these actions effectively produce the desired outcome. Hence, identifying temporal regularities is extremely important for adaptive behavior. Indeed, to guide their behavior, animals operate with temporal information from different orders of magnitude, from microseconds to years. For instance, most (if not all) organisms exhibit endogenous circadian rhythms in physiological [1], metabolic [2,3] and behavioral [4] functions with periods close to 24 h. These cycles are synchronized and entrained by external cycles of light and darkness. In the opposite extreme, birds and some mammals (including humans) are able to use microsecond differences between the times that a sound reaches each ear to localize its source [5].

Relative to microsecond and circadian timing process, millisecond timing and interval timing can be deployed flexibly under animals' willful control; tasks such as coordination of movement (e.g. reaching, walking, dancing, speaking, music execution), perception (e.g. speech comprehension, music appreciation) and some aspects of learning (e.g. classical conditioning; [6]) all require millisecond timing to be properly executed.

Finally, interval timing (i.e. the ability to perceive, estimate and discriminate intervals between events in the range of seconds to minutes to hours) has been identified in organisms as diverse as insects [7], birds [8], fish [9], rat pups [10] and adult rodents [11], primates [12], human infants [13] and adults [14]. Interval timing is critical for important adaptive behaviors. In foraging, animals use temporal estimates to estimate how much reward per time (i.e., the rate of return) any given behavioral strategy or area can provide [15,16]. Timing is also important for decision making [17]; animals can use time as their decision criteria (e.g., decide when to act, or what to do depending on how much time has elapsed) or they can take time into account when comparing two outcomes that are expected to happen at different times. Animals can also easily stretch and contract chains of behaviors. These behaviors can keep their temporal characteristics proportional to the whole

sequence, showing that temporal control is also relevant to co-ordinate movements within a sequence [18]. Additionally, which is perhaps more important, timing can provide most of the information needed to derive sense of proximity, causality and order, which are necessary to implement operant conditioning [19].

Uncovering the underpinning of interval timing might help to elucidate many important cognitive processes in humans. For instance, it has been suggested that interval timing requires rudimentary comparisons and estimations of quantities. These operations could be the basis for high cognitive faculties, such as arithmetics [20]. Moreover, interval timing is not an isolated faculty. It interacts directly with processes such as attention [21,22], memory [23], reward expectation [24] and arousal [25], so that variations in these processes cause temporal delusions. Therefore, Interval timing is not only a primitive ability that is useful to detect relevant patterns from the ever-changing environment and generate anticipatory behaviors. But might underlie most, if not all, high cognitive functions of the human brain. By understanding the brain implements interval timing, we can gain insight into the processes supported by it, and perhaps identify unifying principles of how the nervous systems across species organize information about the environment and behavior.

In contrast to other sensorial modalities (e.g., visual, tactile, etc), timing has no sensorial organ. Hence, the sense of time either emerges from an internal clock mechanism, which generates a trackable time varying signal, or alternatively, arises from learning the temporal statistics of change in sensory and/or motor signals, which vary naturally with time. In either case, the brain must perform temporal estimations in the scale of seconds to minutes using neuronal activity. The Basal Ganglia (BG), and especially the striatum, are necessary for time estimation in the supra-second range [26]. Many models have been proposed on how the brain might perform flexible estimations of time over one second [27,28,29,30,31], some of them directly implicating the BG and the striatum [28,32]. And although some experimental data can support these models, the results are somewhat conflicting. Because of that,

the means by which the BG might perform temporal computations remains elusive.

By combining behavioral, electrophysiological and computational approaches, this work investigated how the rodent nervous system is able to time at supra-second scale and how these estimations are used to generate adaptive behavior.

Psychophysical studies of interval timing

Much of our knowledge about interval timing is derived from psychophysical studies. These studies are based on retrospective and prospective timing methodologies to collect time duration judgments from a subject [33]. Traditionally, the prospective study of time durations is based on the estimation, production, and reproduction of time intervals [34]. Estimation protocols require that a subject observes an interval and reports orally how much time has elapsed. Production protocols, on contrary, inform the subject about a temporal constraints (usually an interval between actions) he/she will have in order to perform an action. Usually a symbolic cue is associated with a particular interval, a spoken communication (e.g., “five seconds”). Because estimation and production protocols require some verbal interaction, most of timing research that uses animal models employ the reproduction protocols. In this protocol the subject is presented to one interval with a given duration criterion, then the subject has to reproduce this interval. Animals are usually deprived of either food or water, so that they are motivated to perform an action (e.g., pressing a lever, pushing a button) in a programmed schedule of time in order to receive a reward (i.e., drop of water, food pellet).

The most often studied interval timing schedule is perhaps the fixed interval (FI) schedule of reinforcement and its variations. During a FI schedule, the behavior is reinforced for the first response (e.g., press of a lever) made after elapse of a pre-determined interval since the previous reinforcement. When the reinforcer is delivered, the cycle restarts. A wide range of animal species (e.g., turtles, fish, cats, primates, humans and bees) trained on the FI protocol exhibit very predictable temporally-regulated behavior that scales with the FI [35]. First, the subjects consume the reward (as explained, the reward

marks the end of the previous and the beginning of the subsequent FI). Secondly, the subjects generally engage in grooming or exploratory behaviors. Thirdly, the animals gradually orient their position and actions towards the response site (e.g., lever). Finally, despite the absence of any external time cues, the animals start to respond after a fixed proportion of the interval has elapsed. The responses under FI schedule generally are manifested in two characteristic patterns. The first one is the scallop performance. This pattern describes an increase in the frequency of responses as the end of the FI approaches. The second pattern, and more frequently observed in over-trained subjects, is the break-and-run. In this pattern, response frequency is kept at a fixed rate from the moment responding starts to the moment of the reinforcement. This fixed rate of response varies together with the reward rate (i.e., magnitude of reward per time in the FI; [36]), and the post reinforcement pause (PRP) of responding is proportional to the length of the interval.

The PRP is the duration of the interval between the acquisition of the reinforcer and the press start time (PST; i.e., the first response) to produce the subsequent reinforcer, and because it is sensitive to the length of the estimated interval, it is the standard metric of timing performance. It has two important features relevant to the interval timing studies: the sensitivity of mean accuracy to the FI and the scalar variance (scalar timing). The mean accuracy sensitivity describes the observed phenomena that PSTs tend to occur in average around one half [35] to two thirds of the length of FI. The scalar variance feature characterizes that the dispersion of PST is a linear function of the average PST. Consequently, it also predicts that the coefficient of variation (standard deviation of PST divided by the average PST) is constant across all FIs. This latter feature is considered to be a manifestation of Weber-Fechner's Law in the time domain, also known as Scalar Timing [37]. The Weber-Fechner's law is obeyed by many sensory modalities [38, 39, 40, 41]. It states that the threshold to detect changes in magnitudes of stimuli (i.e., the just noticeable difference) is proportional to the magnitude. In other words, the just noticeable difference is a constant ratio between the measured magnitudes, for all magnitudes. Scalar timing affects behavior and neuronal activation by making them increasingly less precise as the timed interval lengthens [42].

The Serial Fixed Interval Timing (SFI) task is a variation of FI task used in our lab to sample timing performance from a broad range of intervals. In the SFI task the reward became available at t seconds after the previous reward, provided that the animal has responded. Each reward marked the end of one trial and the start of the next one. t varied in a block-wise fashion over intervals from 12 seconds to 1 minute. The performance in this task was consistent with previous results in dynamic versions of FI task [34, 35, 43, 44, 45, 46] in three aspects. Firstly, average PST is a function of the FI. Secondly, the response rate is proportional to the reward rate. Finally, rodents seem to adopt strategies that take into account for the whole distribution of FIs in the session. So that, PST was relatively later in short FI trials than it was within trials with long FIs. Because they adapted quickly to the new interval, taking less than 5 trials, this violation to the scalar variance property could reflect a strategy to facilitate exploration of intervals. The SFI task offers the possibility to analyze steady and changing timing conditions, while providing statistical power to infer parametric relationships between temporal demands, behavior and neural activity.

Theoretical models of interval timing

Although the long history of psychophysical experiments of interval timing has provided great insight into how temporal perception is manifested through behavior, little is known about the nature of temporal information itself. As stated before, unlike other sensorial modalities, there is no sensory organ for time sensing. Hence, temporal information must be inferred from other sensory modalities or produced by the organism. The idea that animals must produce their temporal representation (instead of directly sensing it) motivated a quest for the internal clock.

In this quest, several models have been suggested to describe animals' performance in timing tasks and explain the mechanisms of interval timing [Franois cited in 47, 48]. These models diverge in how well and how generally they can predict temporal performance, and what are the underlying mechanisms supporting interval timing. Broadly, these models can be grouped into at least three categories that vary in assumptions and explanatory power,

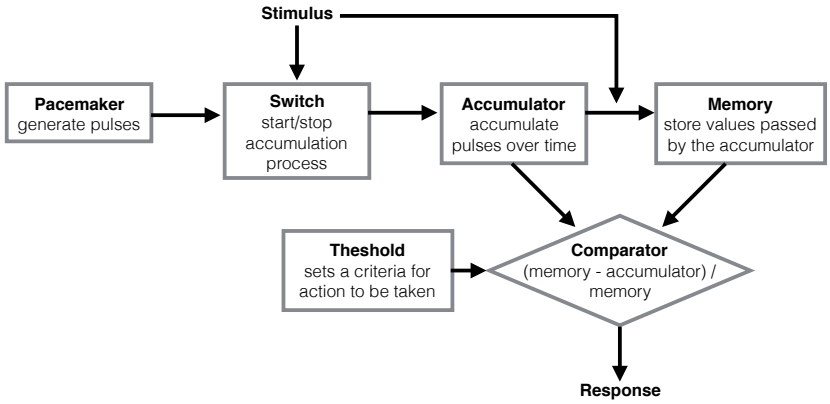

Figure 1.1 | Schematics of the scalar expectancy theory model. Components of the information processing model for time: pacemaker, accumulator, reference memory, switch and comparator. The pacemaker generates pulses through a Poisson-variable process. Environmental stimuli change the switch state, allowing the pulses to go into the accumulator. If the accumulator has a value stored during the moment of the stimulus, this value is passed to the memory and the accumulator is reset to zero. Finally the ratio of the difference between the values stored in the accumulator and the memory is compared with an established threshold to generate a behavioral response.

namely: information-processing models, beat-frequency models and sequential-state models.

Information-processing models were first formulated by Treisman [49] and later developed by Gibbon [50] with the scalar expectancy theory (SET) model (Figure 1.1). SET assumes: an internal poisson-variable pacemaker that generates pulses, an accumulator, a reference memory, a switch and a comparator. When a time marker (cue or reward) is received, the switch allows the pulses to be stored in the accumulator. These pulses were accumulated until a short time after the reinforcement. The rate by which these pulses were generated depended on many other psychological or behavioral variables, such: as arousal, reinforcement magnitude, attention and mood [49]. By the time of the reinforcement, the value stored in the accumulator is transferred to the reference memory and the accumulator is reset to zero. The perceived duration was a monotonic function of the total number of pulses transferred into the accumulator. The behavioral response is dependent on the ratio between the values stored in the accumulator and reference memory. For instance, when the difference falls below a threshold (which may also vary) in a FI task, responding at a steady rate begins. This feature explains that steady-

state measures of time discrimination, such as wait time (i.e., PST, break point) on fixed interval schedules or peak-rate time (on peak procedure), are proportional to the to-be-timed interval (i.e., proportional accuracy sensitivity to the FI; [35]). Because SET posits that the error generated during the accumulation of pulses is proportional to the duration criterion, it presents an explanation for scalar variance sensitivity to the interval. More importantly, SET incorporates two features that have been supported by experimental data. Firstly, the current time estimate (encoding) and the memory for times reinforced in the past (decoding) follow independent laws [27]; and secondly, the behavior is driven by some sort of comparison between current and remembered time of reinforcement [29].

In opposition to information processing models, sequential-state models characterize orderly transitions between different states which can be used to encode time [51,52,53]. The behavior theory of timing (BeT) formulated by Killeen and Fetterman [54] and the learning-to-time (LeT) formulated by Machado inspired by BeT [30] are the most prominent of the sequential state models.

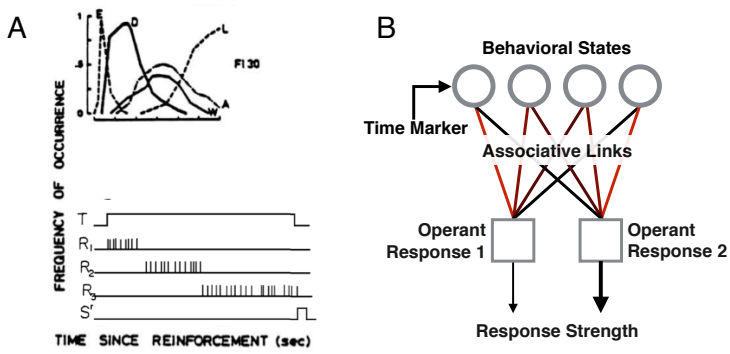

Figure 1.2 | Schematics of sequential state timing models. (**A**) Top: Frequency of occurrence of different activities of two rats over time since reinforcement on fixed interval schedule of 30 s. E = eating, D= drinking, W= in running wheel, L = contact the lever (adapted from Roper in Killeen & Fetterman [51]). Bottom: schematics of the fixed interval schedule of reinforcement paradigm used to acquire the data in the top panel. T= time, R=responses (each subscript is one different response e.g. Eating, Drinking), S = reinforcer, and each vertical line is one occurrence of a response. (**B**) Schematics of Learn to Time model structure (adapted from Machado [30]. After a time marker, a set of states (top circles) is activated in series. The states may be coupled to various degrees (associative links) with one or more operant responses (bottom squares). The strength of each response is determined by the dot product between the vectors of state activation and coupling. Hence, in FI schedules multiple responses over time might be elicited with varying degrees of strength.

These models are based on the empirical observation that sequential chains of behaviors emerge in tasks where reward delivery is contingent on passage of time (e.g., FI, SFI; Figure 1.2A). For instance, in a FI task, behavior would transit from consummatory, to post-consummatory, to exploration, to reorientation to the source of reinforcer and finally to the reinforced behavior across the interval. In BeT, each behavior is associated with a distinct underlying state. Transitions between states occur probabilistically driven by a poisson-variable pacemaker. The speed of this pacemaker depends on the rate of reinforcement, so that increases in reinforcement rate lead to an increase of the speed. The successive underlying states take on the role of a clock process. Consequently, to perform at a temporal criteria, subjects would learn to use their temporally organized behavioral states as discriminative stimuli. Thus, instead of reading an internal clock, subjects are assumed to use their current sensorimotor states to tell time. LeT extends BeT by positing that each underlying state is associated with an operant response, and that association strength varies through means of differential reinforcement in the context they were learned (Figure 1.2B). Therefore, the strength of the operant response at a given moment is the result of the combination between the predominantly active state at that moment, and how strong is the association between this state and the response.

Two major distinctions between information-processing and sequential-state models may argue for the broader explanatory model of the latter models. Firstly, in the former, the decision to respond is made only after the target time interval has elapsed, while in BeT it is done in anticipation to that time interval [53]. Experimental evidence points that accuracy of choice is higher under the prospective conditions than under the retrospective condition. Indeed, under retrospective condition, performance returned to baseline levels [55], suggesting that animals' approach to timing is prospective. Secondly, previous studies have reported contextual effects on timing [56]: having learned the discriminations 1 s (red) vs. 4 s (green) and 4 s (blue) vs. 16 s (yellow), preference for the green over blue key increases with the signal duration. In Information-processing models the memory stores are independent, and because of that this type models have no mechanism to accommodate

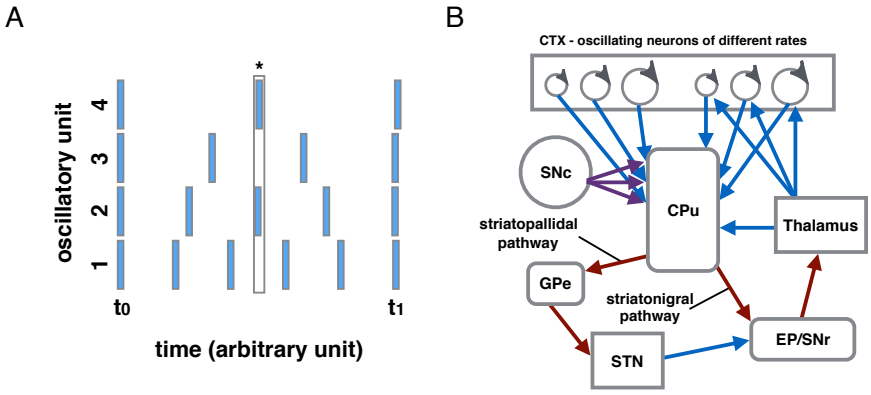

Figure 1.3 | Schematics of beat-frequency timing models. (A) Schematics of oscillation library from a set of units over time (adapted from Miall [57]). On meaningful event at t0, all oscillations are synchronized. After that, they start to oscillate freely. By picking a subset of oscillations and responding to when they synchronize (star symbol), the model can estimate how much time has elapsed. **(B)** Schematics of striatal beat-frequency model (SBF; adapted from Matell [28,58]). Loops involving the cortex (CTX), the basal ganglia (BG) and thalamus implement this mechanism. The striatum act as a coincidence detector of the oscillations provided by the CTX; dopamine signals from the substantia nigra pars compact (SNc) synchronize cortical and thalamic oscillations at every meaningful event (e.g., reward) and serve as the reinforcement signal. Once synchronized neurons oscillate at their inherent periods, allowing the patterns of activity to become meaningful. Striatal spiny neurons fire when a previously reinforced pattern of input is detected, consequently impinging to itself the current oscillatory inputs through the striato-thalamic-cortical loop.

contextual effects. In contrast LeT is sensitive to the errors that occur during the learning of the two discriminations; these errors weaken the connection between the behavioral states and the associated operant responses. Therefore, these errors would bias green keys to be perceived as long and blue as short, regardless the fact that both cues relate to the exact same interval.

The oscillation-based model uses a library of oscillatory pacemaker neurons, which could be independently entrained in different rhythms, to encode a temporal waveform by forming its Fourier series. Torras [cited in 57] said that this combination could be done either by choosing pacemakers with appropriate oscillation periods or through plastic changes to the period of oscillation of each cell. The beat-frequency model (BF; Figure 1.3A) and its updated and more biologically plausible version, the striatal beat-frequency model (SBF; Figure 1.3B), uses “beats” (i.e., frequency at which cells spike

simultaneously) between pairs or groups of oscillatory cells to store time intervals. After resetting the oscillations with a synchronizing event, a specific time can be encoded by selectively weighting the activity of oscillatory cells that are currently active at the time criterion. This process is equivalent to multiplication (e.g., 3 Hz and 5 Hz will first synchronize at 15 Hz), thus providing an efficient process to encode long intervals with neuronal mechanisms which operate in much shorter timescale. The SBF posits that loops involving the cortex (CTX), the basal ganglia and the thalamus implement these mechanisms. More specifically, the striatum would act as a coincidence detector; the DA signals would synchronize cortical and thalamic oscillations at every meaningful event (e.g., reward), hyper-polarizing the striatum membrane, and thereby resetting the integration mechanisms. DA signals would also serve as reinforcement/teaching cues, strengthening the cortico-striatal representation of a particular duration criterion. Once synchronized, neurons oscillate at their inherent periods, allowing the patterns of activity to become meaningful. Striatal spiny neurons fire when a previously reinforced pattern of input is detected, consequently informing that the time criterion was reached. The striatum can entrain itself in the current oscillatory inputs through the striato-thalamic-cortical loop, allowing for alterations of time perception.

Data from striatal neurons during the delay period before an anticipated reward or movement [59,60,61] can equally support any of these models. Hence, it is unclear which model best describes striatal function.

Neurobiological systems involved in interval timing

In our current understanding, interval timing is a complex and primitive function of the brain which engages multiple areas of the brain depending on environmental and behavioral demands. Data from functional magnetic resonance imaging (fMRI) show that multiple areas have time dependent activity which is also affected by task and context, suggesting that interval timing is a distributed and complex process in the brain [62]. But, not all of these areas are required for, or modulate, timing performance equally. For

instance, the primary motor cortex (M1) processes signals correlated with time [63]. Nonetheless, M1's ablation or manipulations do not influence timing reports [64]. The prefrontal cortex (PFC) also has time correlated activity[65]. The PFC seems to play a role modulating time perception. Xu *et al.* [63] demonstrated that time reports change when PFC activity is modulated with cooling. An other study [66] suggests that lesions in the medial prefrontal cortex disrupt the ability to discriminate intervals in the range of seconds. Time correlated signals can be found all over the telencephalon from the PFC [65], to the parietal cortex [67], and even in early sensory areas [68]. As we saw, some models rely on the assumption that the cortex provides the temporal basis for time estimation. But timing experiments done in decorticated animals [64] call this hypothesis into question. These experiments showed that decorticated animals are still able to perform in interval timing tasks.

There is a major consensus that subcortical areas are critical to interval timing. Hence, much of the recent research has been focused on the cerebellum, hippocampus and BG. Data from these researches depict interval timing as a distributed process in which each subcortical area contributes to interval timing in a different and contextually dependent manner. For instance, the cerebellum seems to have a peculiar role in interval timing. Many studies that attempted to affect interval timing through means of cerebellar lesions have failed [69]. Nonetheless, data from stroke patients [70] with lesion in the middle to superior lateral dentate nuclei, especially in the left hemisphere, suggest that the cerebellum is necessary for proper interval timing in durations lower than 12 seconds. Why and how cerebellum contributes to timing in this range is still to be shown. It might coordinate learned actions at a fine timescale [71], playing a mediating role between the sub-second timing [72] and the supra-second timing. The cerebellum receives input from the PFC through the pontine nuclei and connects to the PFC through two paths, both starting at the dentate nuclei: a short (mediodorsal/ventrolateral thalamic nuclei) and a long one (reticulotegmental nucleus, penduculopontine and ventral tegmental). These pathways could be relevant for cerebellum's role in interval timing.

On the other hand, a recent growing body of evidence [73-78] highlights the importance of the hippocampus, an area that is usually associated to spatial learning [79] and explicit memory [80], for interval timing. Gradual changes in hippocampal activity are strongly influenced by time and distance [76]. Additionally, lesions in the dorsal or ventral hippocampus produce leftward or rightward shifts in time estimation respectively [78]. Curiously, the effects that hippocampal inactivations have on time estimation seem to be stronger when the time scale estimated is over one minute [81], and the temporal discrimination is difficult (i.e., intervals with similar durations). Yet, the same group of studies could not provide the evidence that manipulations in the hippocampus produce disruptions on timing of intervals above a second and below one minute. Anatomically, the hippocampus is highly connected with other areas relevant to interval timing such as the nucleus accumbens (Nac; [82]) and the PFC [83]. This connectivity pattern strengthens the argument that the hippocampus has a relevant role in interval timing.

Arguably, the study of interval timing mechanisms in the BG has proven to be more prolific regarding unveiling the biological mechanisms of interval timing. Evidence from multiples sources implicates the BG, and more specifically the striatum, as a locus for the representation of supra-second-below-one-minute timing. Firstly, activity in the striatum is modulated by timing task as shown in studies using ensemble recording techniques in animals [84,85], and regional increase in blood flow captured by fMRI in humans during interval timing tasks [42,86]. Secondly, striatal lesions [26], diseases that affect the BG such as Huntington's [87] and Attention Deficit Disorder [88], all cause interval timing dysfunctions.

Furthermore, patients with disorders that involve meso-striatal dopaminergic pathways, such as schizophrenia [89,90,91] and Parkinson's disease (PD; [92,93]), display impaired performances during interval timing tasks. PD is characterized by a progressive degeneration of nigrostriatal dopaminergic projections, leading to low levels of dopamine (DA) in the striatum. These low levels of DA cause interval timing deficits which can be alleviated by L-dopa (L-3,4-dihydroxyphenylallanine; a precursor of dopamine) treatment [94]. Malapani *et al.* [92,93] leveraged this modulatory effect of DA

over interval timing and the therapeutic effect of L-dopa to segregate storage from retrieval dysfunction in the temporal memory in PD patients. Malapani's data suggest that DA has the power to increase discrimination between intervals on retrieval, to control the speed and the extension of internal representation of time during encoding.

How directly DA affects time perception might be a difficult question to answer, because DA is involved in multiple processes other than timing. For instance, although genetic manipulations that affect the DA system in the BG [95] cause interval timing dysfunctions, a different source of evidence [96] suggests that DA dependent timing deficits might be a cofound of manipulations which affect directly animals' motivation.

Altogether, the multiple areas involved in interval timing seem to constitute not one but multiple "internal clocks", which use diverse sources of information to implement aspects of interval timing. These areas appear to be mutually influenced by each other to generate congruent temporal estimations and subsequent adaptive behavior. A very clear example of such coordination of multiple clocks derives from the interaction among timing mechanisms of different time scales. For instance, the cerebellum exerts an influence in time estimation in the second to sub-second range. It is possible that the cerebellum exerts its influence to the BG either through modulation of thalamic input or through projections to VTA and PFC [97-100]. Conversely, circadian timing mechanisms can affect the interval timing indirectly by regulating DA [101]. Finally, the hippocampus might have a direct effect on the computations done in the striatum, especially in long intervals, in which animals are more likely to move (so distance can be an extra source of information about the rate of change of the environment), and when information about sequence is relevant [74,76].

Organization of the basal ganglia

As it should be clear by now, the BG play a central role in interval timing, and part of this role is derived from its anatomical position and connectivity. The BG are a group of subcortical nuclei localized in the core of the forebrain, ventral to motor cortex, posterior, to PFC and, in rats, anterior to hippocampus and

thalamus [102,103]. The BG are in a strategic position to receive input from most of the areas of the brain and influence both motor and associative processing. A variety of processes including reinforcement learning [104-106], motor control [107-111], limbic [112,115] and associative functions [116-119] depend on the BG. Although it is not yet clear how the BG integrate and modulate information from multiple sources, it is agreed that BG's internal connectivity plays a major role in it.

The BG's internal connectivity is complex as it involves many overlaid pathways through which information passes and is processed across the multiple nuclei of the BG. These nuclei differ drastically from each other in anatomical and histological characteristics. These differences are important because they establish constraints and possibilities for the timing mechanisms we are interested to explain. The classic anatomical description of the BG in

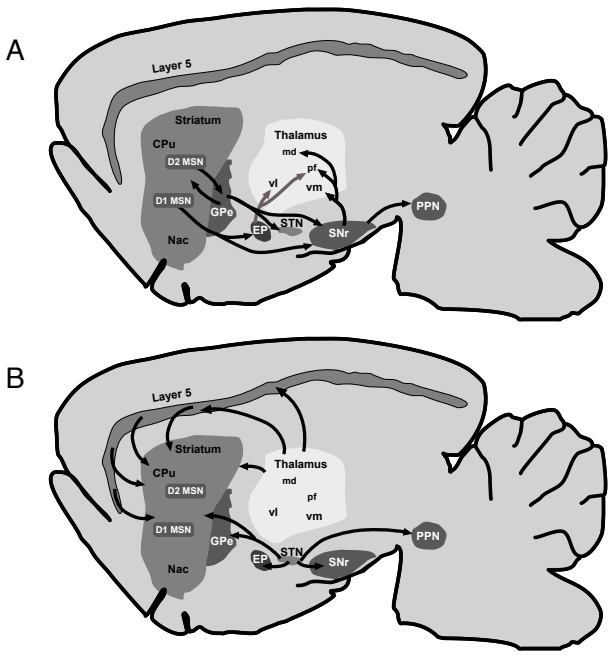

Figure 1.4 | Diagram basal ganglia's connectivity - Diagram of inhibitory **(A)** and excitatory **(B)** inputs and outputs of the BG's nuclei. Striatum (caudate-putamen - CPu and nucleus accumbent - Nac), receives broad excitatory input from the cortical layer 5 and thalamus (B). The striatum inhibits downstream areas through the indirect (from D2 MSN) and direct (from D1 MSN) pathways (A). Globus pallidus pars externa (GPe) and the subthalamic nucleus (STN) belong to the indirect pathway. GPe sends inhibitory projections to the striatum and to the STN (A). STN sends feedback excitatory projections to the GPe and to the striatum, and completes the indirect pathway by exciting the output area of the BG, the entopenducular nucleus/substantial nigra pars reticulata (EP/SNr; B). In the direct pathway, D1 MSNs directly inhibit EP/SNr (A). EP/ SNr outputs are fundamentally inhibitory and project to diverse thalamic nuclei (e.g. md, vl, pf, vm) depending on whether the input to the striatum was associative, limbic or motor. Cortex, thalamus and striatum are connected in loop.

rats is organized as follows (Figure 1.4): rostrodorsally to the other BG nuclei and most close to the CTX lies the largest division of the BG, the striatum (or caudate-putamen); located ventro-medio-posteriorly to the striatum is the globus pallidus (GP, external segment of the globus pallidus in primates) and the entopeduncular nucleus (EP, internal segment of globus pallidus in primates, GPi); the subthalamic nucleus (STN) is located ventroposteriorly to the GP and ventrally to the thalamus; and posterior to all structures is the substantia nigra (SN). The SN is further divided into two main parts, the dorsal pars compacta (SNc) in which the dopaminergic nigrostriatal neurons are located, and the more ventral pars reticulata (SNr). In addition to these structures which are linked to motor and associative functions, there is a ventral division of the BG associated with limbic functions. This limbic division is composed by the ventral striatum or nucleus accumbens (Nac), ventral pallidum and ventral tegmental area (VTA).

As the main input to the BG, the striatum receives glutamatergic input from neurons of layers 2 and 5 from nearly the entire CTX [120-122], strong glutamatergic afferent projections from the thalamus [124,125], dopaminergic input from SNc [126,127] and dense GABAergic input from the GPe [128,129]. Cortical inputs to the striatum are topographically segregated according to associative, motor, oculomotor and limbic functions. This topographical segregation is repeated all over downstream areas of the BG [102], suggesting some sort of parallel processing starting at the striatum. Regarding its outputs, the striatum sends efferent inhibitory projections to the GPe and to SNr/ EP(GPi; [102,103]).

In the other extreme of the BG, the EP (GPi in primates) together with the SNr constitute the main output of the BG. Both areas receive direct inhibitory projections from the striatum (direct or striato-nigral pathway) and from the GPe, in conjunction with glutamatergic excitatory input from the STN. Efferent projections of the EP are inhibitory and target mainly the ventral thalamus.

The GPe is a nucleus of great clinical importance. It is the site where lesions (pallidotomy) and deep-brain stimulation procedures have been applied to alleviate PD symptoms [130]. When it comes to the connectivity, the GPe has an inhibitory feedback with the striatum [128,129]; also it sends inhibitory

projections to the STN and receives glutamatergic excitatory feedback projections [128,130]. This sort of connectivity has been argued to promote an oscillatory activity [130]. It was thought that the BG modulates cortical activity indirectly through inhibitory projections to the thalamus, but a recent study from Saunders *et al.* [131] has demonstrated that the GPe also projects GABAergic/ cholinergic projections to the frontal cortex. The existence of these projections suggests that GPe can directly influence the cortex.

The STN is the next nucleus in the canonical indirect pathway of the BG which has a great clinical relevance. Nowadays it is the favored site for deep-brain stimulation in the treatment of the PD. It receives excitatory projections from the CTX and the thalamus, as well as inhibitory projections from the striatum and the GPe. Additionally, the STN receives cholinergic projections from the pendunculopontine nucleus, a region involved in the control of arousal and alertness. All the output projections that arise from the STN are glutamatergic and excitatory. The STN projects to EP (or GPi in primates), GPe, SNr and to the pendunculopontine nucleus. Finally, the STN also feeds back into the striatum with sparse glutamatergic projections that are poorly branched [132,133], and provides *en passant* excitatory influence over striatal cells [103].

Other output nuclei of the BG is the SN and it is subdivided in SNc and SNr. The SNc sends broadly dopaminergic projections to the whole BG and to other parts of the brain. It has a major modulatory role over the entire brain processing, mostly related to the apparent encoding of errors in reward prediction, value and saliency of events [134,135]. As discussed before, SNr together with EP constitute the main output of the BG. SNr sends inhibitory projections to many different regions in the brain, among which are the pendunculopontine nucleus (PPN), the superior colliculus and the thalamus [136]. Since there is an anatomical segregation of information in all nuclei of the BG, depending on the cortical area from where the signal arises, the thalamic nuclei targeted by these projections differ [137]. For instance, the motor (lateral) circuit, that carries information from motor cortex, outputs to the ventrolateral nucleus pars oralis (VLo), the medial part of the ventrolateral nucleus (Vlm) and to the parvocellular part of the ventral anterior (VApc), from

where projections are sent back to motor areas of the cortex. In associative (medial) circuit, that carries information from higher order cortices, the BG projects to the VApc, the magnocellular part of the ventral anterior nucleus of the thalamus (VAmc), the rostral division of the caudal part of the ventrolateral nucleus (VLcr) and finally, to the lateral part of the mediodorsal nucleus of the thalamus (MDpl). The thalamo-glutamatergic projections from these regions target the lateral orbitofrontal cortex (LOFC) and the dorsolateral prefrontal cortex (DLPFC), the same areas that provide input to this BG-thalamocortical circuit.

Functionally, it has been hypothesized that the BG receive inputs from other areas of the brain and act upon these inputs as a filter. According to this hypothesis, the BG would select information derived from cortical and thalamic activity and send the resulting information back to the cortical source of the information. In parallel, it would also send copy of the same information to other systems of the brain to implement behavior. Since DA modulates the gain of cortico-striatal synapses [138-141], and because reinforcement-based plasticity occurs in the BG, it is thought that this plasticity might influence the input selection process based on previous experience [142]. The striatum and DA are considered to be key components to this filtering process.

The way in which information travels through the multiple nuclei of the BG might offer clues about their functional role. In the canonical perspective of the BG, information from the striatum can pass through the nuclei of the BG by two different parallel circuits: the direct and the indirect pathways (Figure 1.4). Neurons within the striatum can project directly to the EP/SNr that constitute the output nuclei of the BG (direct pathway). Or instead, striatal neurons can project first to intermediate nuclei, namely GPe and STN, and then to the output nuclei EP/SNr (indirect pathway; [143]).

These signaling pathways are regulated by DA in the striatum, and they have been the subject of intense study. It is known that driving activity in the direct pathway increases motor output (i.e., locomotion; [138,141,123]). On the other hand, stimulation of the indirect pathway seems to inhibit behavior [123]. For long it has been hypothesized that the direct pathway encodes the set of behavior plans available to the animals in a given context [19]. Thus, driving

the direct pathway would make these motor plans stronger, and consequently increase the motor output. Complementarily to this hypothesis, the indirect pathway would map the set of competing behaviors which must be suppressed so that the selected behavioral plan can occur with less interference. In this perspective, the BG would be responsible for filtering motor, associative and limbic information using a center-surround-like receptive field in the pertinent space (e.g., behavioral, cognitive) [19].

Anatomy, physiology and histochemistry of striatal neurons

Closer inspection of neuronal population and its characteristics reveals an astonishing complexity that has substantial implications to how the striatum might implement interval timing and other related processes. Most of the neurons with cell bodies within the striatum releases γ-aminobutyric acid (GABA). Since they are inhibitory neurons, it becomes clear that activity inside the striatum is either spontaneous or driven from extrinsic excitatory inputs.

Neurons in the striatum have been characterized anatomically, histochemically and physiologically [144,145]. Regarding their anatomic characteristics, striatal neurons can be either medium spiny projection neurons (MSNs) or aspiny interneurons. MSNs are the most abundant cell type of the striatum, constituting ~95% of striatal neurons [146]. MSNs are driven by extrinsic excitatory input projections from CTX, thalamus and STN and inhibited by interneurons and extrinsic input projections from GPe.

The MSNs are the only output neurons of the striatum [144,147], and they can be further classified into two subpopulations according to their axonal projection targets, the expression of genes for certain peptides, and the expression of DA receptors. These two subpopulations have approximately the same number of cells and they bring about the canonical direct and indirect pathways [143], previously discussed. The first population, striatonigral neurons, give rise to the direct pathway of the BG by sending projections directly to the output neurons of the BG in the EP and SNr. The second population, striatopallidal neurons, are the starting point of the indirect pathway by connecting striatum with the EP/SNr indirectly, through the GPe and STN consecutively. Again, excitation of the direct pathway facilitates movement and

activation of the indirect pathway inhibits movement [143,148]. These functional properties of these two pathways have been tested by Kravitz [149] and colleagues. They excited bilaterally the striatopallidal MSNs in transgenic mice using optogenetic methods and observed that this protocol induced a parkinsonian state (identified by increased freezing, decreased locomotor initiations and bradykinesia). Conversely, activation of striatonigral MSNs caused a decrease in freezing and an increase in locomotion.

MSNs show selective expression of certain peptides and receptors for DA, depending on whether they belong to the direct or indirect pathway. Studies using in situ hybridization histochemistry combined with retrograde labeling of striatonigral neurons suggest that striatonigral MSNs express substance-P, dynorphin and the DA type 1 (D_1, D_2) receptor, and therefore they are also referred to as D_1MSNs. The striatopallidal neurons express enkephalin and the D_2 type receptor (D2, D3, D4), and for that reason they are also known as D_2 MSNs [142].

The remaining 3-5% of striatal neurons are anatomically defined as aspiny interneurons and include among them cholinergic interneurons and several types of GABA-releasing interneurons [150]. Cholinergic interneurons constitute 1-2% of the neurons in the striatum [151]; these neurons are characterized by a large soma, often >50 μm long. They stain positively for choline acetyltransferase (ChAT) and express both D_2 and D_5 receptors as revealed by immunohistochemical analysis [152,153]. The GABAergic interneurons appear to express mainly D_5 receptors [152] and can be divided into at least three groups based on their distinct histochemical and physiological properties [150,154]. Histochemically, striatal GABAergic interneurons can be subdivided into: parvalbumin (PV)-positive; somatostatin-positive, neuropeptide Y-positive, and nitric oxide synthase-positive; and calretinin-positive [154].

The anatomical and histochemical differences discussed so far have physiological consequences in how striatal neurons behave. These three groups of striatal GABAergic interneurons can be further divided into at least two different types based on the firing patterns that they exhibit [154]. While PV-positive neurons display rapid and continued firing rates post current

injection, somatostatin-positive interneurons display lower firing rates and plateau potentials. Consequently, PV-positive neurons are also known as fast spiking (FS) interneurons and somatostatin-positive interneurons are known as low-threshold spiking (LTS) interneurons. Calretinin-positive interneurons appear to share some characteristics of LTS interneurons, but this similarity requires confirmation [155]. Albeit numerically scarce, striatal GABAergic interneurons play a major role regulating spike timing in the MSNs, mainly through feedforward inhibition [155]. Like MSNs, striatal interneurons receive glutamatergic input from cortex, thalamus and STN; and also get GABAergic input from the GPe. But on the contrary to MSNs, interneurons' output is directed primarily to MSNs and other interneurons inside the striatum. This sort of connectivity can strategically grant to GABAergic interneurons a disproportionately strong power to modulate striatal output despite their numerical minority.

Physiologically, the cholinergic interneurons, also known as tonically active neurons (TANs), display almost constant spontaneous activity. TANs are considered to be key mediators of dopamine-dependent striatal plasticity [156] and learning [157]. They exhibit significant hyperpolarization-activated currents, nonetheless TANs display a pause in their tonic firing in the presence of salient cues, including reward [144,158] which are usually followed by a rebound in the activity. Finally, a recent study [159] has found that TANs display fluctuations in their activity that follow changes in behavioral task conditions (e.g., context, task rules). Moreover, these fluctuations are inflexible to particular events (e.g., stimuli or behavior). These facts lead to the idea that TANs encode context-dependent information [159]. Whether these TANs are sensitive to temporal context has yet to be shown.

MSNs' average firing rates vary from 1 to 5 Hz depending on whether the animal is sleeping or awake [160]. Some of MSNs are known to produce spike bursts that are locked to behavior or to action sequence initiation [161]. These characteristics are especially relevant to the study of time, as it might be challenging to separate temporal from behavioral information in MSN's activity.

Because MSNs are the most abundant neurons in the striatum, easy to characterize electrophysiologically and the only output neurons of the striatum, our study focused on the activity of the MSNs in the SFI task.

Decodings and decoders

The brain faces the same elementary problem of communication when it operates on sensorial information and controls its effectors to produce adaptive behaviors. In communication, information from an original source must be transformed into a code that allows this information to be stored and transmitted over space and time in an effective way. This encoded information can be later translated back into a format in which it is meaningful for usage. Advances in communication technology developed our understanding of how to translate information into different codes. We perform these translations across different codes through the usage of encoding and decoding algorithms. We can use these algorithms to understand how neuronal activity might represent environmental events and how animals might use the same information encoded in the neuronal activity to produce behavior. In the particular scope of this thesis, we can use these algorithms to learn about how animals implement interval timing behavior. We can achieve that either by observing how neural time signals might emerge in face of task demands, or by observing how animals might use these temporal signals to produce behavior.

We assume that animals use encoding and decoding processes themselves. Encoding is the process by which animals generate representations of sensorial and behavioral events through the connectivity and activity of neurons [162]; this process can be thought as a mapping between stimuli and neuronal response. To profit from the encoded information, the brain has to be able to infer what is happening in the real world based on the activity dynamics of neurons. This process is called decoding and can either refer to the process of mapping neural activity back to the original stimuli or to behavior [162].

We can use mathematical techniques to exploit responses of one or more neurons and identify the stimulus that they derived from. In

electrophysiological studies, this approach helps us to answer three fundamental questions: What is the stimulus given the neuronal activity? What aspects of the stimulus are important for the neuronal response? What information is extractable from the stimulus by downstream areas and the experimenter (ideal observer analysis)?

The Bayes' theorem is a method to understand how the probability of a hypothesis is affected by the evidence that an other event is true. It can be used to estimate the probability of an event based on knowledge of conditions that might be related to the event. In electrophysiological experiments, we know the probability of the stimuli and the distributions of neural responses for each stimulus. Because of that, we can use Bayes' theorem to generate a model (i.e., decoding function which maps neural response to stimuli) that is able to decode the neural activity. This bayesian decoding procedure usually requires cross validation. Typically, it involves dividing the data set in two subgroups, using one of them to generate the model and using the other to test the predictor. The results of the test data set can be directly compared with the actual conditions in the experiment to address the accuracy, reliability and informational content of the model. Bayesian decoders have been successfully applied to infer discrimination [163] between the values of two different stimuli by a single cell, to extract the value of a stimulus parameter from a population response (i.e., population decoding), and/or to estimate time-varying stimulus from the spike train it evokes (i.e., spike-train decoding; [164]). Thus, these decoders have an established value as a valid analysis tool in neuroscience.

In electrophysiological research of sensorial modalities, the output of a bayesian decoder (the posterior) maps how likely each stimulus is given the current neural activity. The assumption is that the brain is performing a similar computation to come up with a decision or a behavior. To get one single estimate from the posterior distribution, additional assumptions about how to use the posterior distribution are necessary. Typically, the assumption is a classical central tendency measure such as the median, the mean or the mode [165]. This process of estimating the stimulus by observing the most likely one is also known as maximum likelihood decoding.

Decoding information from ongoing behavior

A major point of concern in interval timing research is how to control behavioral artifacts in the data from timing experiments [61]. Ongoing behavior changes over time and their neuronal representations might seem to covary with time but not encode time itself. Furthermore, neuronal activity is not the only form that animals have to encode information. Proponents of the embodied cognition theory state that animals can leverage the idiosyncrasies of their sensors and effectors [166,167] to encode relevant environmental information in the structure of behavior itself [168].

Old methods of behavioral data acquisition are insufficient to address these questions because they lack precision and consistency. Direct observation by trained psychologists and biologists has been the typical method to quantify the topography of behavior [169]. However, this kind of observation has constraints of time, resolution and reliability. Furthermore, this method heavily relies on subjective accounts of the observation, because the exact record of events (i.e., video, raw data) is not usually preserved.

New technologies can help to solve this problem by means of automation. The recent proliferation of high-powered computers, the availability of high quality and inexpensive video cameras, and the increasing need for automated video analysis have promoted the advancement of object tracking algorithms. Tracking, in its simplest form can be defined as estimating the trajectory of an object in the image plane as it moves around a scene. Tracking algorithms open the possibility to use video data to collect large amounts of highly precise and accurate information about the behavior, and then analyze it. This approach is especially suitable to laboratory work with rodents because these animals are small enough to be completely captured inside the video frame, and recording conditions (e.g., lighting, color of the background) can be optimized to make the tracking more efficient.

Every video analysis involves four major steps: digital recording videos of behavioral data, detection of interesting moving objects, tracking of such objects from frame to frame, and analysis of object tracks to recognize their behavior. Each of these steps offers implementation challenges. Constraints on the acquisition speed, video processing and storage of digital information limit

the spatiotemporal extent of video-based tracking. Detecting that an object entered in the field-of-view can be achieved by a process called background subtraction. To do so, we need first to build a representation of the scene, called the background model, and then to find deviations from the model for each incoming frame (i.e., the absolute difference between the current frame and the background image). Any significant (magnitude criteria) change within the image region from the background model indicates a moving object. The pixels constituting the regions undergoing change are marked for further processing. Typically, we estimate the position of the animal by obtaining the regions of neighboring pixels using a connected-components algorithm. When only one animal is in the scene, the largest connected component describes the silhouette of the animal. Tracking the position and pose of the animal can be complex due to: loss of information caused by projection of the 3D world onto a 2D image, noise in images, complex object motion, nonrigid or articulated nature of objects, partial or full object occlusions, complex object shapes and scene illumination changes [170]. Most of these problems can be avoided by controlling the environment to ensure optimal conditions for tracking. For instance, one can impose constraints on the motion and/or appearance of objects such as, assuming linear smooth trajectories, geometric shape or imposing heuristics to decide on ambiguous events data [170]. By following these steps we can produce a time series of behavioral descriptors (positions and poses) which we can use to decode information about the world.

Neural and behavioral dynamics code of interval timing

Animals can support their timing ability either by relying either on neuronal activity or on behavioral strategies. We are interested to understand how the striatum contributes to time perception in the range of seconds to one minute. More specifically, we want to know how striatal activity of rats trained in a dynamic timing task, in which they have to report their estimations of multiple intervals in the range from 12 to 60s, will account for the passage of time and the ongoing behavior that develops in parallel. Thus in this work we aim to:

- Record activity of the striatum while animals were performing this timing task.

- Verify if the striatal activity carries information about the task performance.
- Test the necessity of the recording site activity to perform in the timing task.
- Develop methods to disambiguate variance in neuronal activity due to time and ongoing behavioral activity.
- Observe if behavior in this task is structured so that it could embed information about the intervals.

Structure of the thesis

In the second chapter we investigate the role of the striatal electrical activity in the processing of interval timing. We offer a detailed description of the timing task, the animals' performance, the neural activity of the striatal cells during task performance and how this activity relates to time and behavior. We will also briefly discuss, in light of current timing models, how timing might be encoded and propose a timing mechanism that is relative, scalable and embeds compounded information about time and behavior.

In the third chapter we use simulation as our approach to explore how the neuronal activity observed in the chapter two can leverage reinforcement learning models in order to generate temporally adaptive behaviors. We provide information about how our model reproduces the scalable, multiplexing activity of the striatum; the additional assumptions we adopted to make the model perform in the timing task; and how the model performs when compared with either the experimental data or the timing behavior expected from the literature.

In the fourth chapter we address the problem of separating behavioral information from time information. We describe the computer vision methods to track the animals' behavior with high speed cameras, as well as the decoding methods to extract time information from behavior. We conclude the chapter discussing the main issues and benefits of our approach.

Finally, in the last chapter we discuss our findings in the light of the latest theories about timing. We highlight the limitations of our approach, pointing out some possible solutions that can lead to future lines of research.

REFERENCES

1. Barclay, J. L., Husse, J., Bode, B., Naujokat, N., Meyer-Kovac, J., Schmid, S. M., … Oster, H. (2012). Circadian desynchrony promotes metabolic disruption in a mouse model of shiftwork. PLoS ONE, 7(5). http://doi.org/10.1371/journal.pone.0037150
2. Balsalobre, A., Marcacci, L., & Schibler, U. (2000a). Multiple signaling pathways elicit circadian gene expression in cultured Rat-1 fibroblasts. Current Biology, 10(20), 1291–1294. http://doi.org/10.1016/S0960-9822(00)00758-2
3. Balsalobre, A., Brown, S. A., Marcacci, L., Tronche, F., Kellendonk, C., Reichardt, H. M., … Schibler, U. (2000b). Resetting of circadian time in peripheral tissues by glucocorticoid signaling. Science (New York, N.Y.), 289(5488), 2344–2347. http://doi.org/10.1126/science.289.5488.2344
4. Zhu, L., & Zee, P. C. (2012). Circadian Rhythm Sleep Disorders. Neurologic Clinics. http://doi.org/10.1016/j.ncl.2012.08.011
5. Schnupp, J. W. H., & Carr, C. E. (2009). On hearing with more than one ear: lessons from evolution. Nature Neuroscience, 12(6), 692–697. http://doi.org/10.1038/nn.2325
6. Merchant, H., Harrington, D. L., & Meck, W. H. (2013). Neural basis of the perception and estimation of time. Annual Review of Neuroscience, 36(June), 313–36. http://doi.org/10.1146/annurev-neuro-062012-170349
7. Boisvert, M. J., & Sherry, D. F. (2006). Interval Timing by an Invertebrate, the Bumble Bee Bombus impatiens. Current Biology, 16(16), 1636–1640. http://doi.org/10.1016/j.cub.2006.06.064
8. Buhusi, C. V, Sasaki, A., & Meck, W. H. (2002). Temporal integration as a function of signal and gap intensity in rats (Rattus norvegicus) and pigeons (Columba livia). Journal of Comparative Psychology, 116(4), 381–390. http://doi.org/10.1037/0735-7036.116.4.381
9. Drew, M. R., Zupan, B., Cooke, A., Couvillon, P. A., & Balsam, P. D. (2005). Temporal control of conditioned responding in goldfish. Journal of Experimental Psychology. Animal Behavior Processes, 31(1), 31–39. http://doi.org/10.1037/0097-7403.31.1.31
10. Boulanger Bertolus, J., Hegoburu, C., Ahers, J. L., Londen, E., Rousselot, J., Szyba, K., … Mouly, A.-M. (2014). Infant rats can learn time intervals before the maturation of the striatum: evidence from odor fear conditioning. Frontiers in Behavioral Neuroscience, 8(May), 176. http://doi.org/10.3389/fnbeh.2014.00176
11. Buhusi, C. V, Perera, D., & Meck, W. H. (2005). Memory for timing visual and auditory signals in albino and pigmented rats. Journal of Experimental Psychology. Animal Behavior Processes, 31(1), 18–30. http://doi.org/10.1037/0097-7403.31.1.18

12. Gribova, a, Donchin, O., Bergman, H., Vaadia, E., & Cardoso De Oliveira, S. (2002). Timing of bimanual movements in human and non-human primates in relation to neuronal activity in primary motor cortex and supplementary motor area. Experimental Brain Research. Experimentelle Hirnforschung. Expérimentation Cérébrale, 146(3), 322–35. http://doi.org/10.1007/s00221-002-1174-x

13. Brannon, E. M., Roussel, L. W., Meck, W. H., & Woldorff, M. (2004). Timing in the baby brain. Cognitive Brain Research, 21(2), 227–233. http://doi.org/10.1016/j.cogbrainres.2004.04.007

14. Rakitin, B. C., Gibbon, J., Penney, T. B., Malapani, C., Hinton, S. C., & Meck, W. H. (1998). Scalar expectancy theory and peak-interval timing in humans. Journal of Experimental Psychology. Animal Behavior Processes, 24(1), 15–33. http://doi.org/10.1037/0097-7403.24.1.15

15. Henderson, J., Hurly, T. A., & Healy, S. D. (2006). Spatial relational learning in rufous hummingbirds (Selasphorus rufus). Animal Cognition, 9(3), 201–205. http://doi.org/10.1007/s10071-006-0021-z

16. Kacelnik, A., & Brunner, D. (2002). Timing and foraging: Gibbon's scalar expectancy theory and optimal patch exploitation. Learning and Motivation, 33(1), 177–195. http://doi.org/10.1006/lmot.2001.1110

17. Bateson, M., & Kacelnik, A. (1998). Risk-sensitive foraging: decision making in variable environments. In Cognitive Ecology (pp. 297–340).

18. Bortoletto, M., Lemonis, M. J., & Cunnington, R. (2011). The role of arousal in the preparation for voluntary movement. Biological Psychology, 87(3), 372–378. http://doi.org/10.1016/j.biopsycho.2011.04.008

19. Gallistel, C. R., & Gibbon, J. (2000). Time, rate, and conditioning. Psychological Review, 107(2), 289–344. http://doi.org/10.1037/0033-295X.107.2.289

20. Sohn, M. H., & Carlson, R. A. (2003). Implicit temporal tuning of working memory strategy during cognitive skill acquisition. American Journal of Psychology, 116(2), 239–256.

21. Danckert, J. a., & Allman, a. a a. (2005). Time flies when you're having fun: Temporal estimation and the experience of boredom. Brain and Cognition, 59(3), 236–245. http://doi.org/10.1016/j.bandc.2005.07.002

22. Noreika, V., Falter, C. M., & Rubia, K. (2013). Timing deficits in attention-deficit/hyperactivity disorder (ADHD): Evidence from neurocognitive and neuroimaging studies. Neuropsychologia, 51(2), 235–266. http://doi.org/10.1016/j.neuropsychologia.2012.09.036

23. Pouthas, V., & Perbal, S. (2004). Time perception depends on accurate clock mechanisms as well as unimpaired attention and memory processes. In Acta Neurobiologiae Experimentalis (Vol. 64, pp. 367–385).

24. Galtress, T., & Kirkpatrick, K. (2009). Reward value effects on timing in the peak procedure. Learning and Motivation, 40(2), 109–131. http://doi.org/10.1016/j.lmot.2008.05.004

25. Tamm, M., Uusberg, A., Allik, J., & Kreegipuu, K. (2014). Emotional modulation of attention affects time perception: Evidence from event-related potentials. Acta Psychologica, 149, 148–156. http://doi.org/10.1016/j.actpsy.2014.02.008

26. Meck, W. H. (2006). Neuroanatomical localization of an internal clock: A functional link between mesolimbic, nigrostriatal, and mesocortical dopaminergic systems. Brain Research, 1109(1), 93–107. http://doi.org/10.1016/j.brainres.2006.06.031

27. Gibbon, J., Malapani, C., Dale, C. L., & Gallistel, C. R. (1997). Toward a neurobiology of temporal cognition: Advances and challenges. Current Opinion in Neurobiology. http://doi.org/10.1016/S0959-4388(97)80005-0

28. Matell, M. S., & Meck, W. H. (2000). Neuropsychological mechanisms of interval timing behavior. BioEssays. doi:10.1002/(SICI)1521-1878(200001)22:1<94::AID-BIES14>3.0.CO;2-E

29. Staddon, J. E., & Higa, J. J. (1999). Time and memory: towards a pacemaker-free theory of interval timing. Journal of the Experimental Analysis of Behavior, 71(2), 215–251. http://doi.org/10.1901/jeab.1999.71-215

30. Machado, A. (1997). Learning the temporal dynamics of behavior. Psychological Review, 104(2), 241–265. http://doi.org/10.1037/0033-295X.104.2.241

31. Gershman, S. J., Moustafa, A. a, & Ludvig, E. a. (2014). Time representation in reinforcement learning models of the basal ganglia. Frontiers in Computational Neuroscience, 7(January), 194. http://doi.org/10.3389/fncom.2013.00194

32. Oprisan, S. A., & Buhusi, C. V. (2011). Modeling Pharmacological Clock and Memory Patterns of Interval Timing in a Striatal Beat-Frequency Model with Realistic, Noisy Neurons. Frontiers in Integrative Neuroscience. http://doi.org/10.3389/fnint.2011.00052

33. Brown, S. W., & Smith-Petersen, G. A. (2014). Time perception and temporal order memory. Acta Psychologica, 148, 173–180. doi:10.1016/j.actpsy.2014.02.003

34. Staddon, J. E. R. (2005). Interval timing: Memory, not a clock. Trends in Cognitive Sciences. http://doi.org/10.1016/j.tics.2005.05.013

35. Lejeune, H., & Wearden, J. (1991). The comparative psychology of fixed-interval responding: Some quantitative analyses. Learning and Motivation. http://doi.org/10.1016/0023-9690(91)90018-4

36. Ludvig, E. a., Balci, F., & Spetch, M. L. (2011). Reward magnitude and timing in pigeons. Behavioural Processes, 86(3), 359–363. http://doi.org/10.1016/j.beproc.2011.01.003

37. Gibbon, J. (1977). Scalar expectancy theory and Weber's law in animal timing. Psychological Review. http://doi.org/10.1037/0033-295X.84.3.279

38. Astle, A. T., Li, R. W., Webb, B. S., Levi, D. M., & McGraw, P. V. (2013). A Weber-like law for perceptual learning. Scientific Reports, 3, 1158. http://doi.org/10.1038/srep01158

39. Dehaene, S. (2003). The neural basis of the Weber-Fechner law: A logarithmic mental number line. Trends in Cognitive Sciences. http://doi.org/10.1016/S1364-6613(03)00055-X

40. Johnson, K. O., Hsiao, S. S., & Yoshioka, T. (2002). Neural coding and the basic law of psychophysics. The Neuroscientist : A Review Journal Bringing Neurobiology, Neurology and Psychiatry, 8(2), 111–121. http://doi.org/10.1177/107385840200800207

41. Takahashi, T. (2006). Time-estimation error following Weber-Fechner law may explain subadditive time-discounting. Medical Hypotheses, 67(6), 1372–1374. http://doi.org/10.1016/j.mehy.2006.05.056

42. Hinton, S. C., & Meck, W. H. (2004). Frontal-striatal circuitry activated by human peak-interval timing in the supra-seconds range. Cognitive Brain Research, 21(2), 171–182. http://doi.org/10.1016/j.cogbrainres.2004.08.005

43. Jazayeri, M., & Shadlen, M. N. (2010). Temporal context calibrates interval timing. Nature Neuroscience, 13(8), 1020–1026. http://doi.org/10.1038/nn.2590

44. Innis, N. K., & Staddon, J. E. (1971). Temporal tracking on cyclic-interval reinforcement schedules. Journal of the Experimental Analysis of Behavior, 16(3), 411–423. http://doi.org/10.1901/jeab.1971.16-411

45. Higa, J. J., Moreno, S., & Sparkman, N. (2002). Interval timing in rats: Tracking unsignaled changes in the fixed interval schedule requirement. Behavioural Processes, 58(3), 167–176. http://doi.org/10.1016/S0376-6357(02)00029-3

46. Higa, J. J., Thaw, J. M., & Staddon, J. E. (1993). Pigeons' wait-time responses to transitions in interfood-interval duration: Another look at cyclic schedule performance. Journal of the Experimental Analysis of Behavior, 59(3), 529–541. http://doi.org/10.1901/jeab.1993.59-529

47. Wearden, J. (1991). Do humans possess an internal clock with scalar timing properties? Learning and Motivation, 22(1-2), 59–83. http://doi.org/10.1016/0023-9690(91)90017-3

48. Hoagland, H. (1933). The Physiological Control of Judgments of Duration: Evidence for a Chemical Clock. The Journal of General Psychology. http://doi.org/10.1080/00221309.1933.9920937

49. Treisman, M. (1963). Temporal discrimination and the indifference interval. Implications for a model of the "internal clock". Psychological Monographs, 77(13), 1–31. http://doi.org/10.1037/h0093864

50. Gibbon, J., Church, R. M., & Meck, W. H. (1984). Scalar timing in memory. Annals of the New York Academy of Sciences, 423, 52–77. http://doi.org/10.1111/j.1749-6632.1984.tb23417.x

51. Killeen, P. R., & Fetterman, J. G. (1988). A behavioral theory of timing. Psychological Review, 95(2), 274–295. http://doi.org/10.1037/0033-295X.95.2.274

52. Buonomano, D. V, & Merzenich, M. M. (1995). Temporal information transformed into a spatial code by a neural network with realistic properties. Science (New York, N.Y.), 267(5200), 1028–1030. http://doi.org/10.1126/science.7863330

53. Machado, A., Malheiro, M. T., & Erlhagen, W. (2009). Learning to Time: a perspective. Journal of the Experimental Analysis of Behavior, 92(3), 423–458. http://doi.org/10.1901/jeab.2009.92-423

54. Killeen, P. R., & Fetterman, J. G. (1993). The behavioral theory of timing: transition analyses. Journal of the Experimental Analysis of Behavior, 59(2), 411–422. http://doi.org/10.1901/jeab.1993.59-411

55. Fetterman, J. G., & Killeen, P. R. (2010). Prospective and retrospective timing by pigeons. Learning & Behavior : A Psychonomic Society Publication, 38(2), 119–125. http://doi.org/10.3758/LB.38.2.119

56. Arantes, J. (2008). Comparison of Scalar Expectancy Theory (SET) and the Learning-to-Time (LeT) model in a successive temporal bisection task. Behavioural Processes, 78(2), 269–278. http://doi.org/10.1016/j.beproc.2007.12.008

57. Miall, C. (1989). The Storage of Time Intervals Using Oscillating Neurons. Neural Computation, 1(3), 359–371. http://doi.org/10.1162/neco.1989.1.3.359

58. Matell, M. S., & Meck, W. H. (2004). Cortico-striatal circuits and interval timing: Coincidence detection of oscillatory processes. Cognitive Brain Research, 21(2), 139–170. http://doi.org/10.1016/j.cogbrainres.2004.06.012

59. Hikosaka, O., Sakamoto, M., & Usui, S. (1989). Functional properties of monkey caudate neurons. III. Activities related to expectation of target and reward. Journal of Neurophysiology, 61(4), 814–832.

60. Niki, H., & Watanabe, M. (1979). Prefrontal and cingulate unit activity during timing behavior in the monkey. Brain Research, 171(2), 213–224. http://doi.org/10.1016/0006-8993(79)90328-7

61. Matell, M. S., Meck, W. H., & Nicolelis, M. a L. (2003). Interval timing and the encoding of signal duration by ensembles of cortical and striatal neurons. Behavioral Neuroscience, 117(4), 760–773. http://doi.org/10.1037/0735-7044.117.4.760

62. Wiener, M., Turkeltaub, P., & Coslett, H. B. (2010). The image of time: A voxel-wise meta-analysis. NeuroImage, 49(2), 1728–1740. http://doi.org/10.1016/j.neuroimage.2009.09.064

63. Xu, M., Zhang, S., Dan, Y., & Poo, M. (2014). Representation of interval timing by temporally scalable firing patterns in rat prefrontal cortex. Proceedings of the National Academy of Sciences of the United States of America, 111(1), 480–5. http://doi.org/10.1073/pnas.1321314111

64. Jaldow, E. J., Oakley, D. a., & Davey, G. C. L. (1989). Performance of Decorticated Rats on Fixed Interval and Fixed Time Schedules. Eurpoean Journal of Neuroscience, 1(5), 461–470.

65. Kim, J., Ghim, J.-W., Lee, J. H., & Jung, M. W. (2013). Neural correlates of interval timing in rodent prefrontal cortex. The Journal of Neuroscience : The Official Journal of the Society for Neuroscience, 33(34), 13834–47. http://doi.org/10.1523/JNEUROSCI.1443-13.2013

66. Kim, J., Jung, A. H., Byun, J., Jo, S., & Jung, M. W. (2009). Inactivation of medial prefrontal cortex impairs time interval discrimination in rats. Frontiers in Behavioral Neuroscience, 3(November), 38. http://doi.org/10.3389/neuro.08.038.2009

67. Husain, M., & Nachev, P. (2007). Space and the parietal cortex. Trends in Cognitive Sciences, 11(1), 30–36. http://doi.org/10.1016/j.tics.2006.10.011

68. Hromádka, T., & Zador, A. M. (2009). Representations in auditory cortex. Current Opinion in Neurobiology. http://doi.org/10.1016/j.conb.2009.07.009

69. Harrington, D. L., Lee, R. R., Boyd, L. A., Rapcsak, S. Z., & Knight, R. T. (2004). Does the representation of time depend on the cerebellum? Effect of cerebellar stroke. Brain, 127(3), 561–574. http://doi.org/10.1093/brain/awh065

70. Gooch, C. M., Wiener, M., Wencil, E. B., & Coslett, H. B. (2010). Interval timing disruptions in subjects with cerebellar lesions. Neuropsychologia, 48(4), 1022–1031. http://doi.org/10.1016/j.neuropsychologia.2009.11.028

71. Buonomano, D. V., & Mauk, M. D. (1994). Neural Network Model of the Cerebellum: Temporal Discrimination and the Timing of Motor Responses. Neural Computation, 6(1), 38–55. doi:10.1162/neco.1994.6.1.38

72. Barto, A. G., Fagg, A. H., Sitkoff, N., & Houk, J. C. (1999). A cerebellar model of timing and prediction in the control of reaching. Neural Computation, 11(3), 565–594. http://doi.org/10.1162/089976699300016575

73. Manns, J. R., Howard, M. W., & Eichenbaum, H. (2007). Gradual Changes in Hippocampal Activity Support Remembering the Order of Events. Neuron, 56(3), 530–540. http://doi.org/10.1016/j.neuron.2007.08.017

74. Pastalkova, E., Itskov, V., Amarasingham, A., & Buzsáki, G. (2008). Internally generated cell assembly sequences in the rat hippocampus. Science (New York, N.Y.), 321(5894), 1322–1327. http://doi.org/10.1126/science.1159775

75. MacDonald, C. J., Lepage, K. Q., Eden, U. T., & Eichenbaum, H. (2011). Hippocampal “time cells” bridge the gap in memory for discontiguous events. Neuron, 71(4), 737–749. http://doi.org/10.1016/j.neuron.2011.07.012

76. Kraus, B., Robinson, R., White, J., Eichenbaum, H., & Hasselmo, M. (2013). Hippocampal “Time Cells”: Time versus Path Integration. Neuron, 78(6), 1090–1101. http://doi.org/10.1016/j.neuron.2013.04.015

77. Howard, M. W., MacDonald, C. J., Tiganj, Z., Shankar, K. H., Du, Q., Hasselmo, M. E., & Eichenbaum, H. (2014). A Unified Mathematical Framework for Coding Time, Space, and Sequences in the Hippocampal Region. Journal of Neuroscience, 34(13), 4692–4707. http://doi.org/10.1523/JNEUROSCI.5808-12.2014

78. Yin, B., & Meck, W. H. (2014). Comparison of interval timing behaviour in mice following dorsal or ventral hippocampal lesions with mice having δ-opioid receptor gene deletion. Philosophical Transactions of the Royal Society of London. Series B, Biological Sciences. http://doi.org/10.1098/rstb.2012.0466

79. O’Keefe, J., & Dostrovsky, J. (1971). The hippocampus as a spatial map. Preliminary evidence from unit activity in the freely-moving rat. Brain Research, 34(1), 171–175. http://doi.org/10.1016/0006-8993(71)90358-1

80. Squire, L. R. (1987). The organization and neural substrates of human memory. International Journal of Neurology, 21-22:218-, 218–222.

81. Jacobs, N. S., Allen, T. a, Nguyen, N., & Fortin, N. J. (2013). Critical role of the hippocampus in memory for elapsed time. The Journal of Neuroscience : The Official Journal of the Society for Neuroscience, 33(34), 13888–93. http://doi.org/10.1523/JNEUROSCI.1733-13.2013

82. Goto, Y., & O’Donnell, P. (2001). Synchronous activity in the hippocampus and nucleus accumbens in vivo. The Journal of Neuroscience : The Official Journal of the Society for Neuroscience, 21(4), RC131. http://doi.org/20014996 [pii]

83. Amaral D, Lavenex P (2006). "Ch 3. Hippocampal Neuroanatomy". In Andersen P, Morris R, Amaral D, Bliss T, O'Keefe J. The Hippocampus Book. Oxford University Press. ISBN 978-0-19-510027-3.

84. Coull, J. T., Vidal, F., Nazarian, B., & Macar, F. (2004). Functional anatomy of the attentional modulation of time estimation. Science (New York, N.Y.), 303(5663), 1506–1508. http://doi.org/10.1126/science.1091573

85. Ferrandez, A. M., Hugueville, L., Lehéricy, S., Poline, J. B., Marsault, C., & Pouthas, V. (2003). Basal ganglia and supplementary motor area subtend duration perception: An fMRI study. NeuroImage, 19(4), 1532–1544. http://doi.org/10.1016/S1053-8119(03)00159-9

86. Tanaka, S. C., Okada, G., Ueda, K., Okamoto, Y. and Yamawaki, S.(2004). Prediction of immediate and future rewards differentially recruits cortico-basal ganglia loops. Nature Neuroscience. 7, 887–893.

87. Rowe, K. C., Paulsen, J. S., Langbehn, D. R., Duff, K., Beglinger, L. J., Wang, C., … Moser, D. J. (2010). Self-paced timing detects and tracks change in prodromal Huntington disease. Neuropsychology, 24(4), 435–442. http://doi.org/10.1037/a0018905

88. Rakitin, B. C., Gibbon, J., Penney, T. B., Malapani, C., Hinton, S. C., & Meck, W. H. (1998). Scalar expectancy theory and peak-interval timing in humans. Journal of Experimental Psychology. Animal Behavior Processes, 24(1), 15–33. http://doi.org/10.1037/0097-7403.24.1.15

89. Rammsayer, T. (1990). Temporal discrimination in schizophrenic and affective disorders: evidence for a dopamine-dependent internal clock. The International Journal of Neuroscience, 53(2-4), 111–120. http://doi.org/10.3109/00207459008986593

90. Tracy, J. I., Monaco, C., McMichael, H., Tyson, K., Chambliss, C., Christensen, H. L., & Celenza, M. A. (1998). Information-processing characteristics of explicit time estimation by patients with schizophrenia and normal controls. Perceptual and Motor Skills, 86(2), 515–526. http://doi.org/10.2466/pms.1998.86.2.515

91. Penney, T. B., Meck, W. H., Roberts, S. A., Gibbon, J., & Erlenmeyer-Kimling, L. (2005). Interval-timing deficits in individuals at high risk for schizophrenia. Brain and Cognition, 58(1), 109–118. http://doi.org/10.1016/j.bandc.2004.09.012

92. Malapani, C., Rakitin, B., Levy, R., Meck, W. H., Deweer, B., Dubois, B., & Gibbon, J. (1998). Coupled temporal memories in Parkinson's disease: a dopamine-related dysfunction. Journal of Cognitive Neuroscience, 10(3), 316–331. http://doi.org/10.1162/089892998562762

93. Malapani, C., Deweer, B., & Gibbon, J. (2002). Separating storage from retrieval dysfunction of temporal memory in Parkinson's disease. Journal of Cognitive Neuroscience, 14(2), 311–322. http://doi.org/10.1162/089892902317236920

94. Maricq, A. V., & Church, R. M. (1983). The differential effects of haloperidol and methamphetamine on time estimation in the rat. Psychopharmacology, 79(1), 10–15. http://doi.org/10.1007/BF00433008

95. Ward, R. D., Kellendonk, C., Simpson, E. H., Lipatova, O., Drew, M. R., Fairhurst, S., … Balsam, P. D. (2009). Impaired timing precision produced by striatal D2 receptor overexpression is mediated by cognitive and motivational deficits. Behavioral Neuroscience, 123(4), 720–730. http://doi.org/10.1037/a0016503

96. Boisvert, M. J., & Sherry, D. F. (2006). Interval Timing by an Invertebrate, the Bumble Bee Bombus impatiens. Current Biology, 16(16), 1636–1640. http://doi.org/10.1016/j.cub.2006.06.064

97. Middleton, F. a, & Strick, P. L. (2000). Basal ganglia and cerebellar loops: motor and cognitive circuits. Brain Research. Brain Research Reviews, 31(2-3), 236–50. http://doi.org/10.1016/S0165-0173(99)00040-5

98. Bostan, A. C., & Strick, P. L. (2010). The cerebellum and basal ganglia are interconnected. Neuropsychology Review, 20(3), 261–270. http://doi.org/10.1007/s11065-010-9143-9

99. Hoshi, E., Tremblay, L., Féger, J., Carras, P. L., & Strick, P. L. (2005). The cerebellum communicates with the basal ganglia. Nature Neuroscience, 8(11), 1491–1493. http://doi.org/10.1038/nn1544

100. Kelly, R. M., & Strick, P. L. (2004). Macro-architecture of basal ganglia loops with the cerebral cortex: use of rabies virus to reveal multisynaptic circuits. Progress in Brain Research, 143, 449–459. http://doi.org/10.1016/j.neulet.2011.07.028

101. Bussi, I. L., Levín, G., Golombek, D. a., & Agostino, P. V. (2014). Involvement of dopamine signaling in the circadian modulation of interval timing. European Journal of Neuroscience, 40(1), 2299–2310. http://doi.org/10.1111/ejn.12569

102. Parent, A., & Hazrati, L. N. (1995a). Functional anatomy of the basal ganglia. I. The cortico-basal ganglia-thalamo-cortical loop. Brain Research Reviews. http://doi.org/10.1016/0165-0173(94)00007-C

103. Parent, A., & Hazrati, L. N. (1995b). Functional anatomy of the basal ganglia. II. The place of subthalamic nucleus and external pallidum in basal ganglia circuitry. Brain Research Reviews. http://doi.org/10.1016/0165-0173(94)00008-D

104. Ashby, F. G., Turner, B. O., & Horvitz, J. C. (2010). Cortical and basal ganglia contributions to habit learning and automaticity. Trends in Cognitive Sciences. http://doi.org/10.1016/j.tics.2010.02.001

105. Graybiel, A. M. (1995). Building action repertoires: Memory and learning functions of the basal ganglia. Current Opinion in Neurobiology. http://doi.org/10.1016/0959-4388(95)80100-6

106. Packard, M. G., & Knowlton, B. J. (2002). Learning and memory functions of the Basal Ganglia. Annual Review of Neuroscience, 25, 563–593. http://doi.org/10.1146/annurev.neuro.25.112701.142937

107. Brittain, J. S., & Brown, P. (2014). Oscillations and the basal ganglia: Motor control and beyond. NeuroImage. http://doi.org/10.1016/j.neuroimage.2013.05.084

108. Doya, K. (2000). Complementary roles of basal ganglia and cerebellum in learning and motor control. Current Opinion in Neurobiology, 10, 732–739. http://doi.org/10.1016/S0959-4388(00)00153-7

109. Graybiel, A. M., Aosaki, T., Flaherty, A. W., & Kimura, M. (1994). The basal ganglia and adaptive motor control. Science (New York, N.Y.), 265(5180), 1826–1831. http://doi.org/10.1126/science.8091209

110. Groenewegen, H. J. (2003). The basal ganglia and motor control. Neural Plasticity, 10(1-2), 107–120. http://doi.org/10.1155/NP.2003.107

111.Turner, R. S., & Desmurget, M. (2010). Basal ganglia contributions to motor control: A vigorous tutor. Current Opinion in Neurobiology. http://doi.org/10.1016/j.conb.2010.08.022

112.Buot, A., & Yelnik, J. (2012). Functional anatomy of the basal ganglia: Limbic aspects. Revue Neurologique. http://doi.org/10.1016/j.neurol.2012.06.015

113.Chaudhuri, A., & Behan, P. O. (2000). Fatigue and basal ganglia. Journal of the Neurological Sciences. http://doi.org/10.1016/S0022-510X(00)00411-1

114.Haber, S. N. (2003). The primate basal ganglia: Parallel and integrative networks. In Journal of Chemical Neuroanatomy (Vol. 26, pp. 317–330). http://doi.org/10.1016/j.jchemneu.2003.10.003

115.Haegelen, C., Rouaud, T., Darnault, P., & Morandi, X. (2009). The subthalamic nucleus is a key-structure of limbic basal ganglia functions. Medical Hypotheses, 72(4), 421–426. http://doi.org/10.1016/j.mehy.2008.07.065

116.Grahn, J. A., Parkinson, J. A., & Owen, A. M. (2009). The role of the basal ganglia in learning and memory: Neuropsychological studies. Behavioural Brain Research. http://doi.org/10.1016/j.bbr.2008.11.020

117.Graybiel, A. M. (1995). Building action repertoires: Memory and learning functions of the basal ganglia. Current Opinion in Neurobiology. http://doi.org/10.1016/0959-4388(95)80100-6

118.McNab, F., & Klingberg, T. (2008). Prefrontal cortex and basal ganglia control access to working memory. Nature Neuroscience, 11(1), 103–107. http://doi.org/10.1038/nn2024

119.O'Reilly, R. C., & Frank, M. J. (2006). Making working memory work: a computational model of learning in the prefrontal cortex and basal ganglia. Neural Computation, 18(2), 283–328. http://doi.org/10.1162/089976606775093909

120.Tepper, J. M., Abercrombie, E. D., & Bolam, J. P. (2007). Basal ganglia macrocircuits. Progress in Brain Research. http://doi.org/10.1016/S0079-6123(06)60001-0

121.Parent, A., Cote, P. Y., & Lavoie, B. (1995c). Chemical anatomy of primate basal ganglia. Progress in Neurobiology. http://doi.org/10.1016/0301-0082(95)00001-C

122.Yin, H. H., & Knowlton, B. J. (2006). The role of the basal ganglia in habit formation. Nature Reviews. Neuroscience, 7(6), 464–476. http://doi.org/10.1038/nrn1919

123.Freeze, B. S., Kravitz, A. V, Hammack, N., Berke, J. D., & Kreitzer, A. C. (2013). Control of basal ganglia output by direct and indirect pathway projection neurons. The Journal of Neuroscience : The Official Journal of the Society for Neuroscience, 33(47), 18531–9. http://doi.org/10.1523/JNEUROSCI.1278-13.2013

124.Haber, S. N., & Calzavara, R. (2009). The cortico-basal ganglia integrative network: The role of the thalamus. Brain Research Bulletin. http://doi.org/10.1016/j.brainresbull.2008.09.013

125.Herrero, M. T., Barcia, C., & Navarro, J. M. (2002). Functional anatomy of thalamus and basal ganglia. Child's Nervous System. http://doi.org/10.1007/s00381-002-0604-1

126.Carbon, M., Ma, Y., Barnes, A., Dhawan, V., Chaly, T., Ghilardi, M. F., & Eidelberg, D. (2004). Caudate nucleus: Influence of dopaminergic input on sequence learning and brain activation in Parkinsonism. NeuroImage, 21(4), 1497–1507. http://doi.org/10.1016/j.neuroimage.2003.12.014

127.Joel, D., & Weiner, I. (2000). The connections of the dopaminergic system with the striatum in rats and primates: An analysis with respect to the functional and compartmental organization of the striatum. Neuroscience. http://doi.org/10.1016/S0306-4522(99)00575-8

128.Mallet, N., Micklem, B. R., Henny, P., Brown, M. T., Williams, C., Bolam, J. P., … Magill, P. J. (2012). Dichotomous Organization of the External Globus Pallidus. Neuron, 74(6), 1075–1086. http://doi.org/10.1016/j.neuron.2012.04.027

129.Nevado-Holgado, A. J., Mallet, N., Magill, P. J., & Bogacz, R. (2014). Effective connectivity of the subthalamic nucleus - globus pallidus network during Parkinsonian oscillations. The Journal of Physiology, 7, 1429–1455. http://doi.org/10.1113/jphysiol.2013.259721

130.Hamani, C., Saint-Cyr, J. a., Fraser, J., Kaplitt, M., & Lozano, A. M. (2004). The subthalamic nucleus in the context of movement disorders. Brain, 127(1), 4–20. http://doi.org/10.1093/brain/awh029

131.Saunders, A., Oldenburg, I. a, Berezovskii, V. K., Johnson, C. a, Kingery, N. D., Elliott, H. L., … Sabatini, B. L. (2015). A direct GABAergic output from the basal ganglia to frontal cortex. Nature, 05, [In Press]. http://doi.org/10.1038/nature14179

132.Kita, H., & Kitai, S. T. (1987). Efferent projections of the subthalamic nucleus in the rat: light and electron microscopic analysis with the PHA-L method. Journal of Comparative Neurology, 260(3), 435–452. Retrieved from http://www.ncbi.nlm.nih.gov/entrez/query.fcgi?cmd=Retrieve&db=PubMed&dopt=Citation&list_uids=2439552

133.Smith Y, Hzrati, L.N. & Parent,A. (1990) Efferent projections of the sub thalamic nucleus in the squirrel monkey as studied by the PHA-L anterograde tracing method. Journal of Comparative Neurology; 294: 306-23

134.Bromberg-Martin, E. S., Matsumoto, M., & Hikosaka, O. (2010). Dopamine in Motivational Control: Rewarding, Aversive, and Alerting. Neuron. http://doi.org/10.1016/j.neuron.2010.11.022

135.Matsumoto, M., & Hikosaka, O. (2009). Two types of dopamine neuron distinctly convey positive and negative motivational signals. Nature, 459(7248), 837–841. http://doi.org/10.1038/nature08028

136.Hikosaka, O. (2007). GABAergic output of the basal ganglia. Progress in Brain Research. http://doi.org/10.1016/S0079-6123(06)60012-5

137.Hoover, J. E., & Strick, P. L. (1993). Multiple output channels in the basal ganglia. Science (New York, N.Y.), 259(5096), 819–821. http://doi.org/10.1126/science.7679223

138.Abbott, L. F., Varela, J. A., Sen, K., & Nelson, S. B. (1997). Synaptic depression and cortical gain control. Science (New York, N.Y.), 275(5297), 220–224. http://doi.org/10.1126/science.275.5297.221

139.Montague, P. R., McClure, S. M., Baldwin, P. R., Phillips, P. E. M., Budygin, E. A., Stuber, G. D., … Wightman, R. M. (2004). Dynamic gain control of dopamine delivery in freely moving animals. The Journal of Neuroscience : The Official Journal of the Society for Neuroscience, 24(7), 1754–1759. http://doi.org/10.1523/JNEUROSCI.4279-03.2004

140.Surmeier, D. J., Ding, J., Day, M., Wang, Z., & Shen, W. (2007). D1 and D2 dopamine-receptor modulation of striatal glutamatergic signaling in striatal medium spiny neurons. Trends in Neurosciences. http://doi.org/10.1016/j.tins.2007.03.008

141.Surmeier, D. J., Plotkin, J., & Shen, W. (2009). Dopamine and synaptic plasticity in dorsal striatal circuits controlling action selection. Current Opinion in Neurobiology. http://doi.org/10.1016/j.conb.2009.10.003

142.Gerfen, C. R. (1989). The neostriatal mosaic: striatal patch-matrix organization is related to cortical lamination. Science (New York, N.Y.), 246(4928), 385–388. http://doi.org/10.1126/science.2799392

143.Albin, R. L., Young, A. B., & Penney, J. B. (1989). The functional anatomy of basal ganglia disorders. Trends in Neurosciences, 12(10), 366–375. http://doi.org/10.1016/0166-2236(89)90074-X

144.Wilson, C. J., & Groves, P. M. (1980). Fine structure and synaptic connections of the common spiny neuron of the rat neostriatum: a study employing intracellular inject of horseradish peroxidase. The Journal of Comparative Neurology, 194(3), 599–615. http://doi.org/10.1002/cne.901940308

145.Kawaguchi, Y., Wilson, C. J., Augood, S. J., & Emson, P. C. (1995). Striatal interneurones: chemical, physiological and morphological characterization. Trends in Neurosciences, 18(12), 527–535. http://doi.org/10.1016/0166-2236(95)98374-8

146.Oorschot, D. E. (1996). Total number of neurons in the neostriatal, pallidal, subthalamic, and substantia nigral nuclei of the rat basal ganglia: A stereological study using the cavalieri and optical disector methods. Journal of Comparative Neurology, 366(4), 580–599. http://doi.org/10.1002/(SICI)1096-9861(19960318)366:4<580::AID-CNE3>3.0.CO;2-0

147.Somogyi, P., Bolam, J. P., & Smith, A. D. (1981). Monosynaptic cortical input and local axon collaterals of identified striatonigral neurons. A light and electron microscopic study using the Golgi-peroxidase transport-degeneration procedure. The Journal of Comparative Neurology, 195(4), 567–584. http://doi.org/10.1002/cne.901950403

148.DeLong, M. R. (1990). Primate models of movement disorders of basal ganglia origin. Trends in Neurosciences, 13(7), 281–285. http://doi.org/10.1016/0166-2236(90)90110-V

149.Kravitz, A. V, Freeze, B. S., Parker, P. R. L., Kay, K., Thwin, M. T., Deisseroth, K., & Kreitzer, A. C. (2010). Regulation of parkinsonian motor behaviours by optogenetic control of basal ganglia circuitry. Nature, 466(7306), 622–626. http://doi.org/10.1038/nature09159

150.Kawaguchi, Y. (1993). Physiological, morphological, and histochemical characterization of three classes of interneurons in rat neostriatum. The Journal of Neuroscience, 13(11), 4908–4923. http://doi.org/10.1016/S0921-8696(05)81133-8

151.Bolam, J. P., Wainer, B. H., & Smith, A. D. (1984). Characterization of cholinergic neurons in the rat neostriatum. A combination of choline acetyltransferase immunocytochemistry, Golgi-impregnation and electron microscopy. Neuroscience, 12(3), 711–718. http://doi.org/10.1016/0306-4522(84)90165-9

152.Rivera, A., Alberti, I., Martín, A. B., Narváez, J. A., De la Calle, A., & Moratalla, R. (2002). Molecular phenotype of rat striatal neurons expressing the dopamine D5 receptor subtype. European Journal of Neuroscience, 16(11), 2049–2058. http://doi.org/10.1046/j.1460-9568.2002.02280.x

153.Yan, Z., Song, W. J., & Surmeier, J. (1997). D2 dopamine receptors reduce N-type Ca2+ currents in rat neostriatal cholinergic interneurons through a membrane-delimited, protein-kinase-C-insensitive pathway. Journal of Neurophysiology, 77(2), 1003–1015.

154.Kubota, Y., Mikawa, S., & Kawaguchi, Y. (1993). Neostriatal GABAergic interneurones contain NOS, calretinin or parvalbumin. Neuroreport. http://doi.org/10.1097/00001756-199312000-00004

155.Koós, T., & Tepper, J. M. (1999). Inhibitory control of neostriatal projection neurons by GABAergic interneurons. Nature Neuroscience, 2(5), 467–472. http://doi.org/10.1038/8138

156.Wang, Z., Kai, L., Day, M., Ronesi, J., Yin, H. H., Ding, J., … Surmeier, D. J. (2006). Dopaminergic Control of Corticostriatal Long-Term Synaptic Depression in Medium Spiny Neurons Is Mediated by Cholinergic Interneurons. Neuron, 50(3), 443–452. http://doi.org/10.1016/j.neuron.2006.04.010

157.English, D. F., Ibanez-Sandoval, O., Stark, E., Tecuapetla, F., Buzsáki, G., Deisseroth, K., … Koos, T. (2011). GABAergic circuits mediate the

reinforcement-related signals of striatal cholinergic interneurons. Nature Neuroscience. http://doi.org/10.1038/nn.2984

158.Morris, G., Arkadir, D., Nevet, A., Vaadia, E., & Bergman, H. (2004). Coincident but distinct messages of midbrain dopamine and striatal tonically active neurons. Neuron, 43(1), 133–143. http://doi.org/10.1016/j.neuron.2004.06.012

159.Benhamou, L., Kehat, O., & Cohen, D. (2014). Firing pattern characteristics of tonically active neurons in rat striatum: context dependent or species divergent? The Journal of Neuroscience : The Official Journal of the Society for Neuroscience, 34(6), 2299–304. http://doi.org/10.1523/JNEUROSCI.1798-13.2014

160.Mahon, S., Vautrelle, N., Pezard, L., Slaght, S. J., Deniau, J.-M., Chouvet, G., & Charpier, S. (2006). Distinct patterns of striatal medium spiny neuron activity during the natural sleep-wake cycle. The Journal of Neuroscience : The Official Journal of the Society for Neuroscience, 26(48), 12587–12595. http://doi.org/10.1523/JNEUROSCI.3987-06.2006

161.Jin, X., and Costa, R.M. (2010). Start/stop signals emerge in nigrostriatal circuits during sequence learning. Nature 466, 457-462.

162.Quian Quiroga, R., & Panzeri, S. (2009). Extracting information from neuronal populations: information theory and decoding approaches. Nature Reviews. Neuroscience, 10(3), 173–185. http://doi.org/10.1038/nrn2578

163.Britten, K. H., Shadlen, M. N., Newsome, W. T., & Movshon, J. A. (1992). The analysis of visual motion: a comparison of neuronal and psychophysical performance. The Journal of Neuroscience, 12(12), 4745–4765. http://doi.org/10.1.1.123.9899

164.Shpigelman, L., Singer, Y., Paz, R., & Vaadia, E. (2005). Spikernels: predicting arm movements by embedding population spike rate patterns in inner-product spaces. Neural Computation, 17(3), 671–90. http://doi.org/10.1162/0899766053019944

165.Jazayeri, M. (2008). Probabilistic sensory recoding. Current Opinion in Neurobiology. http://doi.org/10.1016/j.conb.2008.09.004

166.Brooks, R. a. (1990). Elephants don't play chess. Robotics and Autonomous Systems, 6(1-2), 3–15. http://doi.org/10.1016/S0921-8890(05)80025-9

167.Critchley, H. D., & Harrison, N. a. (2013). Visceral Influences on Brain and Behavior. Neuron, 77(4), 624–638. http://doi.org/10.1016/j.neuron.2013.02.008

168.Wilson, A. D., & Golonka, S. (2013). Embodied Cognition is Not What you Think it is. Frontiers in Psychology, 4(February), 58. http://doi.org/10.3389/fpsyg.2013.00058

169.Altmann, J. (1974). Observational study of behavior: sampling methods. Behaviour, 49(3), 227–267. http://doi.org/10.1163/156853974X00534

170. Dell, A. I., Bender, J. a., Branson, K., Couzin, I. D., de Polavieja, G. G., Noldus, L. P. J. J., … Brose, U. (2014). Automated image-based tracking and its application in ecology. Trends in Ecology and Evolution, 29(7), 417–428. http://doi.org/10.1016/j.tree.2014.05.004

CHAPTER 2: A scalable population code for time in the striatum

All data discussed in this chapter was published as the following publication: Mello, G. B. M., Soares, S., & Paton, J. J. (2015). A Scalable Population Code for Time in the Striatum. *Current Biology*, *25*(9), 1113–1122. http://doi.org/10.1016/j.cub.2015.02.036

SUMMARY

To guide behavior and learn from its consequences, the brain must represent time over many scales. Yet, the neural signals used to encode time in the seconds to minute range are not known. The striatum is a major input area of the basal ganglia associated with learning and motor function. Previous studies have also shown that the striatum is necessary for normal timing behavior. To address how striatal signals might be involved in timing, we recorded from striatal neurons in rats performing an interval timing task. We found that neurons fired at delays spanning tens of seconds and that this pattern of responding reflected the interaction between time and the animals' ongoing sensorimotor state. Surprisingly, cells rescaled responses in time when intervals changed, indicating that striatal populations encoded relative time. Moreover, time estimates decoded from activity predicted timing behavior as animals adjusted to new intervals, and disrupting striatal function led to a decrease in timing performance. These results suggest that striatal activity forms a scalable population code for time, providing timing signals that animals use to guide their actions.

INTRODUCTION

To behave adaptively in ever-changing environments animals must learn which actions to take in a particular context based on their past experience. However, to learn about the sometimes delayed consequences of actions and to guide future behavior, it is absolutely necessary that the brain represents not only

actions and consequences, but also temporal information about when those actions and consequences occur [1].

Multiple lines of evidence implicate the Basal Ganglia (BG) as a locus for the representation of such temporal information. Lesions of the striatum [2], disease states that affect the BG such as Parkinson's [3] and Huntington's disease [4], drugs that affect dopamine (DA) signaling [5] , and genetic manipulations that affect the DA system in the BG [6] all cause interval timing dysfunction. Furthermore, human functional magnetic resonance imaging studies have found that the striatum, a main input area of the BG, is activated by tasks that involve the processing of interval information [7,8].

In addition, many theoretical models have been proposed to explain timing behavior. These models can be grouped into at least three categories. Pacemaker-accumulator models integrate pulses emitted from a central pacemaker to measure elapsed time [9,10]. Beat frequency models detect patterns of activation across re-settable oscillatory processes at different frequencies to encode time delays from some resetting event [11]. Sequential state models contain orderly transitions between different activity states that can be used to encode time [12-14]. These theories reproduce various aspects of timing behavior in many interval timing tasks. However, neural data in conflict or in support of the various theories is lacking.

To understand how time is encoded in neural circuits, we recorded the spiking activity of neurons as rats performed an interval timing task. Specifically, given the apparent localization of timing function in striatal tissue, we asked whether striatal neural activity could encode elapsed time over durations of tens of seconds to one minute while we measured behavior that reflected animals' estimates of time.

We found that different striatal neurons fired maximally at different delays from reward receipt, and that information about animals' time estimates could be extracted from striatal populations by simply treating neurons as tuned for time. Importantly, this tuning for time, while affected by sensorimotor event-related neural responses, could not be fully explained by ongoing behavior, as even cells that displayed responses locked to a specific behavior varied their responses depending on when that behavior was executed within a given

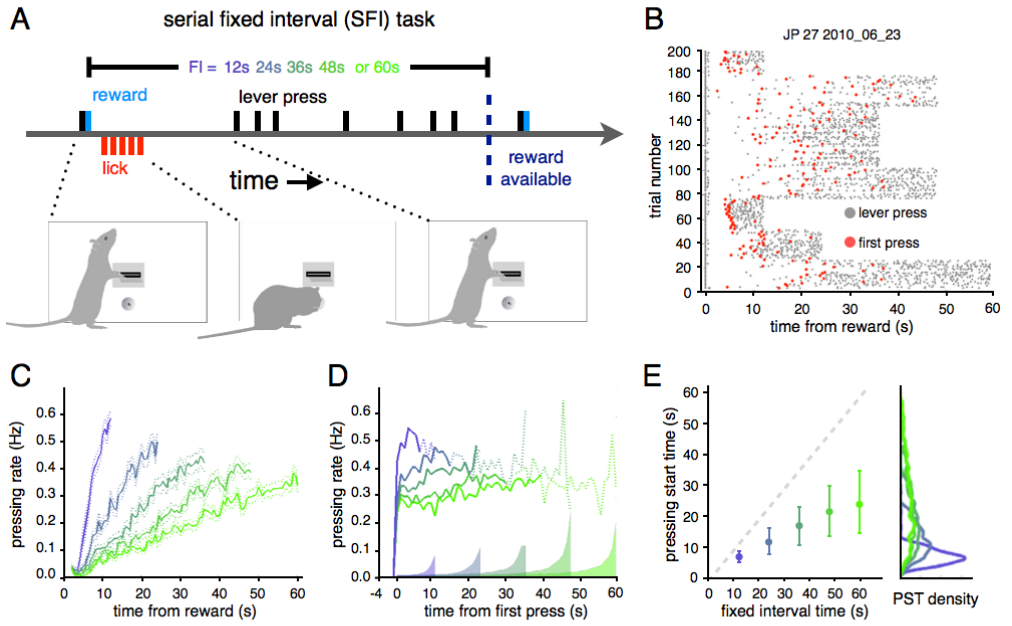

Figure 2.1 | The SFI task produces systematic changes in lever pressing start time (PST). (**A**) Task structure. The following color code will be commonly used: blue represents short FIs and green represents longer FIs. (**B**) Example of lever pressing behavior in a single session of the SFI task. Grey markers indicate a lever press, red markers indicate the PST. (**C**) Average lever pressing rate in each of the five FIs, aligned with preceding reward. Dashed lines represent SEM. (**D**) Average rate of lever pressing in each block, aligned with PST. Traces are plotted in a solid line for the period for which more than half of the trials contribute data, and a dotted line after that point. Shaded patches along the horizontal axis represent SEM. Bins of 1 second in (C) and (D). (**E**) Median and interquartile range of PST for each of the five FIs. Smoothed density functions depicting the full distributions of PST are shown on the right. See also Figure S2.1.

interval. Strikingly, we found that temporal tuning stretched or contracted, rescaling with the interval being timed. Thus, striatal populations encoded relative time, flexibly adapting to the immediate demands of the environment. These results provide important biological insight into how a major brain system encodes time during behavior.

RESULTS

Lever pressing start time under fixed interval reinforcement schedules is a behavioral measure of rats' expectation of time until reward

To elicit robust time-dependent behavior over a broad range of timescales we employed operant conditioning procedures under fixed interval (FI) schedules of reinforcement (Figure 2.1A). Briefly, rats were placed in a behavioral box containing a lever positioned over a liquid delivery port and were trained to press the lever to receive water reward. Reward delivery triggered a timer and reward became available again only after the timer exceeded a FI ranging from 12s to 60s in multiples of 12s. Lever presses occurring after reward delivery but before the FI had elapsed were not reinforced. A FI was maintained for between 18 and 40 rewards before changing to another FI, randomly chosen from the interval set.

On single sessions, rats tended to distribute lever pressing toward the latter portion of the FI, shifting when they responded as FI changes occurred (Figure 2.1B, S2.1A). This pattern of responding produced ramps in block-wise averaged pressing as a function of time that varied in slope in relation to FI (Figure 2.1C, S2.1B). However, this did not reflect the pattern of responding on single trials. We asked how pressing evolved after pressing onset (pressing start times, PST) on each trial by aligning on the PST and averaging lever press rates across trials and within blocks of the same FI (Figure 2.1D). Rats pressed at a relatively constant rate after the first press on each trial, with a rate determined by the experienced reward rate (Figure S2.1C). The ramps in the reward-aligned pressing as a function of time largely result from changing distributions of PSTs (Figure 2.1E), as these vary systematically with FI, and averaging a group of step functions with onset times drawn from these distributions will produce ramps of varying slope.

This serial fixed interval (SFI) lever pressing task produced systematic variation in the distributions of PSTs of bouts of anticipatory pressing, consistent with previous timing studies employing FI schedules of reinforcement [9]. These bouts were of a relatively constant rate that varied with reward rate over time (Figure 2.1D, S2.1C). The PST thus provided a behavioral metric that covaried with the animals' changing expectation about

time until the next available reward, which we compared to the activity of neurons recorded in the striatum during performance of the task as described below.

Striatal neurons display temporal tuning

In the SFI task, reward delivery was both the timing cue, and the reinforcer. Since animals reported knowledge of time between reward availability by when they began to press a lever, we asked whether neuronal responses in the striatum aligned with reward might reveal a signal that animals could use to guide the decision of when to begin pressing. We recorded broadly in the dorsal striatum, so as to sample neurons from regions previously shown to be important for interval timing behavior [2] (inset in Figure S2.1D), and the vast majority of units we recorded exhibited average firing rates of less than five spikes per second, consistent with a population made up of mostly medium spiny projection neurons ([15]; Figure S2.1D).

Aligned with reward delivery, the population of recorded cells exhibited a broad distribution of activity patterns, as reflected in the normalized spike density functions (SDF, see Methods for details) shown in Figure 2.2A. Some cells fired just after reward delivery, others in the middle of the delay, others leading up to the next reward (Figure 2.2A, S2.2 and S2.3). This produced a

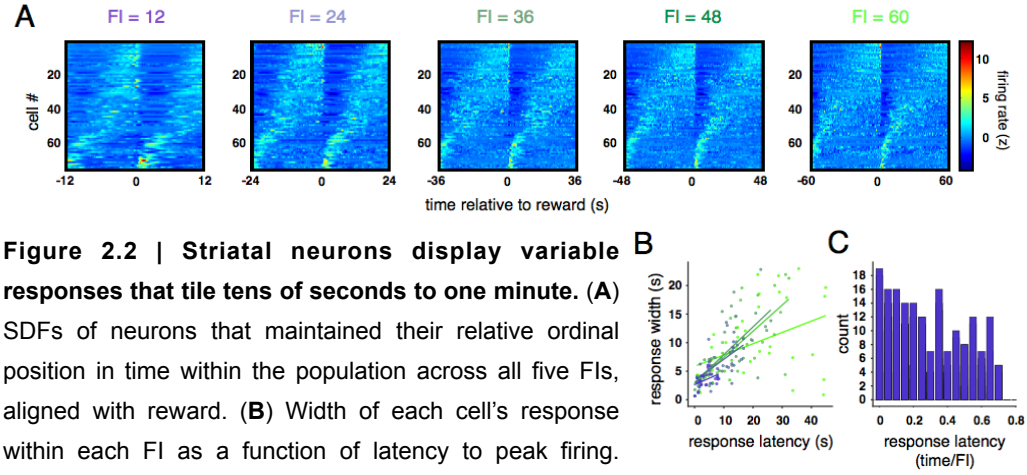

Figure 2.2 | Striatal neurons display variable responses that tile tens of seconds to one minute. (**A**) SDFs of neurons that maintained their relative ordinal position in time within the population across all five FIs, aligned with reward. (**B**) Width of each cell's response within each FI as a function of latency to peak firing. Colored lines represent the best linear fit to the data. (**C**) Histogram of relative peak latencies pooled over all FIs, using data shown in (B) See also Figure S2.2.

slow moving “bump” of activity that traversed the population during each FI. In theory, reading out the location of this bump in the population could provide an estimate of time within the FI. However, a core feature of interval timing behavior is that timing accuracy decreases with the magnitude of the interval being timed [9]. Two features of the neural data could potentially contribute to this phenomenon: an increased spread of each neurons’ response as a function of their peak latency, and a decreasing density of neurons displaying peak firing rates as time progresses. We found that the widths of responses were indeed correlated with their latencies to peak firing within each FI (Figure 2.2B, linear regression, FI 12s, $R = 0.4443$, $p < 0.001$; FI 24s, $R = 0.7563$, $p < 0.001$; FI 36s $R = 0.7188$, $p < 0.001$; FI 48s, $R = 0.5910$, $p < 0.001$; FI 60s $R = 0.4733$, $p < 0.001$, see Methods). In addition, the density of peak firing rate latencies in our population decreased over time within the FI (Figure 2.2C). Thus, the bump in activity within the striatum population moved progressively slower as the FI wore on. Strikingly, the overall time taken by this bump to traverse the population appeared to scale with the FI (Figure 2.2A, S2.4A). To begin to assess apparent scaling of response times, we first selected cells that we had recorded in all five FIs and that maintained their ordinal position within the population when responses within each FI were ordered by firing dynamics [16]. Of the 112 neurons recorded in all FIs, we found that 76 neurons (68%) maintained their ordinal position in time across the population (see Methods for details). The responses of these neurons can be observed in Figure 2.2A, wherein the position of cells along the y axis is the same across the panels displaying average responses in each of the FIs (for all recorded cells, see Figure S2.4A).

To quantify to what degree responses rescaled, we computed a scale factor for each neuron as the ratio of the center of mass (COM) of the SDF in the 12s FI over the COM of the SDF in each of the other four FIs (Figure 2.3A). The distributions of these scale factors were sharper than and significantly different from null distributions generated by shuffling cell identity across FIs and recomputing the scale factors (red distributions in Figure 2.3A, Kolmogorov-Smirnov test, $p < 0.001$ for all pairwise comparisons). The medians of these distributions, were the population to have rescaled its

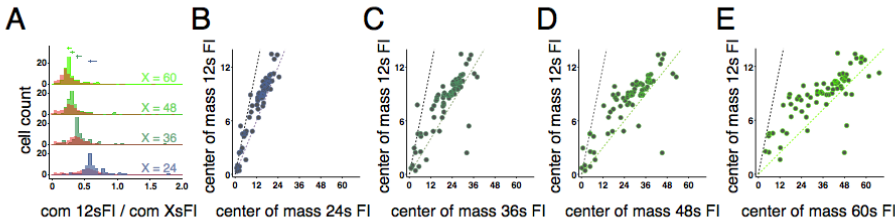

Figure 2.3 | Striatal neurons rescale their response time with FI. (**A**) Distributions of scale factors obtained by calculating the ratio of the center of mass (COM) of the SDF between the 12s FI and Xs FI (24s, 36s, 48s, and 60s, respectively, from blue to green) for each cell. For each distribution of scale factors a null distribution was generated by shuffling cell identity across FIs and recomputing the scale factors (red). (**B, C**, **D**, **E**) COM of each cell's SDF in the 12 second FI against each that of the other FIs. The black dotted line signifies no change in COM from block to block. The colored dotted line signifies a change in COM that is proportional to the change in FI relative to the 12s FI. See also Figure S2.3.

responses in direct proportion to the FI, should lie at 1/2, 1/3, 1/4, and 1/5 for the scale factors corresponding to 12/24, 12/36, 12/48, and 12/60s FIs, respectively. We observed median values of 0.59, 0.39, 0.30, 0.24, for the corresponding distributions, indicating near-proportional rescaling of response times across the recorded striatal population. A more complete description of the relative scale of responses can be seen in Figures 2.3B-E, where the COM of each cell's SDF in the 12s FI against each that of the other FIs are displayed. These data demonstrate a strong tendency for rescaling of neural responses across the population suggesting that the state of striatal populations may convey relative elapsed time information scaled to the animal's estimate of the current behaviorally relevant timescale in the environment. We explore this hypothesis in greater detail below.

Striatal populations encode information about timing behavior

The above analyses of striatal neural responses indicate a correspondence between striatal activity and timing behavior across trial blocks, suggesting that striatal activity patterns might guide decisions about when to begin pressing the lever during each FI. To test this hypothesis, we applied a decoding approach to data collected from single trials near block transitions, wherein animals systematically changed the time that they began to press the lever. Specifically, we asked three questions. Firstly, we asked whether decoded time

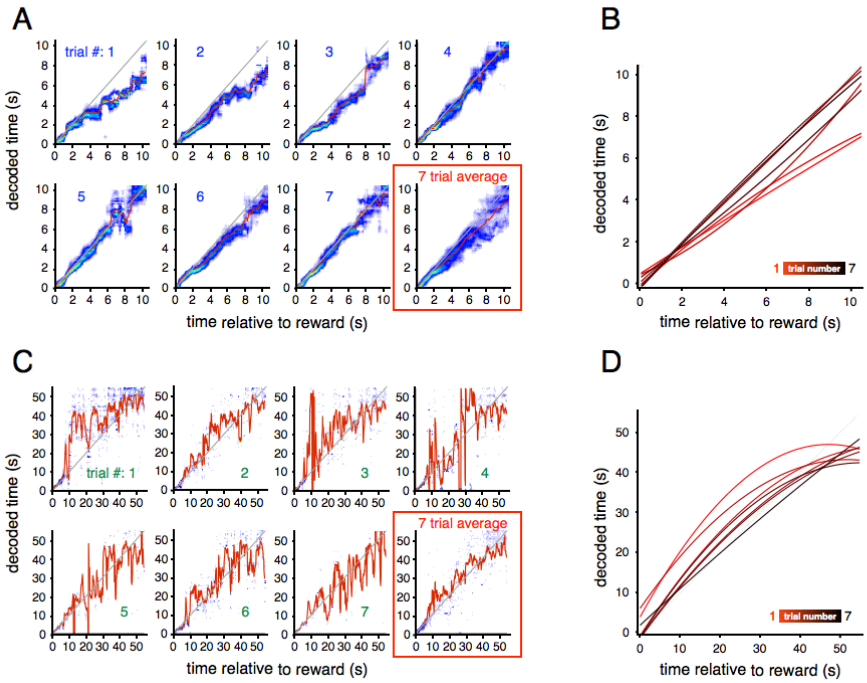

Figure 2.4 | Single trial estimates of elapsed time decoded from the population response correlate with true time during initial trials of 12s and 60s FI blocks. (**A**) Decoded population estimates of elapsed time from reward on single trials, for the first 7 trials of the 12s FI block plotted against true time. Red traces indicate the mean of the population likelihood function, and the underlying heat map indicates the population likelihood function. The last panel shows a 7 trial average likelihood function using the first 7 trials of the 12s block. (**B**) Decoded estimates of elapsed time for the first 7 trials of the 12s FI block plotted in the same axis. Curves are quadratic fits to the mean likelihood function of each individual trial (red lines in first 7 panels). Red curves represent early trials and black curves represent later trials. (**C**) Same description as in (A) but for the 60s FI. (**D**) Same description as in (B) but for the 60s FI. See also Figure S2.4.

estimates covaried with true time. Secondly, we asked whether systematic errors in estimated time as compared to true time occurred at these block transitions. Lastly, we asked whether any observed errors in time encoding correlated with timing behavior.

We first built a probabilistic decoder to derive an estimate of elapsed time from reward on single trials given the observed spiking response of the population. We focused on the first trials of the 12s and the 60s FI blocks because these blocks were the shortest and longest FIs employed, respectively. Thus, animals consistently over- and underestimated the amount of time remaining until reward as they entered 12s and 60s blocks. Briefly, our

decoder was constructed as follows. On each of the first 7 trials of a block, we counted spikes within defined time bins and asked how likely we were to have observed that number of spikes at each time given the observed distributions of spike counts on trials 8 onward of the corresponding block. This generated a likelihood function for current time given an observed spike count in each bin, for each individual cell. To derive a measure of the population's estimate of the likelihood for current time, we multiplied together the individual cells' likelihood functions. We then took the mean of this likelihood function as our estimate for current time [17].

In Figure 2.4A and 2.4C we display decoded estimates as a function of time for the first 7 trials of 12s and 60s FI blocks. We found that decoded estimates tracked true time, but that systematic errors between estimates and true time were present in the first few trials of the 12s and 60s FI blocks. This feature can be observed more readily when estimates derived from multiple trials are plotted on the same axes (Figures 2.4B, 2.4D, quadratic fits). Initial estimates are relatively slow and fast on the first trials of the 12s and 60s FI blocks respectively, and become more accurate after the first few trials.

Next we asked whether such timing signals may be used by animals to guide timing behavior. We first asked if errors in decoded time estimates over the first trials of blocks were correlated with timing behavior. We found that the mean PST was significantly correlated with the errors in time estimates derived from the population over the first seven trials of 12s and 60s FI blocks (Figure 2.5, FI=12 R2 = 0.63, p = 0.03, FI=60, R2 = 0.64, p = 0.03). On the initial trials of the 12s FI block, rats began pressing late relative to subsequent trials, and likewise the decoded estimate of time relative to reward ran slow (Figures 2.4B and 2.5). The first trials of the 60s FI block showed a similar relationship, yet

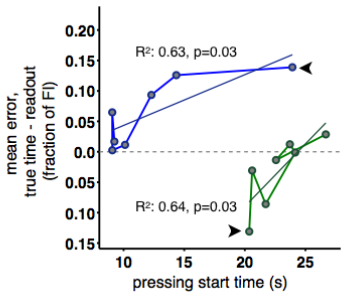

Figure 2.5 | Errors in decoded time predicted timing behavior. Mean error between true time and the decoded population estimate on the first seven trials of the 12s (blue) and 60s (green) FI blocks. Contiguous trials are connected by solid lines to display the trajectory of the data over trials, and the first trial on each block is indicated by the black arrow. Dashed horizontal gray line represents zero error average decoding as compared to true time. See also Figure S2.5.

opposite in direction: the decoded estimate ran quickly on early trials, and rats were early to press (Figures 2.4D and 2.5). We then tested in two control animals whether manipulating striatal circuitry via bilateral infusions of the GABAa agonist muscimol produced deficits in timing behavior (Figure S2.5). Indeed, at a dose that rendered rats able to perform the task, muscimol reversibly and significantly diminished the relationship between PST and FI (linear regression, likelihood ratio test, significant effect of treatment, $p < 0.001$), showing that a normally functioning striatum is critical for normal timing behavior. The consistency between time estimates decoded from striatal populations, and trial-by-trial variations in timing behavior at block transitions, together with observed dependence of a normally functioning striatum for normal timing behavior, suggested that the brain used a population code for time that samples broadly from striatal neurons to guide decisions about when to act.

Striatal neurons multiplexed information about action and time.

Based on previous studies [18-20], we expected that striatal neurons would display significant modulation by behaviors during the FI. Could behaviors that accompany task performance fully explain the sequential neural responses we have observed? Several features of the data argued against this possibility. Rats consistently licked at the reward port from 0.5s to 5.5s after reward delivery (Figure S2.4B), and yet our ability to decode time was unaffected by the animal being engaged in a fixed behavior over this time (see initial ~5s of decoded time estimates in Figures 2.4A and 2.4C). After departing from the reward port, however, it was possible that observed dynamics in neural responses were accounted for by ongoing behaviors. If it were the case, responses related to a particular behavior should not vary depending on when in a trial the rat engaged in that behavior. To identify neurons that were significantly modulated by a measured behavior in our task, we focused on a 2.5 seconds centered on the PST in each trial. We found that of the 76 neurons displayed in Figure 2.2A, 31 exhibited significant modulations around the onset of lever pressing. Next we asked if spiking observed in time bins aligned with the PST was additionally correlated with the time, relative to the FI, that

pressing onset occurred. More than half of pressing onset modulated neurons (16/31, 52%) displayed a significant correlation between spiking around each press initiation and the relative time that press onset occurred within the FI (Pearson's linear regression, $p < 0.01$). Figures 2.6A-D show examples of four such neurons from three different animals, all of which vary in their responses around the PST, from none at all to robust firing.

The regression approach described above is only expected to identify neurons that display a monotonic relationship between pressing onset response and the relative time of pressing onset. Other cells may have displayed significant time-dependent modulations in pressing onset response

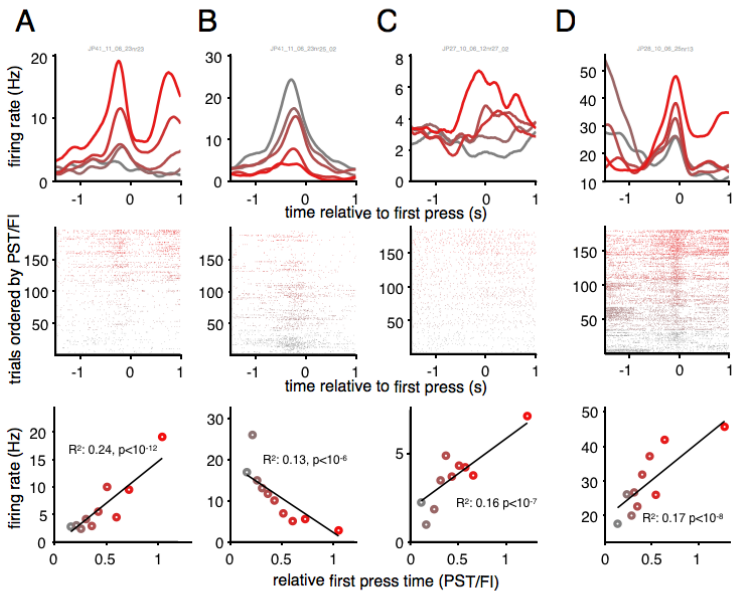

Figure 2.6 | Pressing onset responsive neurons display sensitivity to the time relative to the FIs. (**A**-**D**) Four single neuron peri-stimulus time histograms (top) and raster plots (middle) of 2.5 second periods aligned with pressing onset event (from three animals, the first two columns display data from two neurons recorded in the same animal and same session). Trials were sorted in ascendent fashion from bottom to top in the vertical axis by the pressing onset time relative to the FI (middle) and grouped into quintiles. Here, the colors from grey to red represent the 1st to the 5th quintile, respectively (middle and top panels). (**A**-**D** bottom) Correlation between the firing rate of the respective neuron and the time of the pressing onset relative to FI. Each datapoint is color coded from grey to red for the 1st to the 10th decile of the relative pressing onset time. Firing rates were extracted from the most modulated 500 ms bin of the 4 bins surrounding the pressing onset event.

that were not monotonic (for example, see Figures S2.2B and S2.3A). To identify such cells, we asked whether the median of distributions of spikes counts, collected around pressing onsets and falling into each of five quintiles of relative PSTs, differed from each other. We found that 53 out of 76 neurons (70%) displayed in Figure 2.2A exhibited significantly different median spike counts across relative time within the FI ($p < 0.01$, Kruskal-Wallis). Of these, 9 cells were significantly modulated by the onset of lever pressing and were not identified in the linear regression analysis. Overall, only 6 cells that displayed response modulation around PST did not exhibit additional modulation by relative time in the FI as assessed by linear regression and/or nonparametric testing for median difference in spike count. These results suggest that striatal neurons multiplex information about time and immediate sensorimotor state of the animal, and argue strongly against the possibility that the striatal population responses we observed can be explained by purely non time-related responses to specific sensory or motor components of ongoing behavior.

DISCUSSION

Time is a fundamental dimension of animals' experience in the world. As such, it plays an integral role in many brain processes from perception, to motor control, to learning and memory formation. What is the role of temporal representation within the BG? A dominant view supported by a wide range of neurobiological data posits that the BG implement aspects of reinforcement learning (RL) [1,20,22-25], learning how an organism ought to act in order to maximize reward. However, to learn about the sometimes delayed consequences of actions and to guide future behavior towards rewarding outcomes, it is necessary that the brain represent situations and actions through time [1,26]. Indeed, temporal relations amongst actions and events contain the causal information that learning systems have evolved to detect through a process sometimes referred to as credit assignment [27]. Once credit for the occurrence of predictable events has been assigned, this information must be used to profitably guide the course and timing of action as situations arise. This continuous learning-behaving cycle is what RL algorithms naturally account for [26]. And yet, it is not known how the BG, the brain

system most often associated with RL, represents temporal relationships over the durations necessary to explain its role in animal learning and behavior.

The sequential neural states that we described in the striatum during timing behavior could provide a unifying view of the BG's role in timing and RL. These signals are similar to temporal basis functions proposed in existing learning models as more neurally plausible and efficient representations of time [21,28,29]. Such models operate by learning a set of weights used in a weighted sum of the temporal bases to construct a moment by moment prediction about future events such as expected reward. In theory a weighted combination of activity patterns in the cortical or thalamic inputs to the striatum could act as such temporal bases and modulate the responses of striatal neurons that we observed. Despite the similarity between our data and the basis functions proposed by RL models discussed, It is not clear that our data can be used to generate timing behavior similar to what we observed experimentally. Our data suggest that striatal activity multiplexes information about behavior and time. It might be the case that behavioral contributions to the timing signal disrupt temporal information. This issue can be addressed by modeling the striatal signals we observed and integrating them as basis functions into a RL model that performs the SFI task.

An important question for future studies concerns the mechanism that generated the striatal dynamics we observed. Although several modeling studies suggest mechanisms for generating sequential activity states using striatum-like circuitry over shorter timescales [30]; given the duration of the intervals we examined, we find it unlikely that striatal dynamics were purely locally generated. Indeed the signals we used to decode time were affected, but not fully explained by, the ongoing sensorimotor state of the animal. Thus, our decoding approach implicitly endorses a number of prominent interval timing theories positing that animals may use behavioral [12,14] or sensory state [31] transitions to learn to time events in the environment and their own behavior.

Our data appears most consistent with theoretical models that suggest distributed representations of time encoded by the joint activity of populations of neurons [32]. Indeed, the decoder used in the current study assumes that

time information might be present in many different neurons. However, we cannot rule out that there may exist other forms of temporal representations upstream from the population we recorded in the striatum. For instance, an accumulating process such as the one contained within pacemaker accumulator models Gibbon [9] might act to trigger neurons to become active at different delays as the accumulator passes a series of thresholds.

We showed that sequential neural activation in the striatum could be used to encode time on a scale of tens of seconds up to one minute. These results added to a growing list of studies that demonstrate sequential activation of neurons over multi-second timescales in other brain areas such as the hippocampus [33,34], the cerebellum [32], and the parietal [35] and prefrontal cortex [36-38]. Unlike previous studies, we found that many individual striatal neurons exhibited responses that dynamically rescaled with the timing of events in the environment and that this scaling of responses produced changes in time encoding by the population that correlated with timing behavior. Combined with previous studies highlighting the importance of a normally functioning striatum for timing behavior [2-4,6], the effect of striatal inactivation in the current study, and other work that demonstrated time encoding by striatal populations over shorter timescales [39], our results suggest that information about where in time a subject finds itself relative to anticipated events in the environment is present in populations of striatal neurons and is used to guide behavior.

Similar timing signals observed in areas other than the striatum are viewed within the larger context of the functional role of those areas where they were recorded. Timing signals in the hippocampus might endow explicit memories with accurate information about the order and temporal context of events [40], and timing signals in the cerebellum might coordinate learned actions at a fine timescale [32], while timing signals in premotor cortex might enable accurate timing of movement in general [39]. The striatal neurons we observed appear to multiplex temporal information with other, non-temporal types of information, such as signals related to the ongoing sensorimotor state of the animal, and likely other previously identified striatal signals related to actions, motor sequences, or reinforcement [19,23-25]. Such multiplexing of

temporal and other information in populations of striatal neurons as observed in the current study is likely to be critical to the previously ascribed and often studied function of the BG in learning and action selection.

METHODS

Behavior

Five male Long-Evans hooded rats were trained in an operant lever pressing paradigm reinforced with 0.015mL of water on a fixed interval (FI) reinforcement schedule (Figure 2.1A). The FI was varied randomly in blocks of >= 18 trials among five intervals ranging in multiples of 12 from 12s to 60s. A real-time LINUX state machine directed by custom software in MATLAB (bcontrol/mathworks) controlled the task. To remove incidental lever depressions that sometimes occurred as animals explored the box, pressing start time (PST) was computed as the first press on each trial where the interval until the next press fell below the 85th percentile of the inter-press interval distribution of the entire session.

Neurophysiology

Movable arrays of 32 tungsten microwires (CD neural systems) were implanted unilaterally in the striatum under isoflurane anesthesia. Neural signals recorded during behavior were amplified and high pass filtered at 100 Hz or 250 Hz (i2smicro), and waveforms corresponding to action potentials from single neurons were sorted offline using principal components analysis (PCA) (offline sorter, Plexon). All isolated units (179 total from 5 rats, 25 R1, 9 R2, 21 R3, 28 R4, 96 R5) recorded for at least three blocks in sessions in which PSTs correlated significantly with FI ($p < 0.05$) were included in subsequent analyses.

To construct spike density functions (SDF), spikes were counted in bins of 20 ms. This histogram was then divided by the number of trials, smoothed with a half gaussian kernel with a standard deviation of 500 ms, and z-scored by subtracting the mean and dividing by the standard deviation of the time series.

We applied principal component analysis (PCA) to the SDFs of all recorded neurons within each FI separately (Figure S2.4A), or the concatenated SDFs of a subset of neurons across all FIs together (Figure 2.2A). SDFs were aligned with reward, including activity from reward delivery minus one FI to reward delivery plus one FI. As has been done previously, we applied an ordering procedure wherein SDFs were ordered by their angular position within a plane defined by the contributions made by the first two PCs to SDFs, rotating around the origin [16]. This method has the advantage that it orders cells with respect to their dynamics while taking into account the full firing profile of each neuron over time, as opposed to methods that order by peak response time that only take into account one moment in the cell's average firing profile.

Selection for cells with consistent relative response profiles

To identify cells that maintained their position in the population across the FIs we performed the following selection. First, The PCA-based ordering process was applied to all neurons that were recorded in all five FIs (n = 112). Importantly, for this analysis PCA was run separately on data collected in each FI so that each cell's ordered position within the population was free to change across FI. Next, each within-FI position was converted to a unit vector, at an angle determined by its ordered position. These unit vectors were then averaged, and those average vectors with a length of 0.75 or greater (n = 76/112, 68%) were identified as having consistent ordinal positions within the population across FIs.

Scale factors

To quantify the temporal rescaling observed in striatal neurons across the different FIs, we computed a scale factor for each neuron in the 24s, 36s, 48s, and 60s FIs as the ratio of the center of mass of neural firing in the 12s FI, over the center of mass of neural firing in each of the four other FIs (Figure 2.3). We then generated null distributions by recomputing scale factors using the same data but where scale factors were repeatedly computed across cells instead of within single cells (100 repetitions). We then tested for significant differences

between the data distributions and the null distributions for each of the four sets of ratios using a Kolmogorov-Smirnov test ($p < 0.001$).

Latency and width of responses

To quantify the latency and the spread of the observed striatal responses (Figure 2.2B), we estimated the time of the peak firing rate in each FI and the width at its half-height from a smoothed peri-stimulus time histogram (PSTH) aligned with reward delivery. 10 ms bins were used to build the PSTH, smoothed with a gaussian kernel with a standard deviation that was inversely proportional to the median firing rate of the neuron (sd = 11/median firing rate). We selected the firing mode as the time of the peak of the smoothed PSTH, and the width of the peak at the half height between the trough (minimum) and the peak (maximum) of the smoothed PSTH as our measure of spread. To prevent edge effects, peaks occurring later than three quarters of the FI were removed from the analysis. We asked whether each cell's spread was correlated with its delay to peak firing by linear regression. (FI 12s, $R = 0.4443$, $p < 0.001$; FI 24s, $R = 0.7563$, $p < 0.001$; FI 36s $R = 0.7188$, $p < 0.001$; FI 48s, $R = 0.5910$, $p < 0.001$; FI 60s $R = 0.4733$, $p < 0.001$).

Decoding methods

We built a maximum likelihood (Ml) decoder to estimate current time within our task given the pattern of activity across the population. To best control for conditions across sessions, we focus on the first seven trials of the 12s and 60s FI blocks.

In 12s FI trials, spikes were counted in 1.5s bins beginning with the earlier edge aligned to reward delivery and moved in 100 ms steps until the latter edge reached 12s. In 60s FI trials,spikes were counted in 5s bins beginning with the earlier edge aligned to reward delivery and moved in 100 ms steps until the latter edge reached 60s. Time labels were placed at the earlier edge of the bins. To build distributions of spikes counts used to generate the single cell likelihood functions, $p(t|r)$, meaning the probability of it being any moment in time given the observed spike count, we did the following: first we counted the number of spikes observed for trials 8 onward since a block

switch, and for all time bins. To estimate the underlying probability density we smoothed the resulting histograms using local regression within a window of 30 spikes. We then counted spikes within the same time bins during trials 1 through 7 since the block switch. For each spike count, we determined the likelihood of observing that many spikes in each time bin, given the data from the latter trials. These single cell likelihood functions from every cell recorded (n = 179) were multiplied together to derive a population estimate of current time given the number of spikes observed from each cell in the population. To derive a single estimate from this likelihood function derived from the population, we took the mean [17].

Muscimol infusions

We implanted 24-gauge stainless steel cannulas bilaterally into the striatum of two rats under isoflurane anesthesia. Coordinates: anteroposterior (AP) +2.0mm from bregma; mediolateral (ML) ±2.7mm; dorsoventral (DV) −4.0 mm from the skull surface. After one week of recovery from surgery, rats were allowed to perform the SFI task. Once the rats performed well (5 block switches with significant regression of PST vs. FI) in the SFI task, we injected saline (PBS, 1x), muscimol (GABAa agonist, Sigma™) and saline in three successive days. To perform the injections, rats were anesthetized using 1.5-2.5% isoflurane (v/v). Muscimol or saline solution was delivered using a 1 µl (Hamilton) syringe attached to an injection pump (Harvard Apparatus™, HA11D 702209) through a 24-gauge injector. The injector extended 1.5 mm beyond the tip of the guide cannulas. We used a muscimol concentration of 22.2 ng/µL in saline, injecting 0.6 µL during 2.5 min. The injector was left in place for an additional 1.5 min and the rats were placed for a 45 min recovery period in a home-cage before starting the test session. Both rats received the saline vehicle injections using the same parameters as the muscimol treatment.

Identification of pressing onset related neurons

To identify neurons modulated by the onset of lever pressing, we compared distributions of “test” spike counts in time bins of 500 ms during two

seconds centered on lever pressing onset, to distributions of “baseline” spike counts from 500 ms time bins situated between 2.5 and 1s before lever pressing onset [19]. Baseline time bins consisted of 3 non-overlapping 500 ms time bins, while test time bins consisted of 500 ms bins that were moved in 10 ms steps starting with the trailing edge at 1s before lever pressing onset, until the leading edge met 1s after lever pressing onset. Cells were considered significantly modulated around lever press onset if at least 50 consecutive test bins were significantly different from a baseline distribution constructed by pooling spike counts in the three non-overlapping baseline bins Kruskal-Wallis test, $p < 0.05$).

Identification of press start time modulated neurons

To identify neurons displaying press onset responses that varied additionally with time, we compared observed spike counts in four bins of 500 ms centered on the PST in each trial. Given the observed rescaling in striatal neurons during the task, we first normalized PSTs by dividing each PST by the FI of the block in which it occurred, resulting in fractional PSTs. We then used two methods to identify neurons that exhibited responses aligned with the PST that varied with fractional PST. First we performed linear regression, using fractional PST to predict spike counts in each time bin. We performed an additional analysis to test for differences in median spike count observed across trials that had been binned with respect to fractional PST. Fractional PSTs were separated into five bins, the edges of which corresponded to 0, 20, 40, 60, 80 and 100th percentiles. Responses were considered not to be uniform with respect to fractional PST if trials in at least one bin displayed a median spike count that was significantly different from the rest (Kruskal-Wallis, $p < 0.01$)

AUTHOR CONTRIBUTIONS

G.M. and J.J.P. designed experiments. G.M. and S.S. carried out experiments. G.M., S.S., and J.J.P. analyzed the data and wrote the manuscript.

ACKNOWLEDGEMENTS

We thank Bassam Atallah, Brian Lau, Kenway Louie, Christian Machens, Zachary Mainen, Thiago Gouvêa, Eric DeWitt, Alfonso Renart and Masayoshi Murakami for critical comments on versions of the manuscript and discussions. We thank the Histopathology and the Vivarium staff from the Champalimaud Scientific and Technological Platforms for the support. The work was supported by Champalimaud and Gulbenkian Foundations, and fellowships to G.M. and S.S from the Portuguese Foundation for Science and Technology.

REFERENCES

1. Schultz, W., Dayan, P., & Montague, P. R. (1997). A neural substrate of prediction and reward. Science (New York, N.Y.), 275(5306), 1593–1599. http://doi.org/10.1126/science.275.5306.1593
2. Meck, W. H. (2006). Neuroanatomical localization of an internal clock: A functional link between mesolimbic, nigrostriatal, and mesocortical dopaminergic systems. Brain Research, 1109(1), 93–107. http://doi.org/10.1016/j.brainres.2006.06.031
3. Malapani, C., Rakitin, B., Levy, R., Meck, W. H., Deweer, B., Dubois, B., … J., G. (1998). Coupled temporal memories in Parkinson's disease: a dopamine-related dysfunction. Journal of Cognitive Neuroscience, 10(3), 316–331. http://doi.org/10.1162/089892998562762
4. Rowe, K. C., Paulsen, J. S., Langbehn, D. R., Duff, K., Beglinger, L. J., Wang, C., … Moser, D. J. (2010). Self-paced timing detects and tracks change in prodromal Huntington disease. Neuropsychology, 24(4), 435–442. http://doi.org/10.1037/a0018905
5. Maricq, A. V., & Church, R. M. (1983). The differential effects of haloperidol and methamphetamine on time estimation in the rat. Psychopharmacology, 79(1), 10–15. http://doi.org/10.1007/BF00433008
6. Ward, R. D., Kellendonk, C., Simpson, E. H., Lipatova, O., Drew, M. R., Fairhurst, S., … Balsam, P. D. (2009). Impaired timing precision produced by striatal D2 receptor overexpression is mediated by cognitive and motivational deficits. Behavioral Neuroscience, 123(4), 720–730. http://doi.org/10.1037/a0016503
7. Hinton, S. C., & Meck, W. H. (2004). Frontal-striatal circuitry activated by human peak-interval timing in the supra-seconds range. Cognitive Brain Research, 21(2), 171–182. http://doi.org/10.1016/j.cogbrainres.2004.08.005
8. Tanaka, S. C., Doya, K., Okada, G., Ueda, K., Okamoto, Y., & Yamawaki, S. (2004). Prediction of immediate and future rewards differentially recruits

cortico-basal ganglia loops. Nature Neuroscience, 7(8), 887–893. http://doi.org/10.1038/nn1279

9. Gibbon, J. (1977). Scalar expectancy theory and Weber's law in animal timing. Psychological Review, 84(3), 279–325. http://doi.org/10.1037/0033-295X.84.3.279

10. Simen, P., Balci, F., de Souza, L., Cohen, J. D., & Holmes, P. (2011). A model of interval timing by neural integration. The Journal of Neuroscience : The Official Journal of the Society for Neuroscience, 31(25), 9238–9253. http://doi.org/10.1523/JNEUROSCI.3121-10.2011

11. Meck, W. H., Penney, T. B., & Pouthas, V. (2008). Cortico-striatal representation of time in animals and humans. Current Opinion in Neurobiology, 18(2), 145–152. http://doi.org/10.1016/j.conb.2008.08.002

12. Killeen, P. R., & Fetterman, J. G. (1988). A behavioral theory of timing. Psychological Review, 95(2), 274–295. http://doi.org/10.1037/0033-295X.95.2.274

13. Buonomano, D. V, & Merzenich, M. M. (1995). Temporal information transformed into a spatial code by a neural network with realistic properties. Science (New York, N.Y.), 267(5200), 1028–1030. http://doi.org/10.1126/science.7863330

14. Machado, A., Malheiro, M. T., & Erlhagen, W. (2009). Learning to Time: a perspective. Journal of the Experimental Analysis of Behavior, 92(3), 423–458. http://doi.org/10.1901/jeab.2009.92-423

15. Gage, G. J., Stoetzner, C. R., Wiltschko, A. B., & Berke, J. D. (2010). Selective Activation of Striatal Fast-Spiking Interneurons during Choice Execution. Neuron, 67(3), 466–479. http://doi.org/10.1016/j.neuron.2010.06.034

16. Geffen, M. N., Broome, B. M., Laurent, G., & Meister, M. (2009). Neural Encoding of Rapidly Fluctuating Odors. Neuron, 61(4), 570–586. http://doi.org/10.1016/j.neuron.2009.01.021

17. Dayan, P. and Abbott, L. F. (2005). Theoretical neuroscience. Second Edition (Cambridge: The MIT Press).

18. Mink, J. W. (1996). The basal ganglia: Focused selection and inhibition of competing motor programs. Progress in Neurobiology, 50(4), 381–425. http://doi.org/10.1016/S0301-0082(96)00042-1

19. Jin, X., & Costa, R. M. (2010). Start/stop signals emerge in nigrostriatal circuits during sequence learning. Nature, 466(7305), 457–462. http://doi.org/10.1038/nature09263

20. Kim, H., Sul, J. H., Huh, N., Lee, D., & Jung, M. W. (2009). Role of striatum in updating values of chosen actions. The Journal of Neuroscience : The Official Journal of the Society for Neuroscience, 29(47), 14701–14712. http://doi.org/10.1523/JNEUROSCI.2728-09.2009

21. Grossberg, S., & Schmajuk, N. A. (1989). Neural dynamics of adaptive timing and temporal discrimination during associative learning. Neural Networks, 2(2), 79–102. http://doi.org/10.1016/0893-6080(89)90026-9

22. Doya, K. (1999). What are the computations of the cerebellum, the basal ganglia and the cerebral cortex? Neural Networks, 12(7-8), 961–974. http://doi.org/10.1016/S0893-6080(99)00046-5

23. Lauwereyns, J., Watanabe, K., Coe, B., & Hikosaka, O. (2002). A neural correlate of response bias in monkey caudate nucleus. Nature, 418(6896), 413–417. http://doi.org/10.1038/nature00892

24. Samejima, K., Ueda, Y., Doya, K., & Kimura, M. (2005). Representation of action-specific reward values in the striatum. Science (New York, N.Y.), 310(5752), 1337–1340. http://doi.org/10.1126/science.1115270

25. Lau, B., & Glimcher, P. W. (2008). Value Representations in the Primate Striatum during Matching Behavior. Neuron, 58(3), 451–463. http://doi.org/10.1016/j.neuron.2008.02.021

26. Sutton, R. S., & Barto, A. G. (1998). Reinforcement Learning: An Introduction. IEEE Transactions on Neural Networks, 9(5), 1054–1054. http://doi.org/10.1109/TNN.1998.712192

27. Balsam, P. D., & Gallistel, C. R. (2009). Temporal maps and informativeness in associative learning. Trends in Neurosciences, 32(2), 73–78. http://doi.org/10.1016/j.tins.2008.10.004

28. Suri, R. E., & Schultz, W. (1999). A neural network model with dopamine-like reinforcement signal that learns a spatial delayed response task. Neuroscience, 91(3), 871–890. http://doi.org/10.1016/S0306-4522(98)00697-6

29. Ludvig, E. a, Sutton, R. S., & Kehoe, E. J. (2008). Stimulus representation and the timing of reward-prediction errors in models of the dopamine system. Neural Computation, 20(12), 3034–3054. http://doi.org/10.1162/neco.2008.11-07-654

30. Ponzi, A., & Wickens, J. (2010). Sequentially switching cell assemblies in random inhibitory networks of spiking neurons in the striatum. The Journal of Neuroscience : The Official Journal of the Society for Neuroscience, 30(17), 5894–5911. http://doi.org/10.1523/JNEUROSCI.5540-09.2010

31. Ahrens, M. B., & Sahani, M. (2011). Observers exploit stochastic models of sensory change to help judge the passage of time. Current Biology, 21(3), 200–206. http://doi.org/10.1016/j.cub.2010.12.043

32. Buonomano, D. V., & Mauk, M. D. (1994). Neural Network Model of the Cerebellum: Temporal Discrimination and the Timing of Motor Responses. Neural Computation, 6(1), 38–55. http://doi.org/10.1162/neco.1994.6.1.38

33. Pastalkova, E., Itskov, V., Amarasingham, A., & Buzsáki, G. (2008). Internally generated cell assembly sequences in the rat hippocampus.

Science (New York, N.Y.), 321(5894), 1322–1327. http://doi.org/10.1126/science.1159775

34. MacDonald, C. J., Lepage, K. Q., Eden, U. T., & Eichenbaum, H. (2011). Hippocampal “time cells” bridge the gap in memory for discontiguous events. Neuron, 71(4), 737–749. http://doi.org/10.1016/j.neuron.2011.07.012

35. Harvey, C. D., Coen, P., & Tank, D. W. (2012). Choice-specific sequences in parietal cortex during a virtual-navigation decision task. Nature, 484(7392), 62–68. http://doi.org/10.1038/nature10918

36. Machens, C. K., Romo, R., & Brody, C. D. (2010). Functional, but not anatomical, separation of “what” and “when” in prefrontal cortex. The Journal of Neuroscience : The Official Journal of the Society for Neuroscience, 30(1), 350–360. http://doi.org/10.1523/JNEUROSCI.3276-09.2010

37. Shinomoto, S., Omi, T., Mita, A., Mushiake, H., Shima, K., Matsuzaka, Y., & Tanji, J. (2011). Deciphering elapsed time and predicting action timing from neuronal population signals. Frontiers in Computational Neuroscience, 5(June), 29. http://doi.org/10.3389/fncom.2011.00029

38. Kim, J., Ghim, J.-W., Lee, J. H., & Jung, M. W. (2013). Neural correlates of interval timing in rodent prefrontal cortex. The Journal of Neuroscience : The Official Journal of the Society for Neuroscience, 33(34), 13834–47. http://doi.org/10.1523/JNEUROSCI.1443-13.2013

39. Merchant, H., Pérez, O., Zarco, W., & Gámez, J. (2013). Interval Tuning in the Primate Medial Premotor Cortex as a General Timing Mechanism. The Journal of Neuroscience, 33(21), 9082–9096. http://doi.org/10.1523/JNEUROSCI.5513-12.2013

40. Howard, M. W., MacDonald, C. J., Tiganj, Z., Shankar, K. H., Du, Q., Hasselmo, M. E., & Eichenbaum, H. (2014). A Unified Mathematical Framework for Coding Time, Space, and Sequences in the Hippocampal Region. Journal of Neuroscience, 34(13), 4692–4707. http://doi.org/10.1523/JNEUROSCI.5808-12.2014

Chapter 2
Appendice A: Supplementary figures

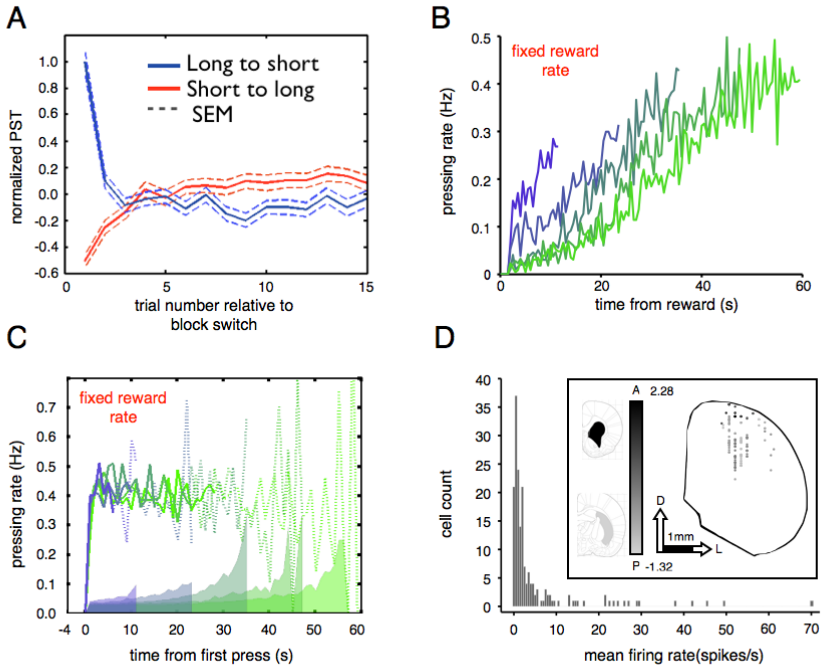

Figure S2.1 | Rats adjust their PSTs rapidly after a block switch. In a fixed reward rate condition, rats' constant pressing rate after pressing onset is insensitive to FI. See also Figure 2.1. (**A**) Normalized PST for the first 15 trials after block switch. Solid blue trace represents block switches from any FI to the 12s FI block (long to short). The solid red trace represents block switches from any FI to the 60s FI (short to long). Dashed lines show the SEM. PSTs were normalized by subtracting the mean within-FI PST, and dividing by the within-FI standard deviation, across all sessions. (**B**-**C**) Conventions as in Figure 2.1C, D. Average pressing rate aligned with reward time (B) and on first press (C), for 12 sessions from two control animals where reward amount varied in proportion to the current FI, holding reward volume over time constant during the session. (**D**) Distribution of average overall firing rates (bin size of 1spike/s), calculated using all recorded spikes from each neuron. Inset represents the reconstruction of recording sites in the striatum. Data from all five rats were projected onto one coronal silhouette of the striatum. Each data point corresponds to one recording site. Black-gray color coding indicates position along the anterior-posterior (AP) axis, from black to gray respectively. Coronal slices at the extreme anterior and posterior positions are shown for reference at +2.28mm and -1.32 mm AP coordinates measured from Bregma. A - Anterior, P - Posterior, D - Dorsal, L - Lateral.

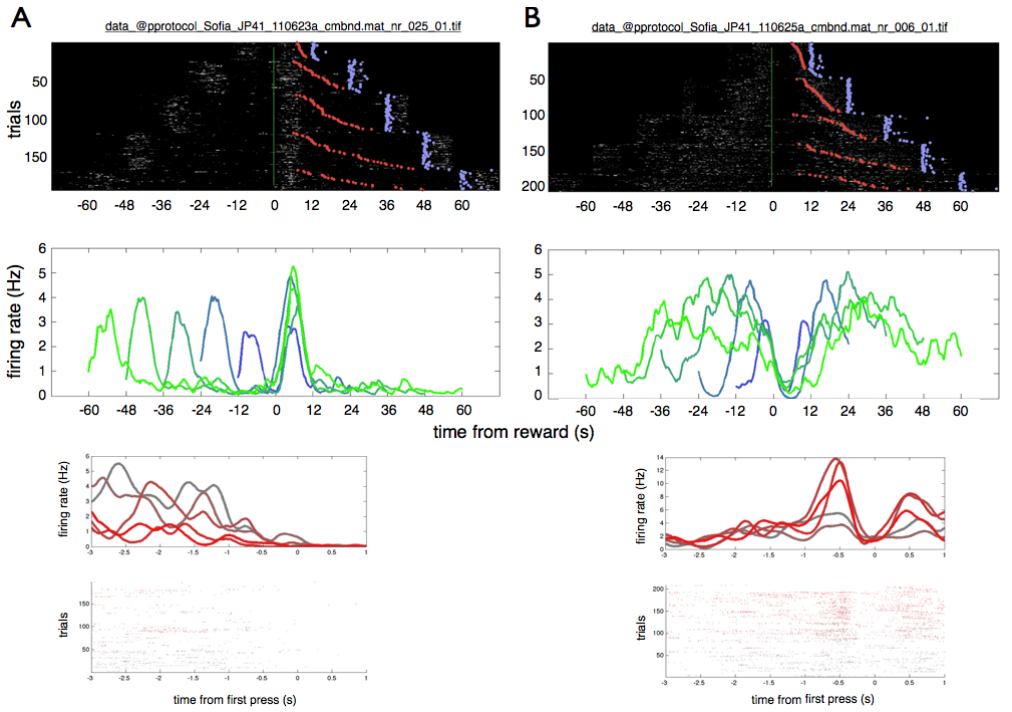

Figure S2.2 | Examples of single neurons recorded from the striatum during performance of the SFI task reflect neurons with different time courses of response that rescale with FI. See also Figure 2.2. (A-B) Top panel depicts single trial peri-stimulus time histograms, aligned with reward delivery (green line), with a bin size of 20 ms. Red tick marks indicate the onset of pressing and purple tick marks indicate reward delivery. Trials are ordered by FI, and within each FI by pressing onset time. Middle panel depicts SDFs for each FI block, aligned with reward delivery. Blue trace depicts the shortest FI, 12s, and the green trace depicts the longest FI, 60s with intermediate FIs depicted using intermediate colors. Bottom panel shows, using the same conventions as in Figure 2.6 A-D top and middle, the peri-event time histogram (top of the panel) and the raster plot (bottom of the panel) aligned with pressing onset for the same neuron.

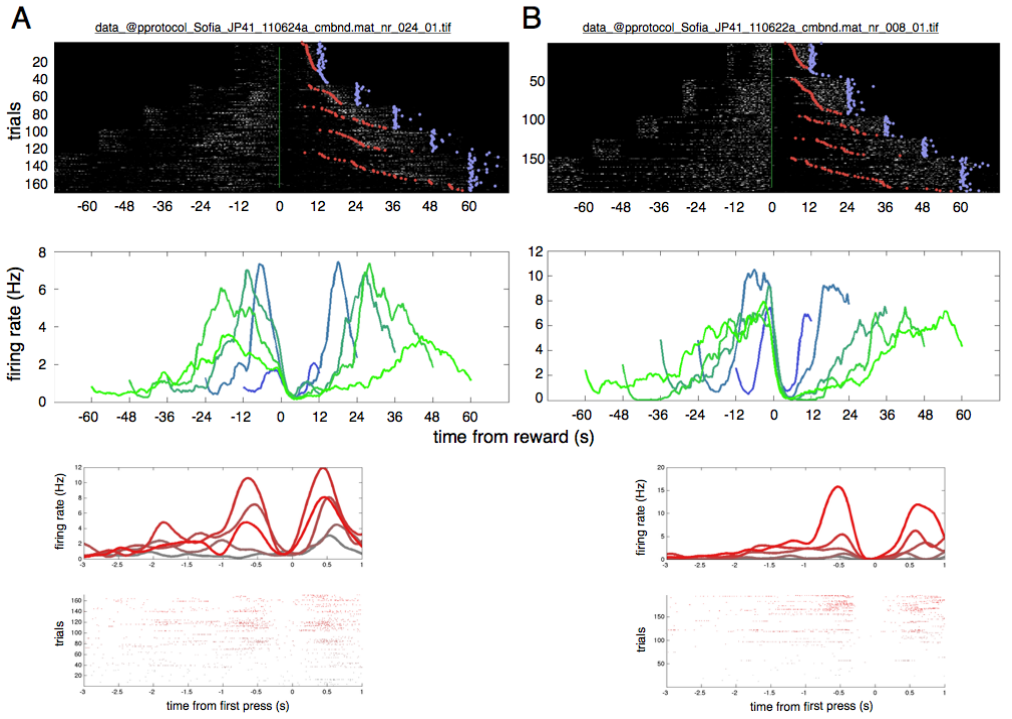

Figure S2.3 | Examples of single neurons recorded from the striatum during performance of the SFI task reflect neurons with different time courses of response that rescale with FI. See also Figure 2.3. (A-B) As in Figure S2.2, top panel depicts single trial peri-stimulus time histograms, aligned with reward delivery (green line), with a bin size of 20ms. Red tick marks indicate the onset of pressing and purple tick marks indicate reward delivery. Trials are ordered by FI, and within each FI by pressing onset time. Middle panel depicts SDFs for each FI block, aligned with reward delivery. Blue trace depicts the shortest FI, 12s, and the green trace depicts the longest FI, 60s with intermediate FIs depicted by the intermediate colors. Bottom panel shows, using the same conventions as in Figure 2.6 A-D top and middle, the peri- event time histogram (top of the panel) and the raster plot (bottom of the panel) aligned with pressing onset for the same neuron.

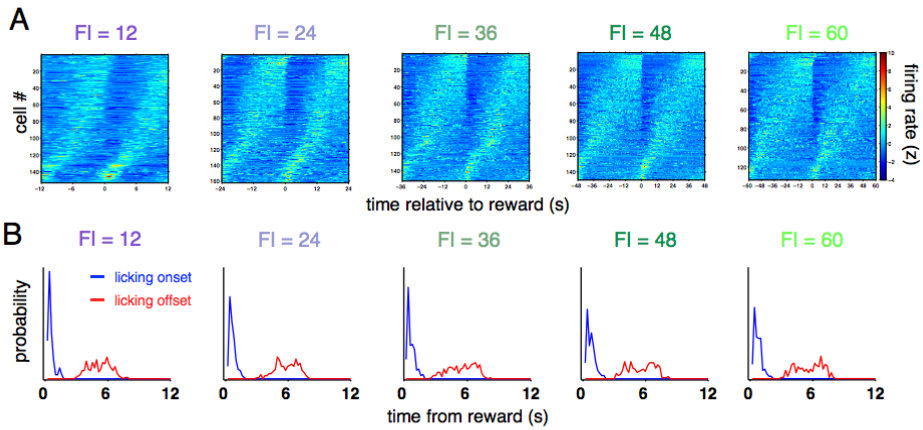

Figure S2.4 | Neuronal averages display slow moving bump of activity that scales with FI. See also Figure 2.4. (A) SDFs of all isolated neurons aligned with reward. **(B)** Probability of licking sequence onset (blue) and licking sequence offset (red) in the first 12s of all five FIs.

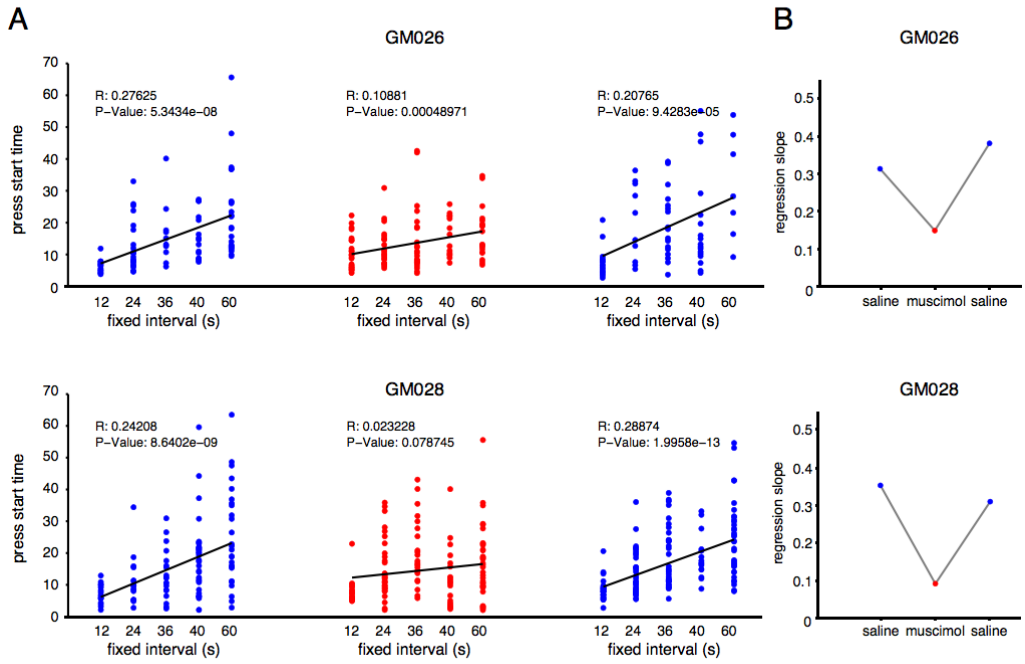

Figure S2.5 | Striatal muscimol infusion diminishes PST relationship to the FI. See also Figure 2.5. (**A**) Pressing start times per FI of three successive sessions (from left to right) and their respective regression slopes (black line) for two rats (top and bottom). Muscimol treatment session is depicted in red and saline treatment in blue. (**B**) Regression slopes for the same three sessions depicted in (A), same color code is applied.

CHAPTER 3: Simulation of timing behavior from a multiplexing sequential neural state based reinforcement learning model

Part of the data discussed in this chapter was published as the following manuscript: Mello, G. B. M., Soares, S., & Paton, J. J. (2015). A Scalable Population Code for Time in the Striatum. *Current Biology*, *25*(9), 1113–1122. http://doi.org/10.1016/j.cub.2015.02.036

SUMMARY

In a previous study we found neural signals in the striatum that might be used to encode time in the range of seconds to minutes. These striatal neurons fired at sequential delays spanning tens of seconds, and reflected the interactions between time and sensorimotor state. These cells rescaled their responses in time, preserving their sequence when intervals changed, implying relative time coding. Nonetheless, It was not clear whether the activity observed was sufficient to produce the temporally adaptive behavior performed by the animals. Because behavioral contributions to the timing signal might disrupt the information about time, it is unknown how behavior would affect temporal representations. To address these questions, we built a model to simulate rats' performance in the same task. Our simulation used a set of basis functions resembling the striatal activity, a delta learning rule, behavior-locked contributions to the neural activity and a reward rate sensitive pressing rate. We observed that press-locked contributions caused a slight left shift in temporal estimations. The behavior of the simulation manifested both accuracy sensitivity and scalar variance sensitivity to the FI, both classically accepted features of timing behavior. We also observed that compliance with scalar timing is the major distinction between simulation's and animals' behavior. This work is a proof of principle that neural responses resembling ones we observed in the striatum are suitable for being used as a basis for timing behavior in the range of seconds to one minute.

INTRODUCTION

In order to survive, animals have to maximize positive outcomes while minimizing effort. Actions taken too early or too late can change the outcome of actions and represent the difference between life and death (e.g., to get caught by a predator, to lose an opportunity to get food or a mate, to waste vital calories). Hence, animals rely on their ability to estimate intervals in the scale of tens of seconds (interval timing) to generate behaviors that are temporally adapted.

Learning how to act to maximize the outcome and minimize the effort in an ever changing environment is called reinforcement learning (RL; [1-3]). Multiple sources of evidence have highlighted the importance of the striatum to RL [4-10] and interval timing [11-17] processes. Additionally, Gershman [18] suggested that a single computational system can support both RL and interval timing by incorporating a time-sensitive action selection mechanism into RL models.

We found evidence that might support Gershman's claim. In the previous research [19], we recorded the activity of striatal neurons of rats as they performed a serial fixed interval (SFI) timing task. We identified striatal neurons which fired as they had temporal receptive fields that stretched or contracted, rescaling accordingly with longer or shorter timed intervals. The activity of these neurons combined information about time and behavior, which suggested an intimate interplay between action planning/selection/performance and timing.

Nonetheless, it is not clear how the behavioral contribution to the striatal timing signal might affect the temporal estimation. These behavioral contributions could improve or disrupt time estimations derived from striatal population activity. Indeed, there are many examples showing that timing is affected by behavioral [20,21], sensorial states [22], and vice versa [23], so that distortions in temporal estimations derived from behavior are expected. We want to know if there is a systematic shift in temporal estimation derived from behavioral contribution.

It has been demonstrated that striatal activity is necessary for interval timing performance [11,19], but (to the extent of our knowledge) its sufficiency for interval timing has never been investigated. To test whether striatum is

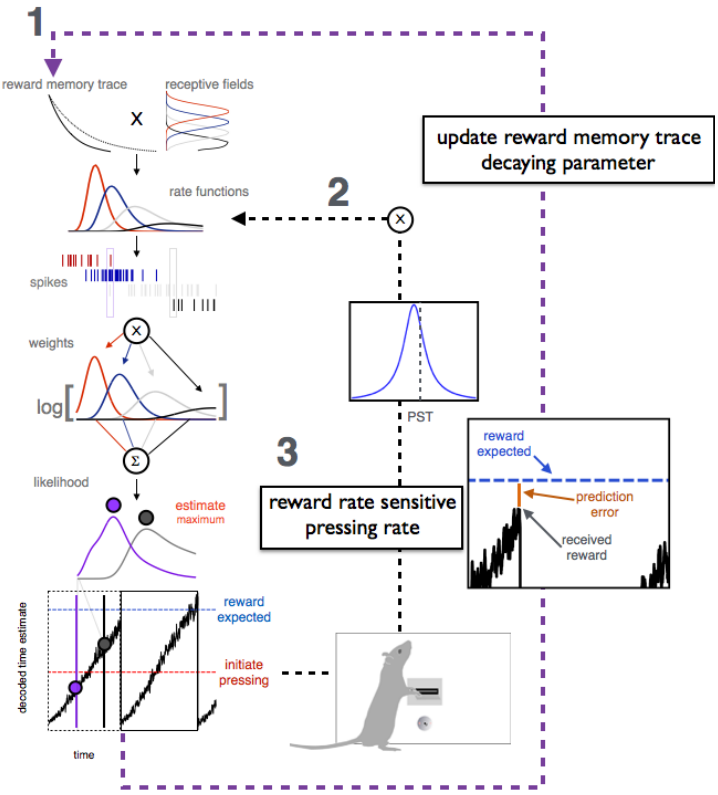

Figure 3.1 | Model of timing behavior in SFI was inspired by multiplexing and scalable population activity from experimental data. Striatal neurons' spike times were modeled based on receptive fields for the height of a decaying trace. This decaying trace was reset in every trial by the reward delivery (left in the top left). This trace could decay faster (solid line) or slower (dotted line) by adjusting the parameter gamma. The gaussian functions (right part in the top left drawing) represent receptive fields evenly spaced along the height of the trace function. The trace function was multiplied by the receptive fields to generate rate functions. These rate functions stretched and compressed over time accordance with the memory trace function decay rate. Spike counts observed within defined time bins were then multiplied by the logarithm of their respective rate functions and summed to compute the population log-likelihood function for current time given the population response, from t=0 to t=FI (middle left). The maximum of this likelihood function was used to derive our estimate for current time relative to reward, for each time bin (bottom left). Decoded time estimates can run faster or slower depending on whether the trace function decays quickly or slowly. For each trial, when the decoded time estimate reached a given threshold (red dotted line in the bottom left), we started a probabilistic pressing process. After the fixed interval has elapsed, the very first response produced the reward; at this moment internal estimate of current time was compared with the expected time of reward (right panel in the purple arrow line). The difference between current estimate and expected time was the prediction error that was then used to update the gamma parameter of the memory trace function (**1**). Also a press-locked response (**2**) was incremented to the rate function (black dotted path line in the center) on every press to take behavioral multiplexing into account. And additionally (**3**) a coefficient mapped the pressing rate as a function of reward rate.

sufficient to implement interval timing in a living organism would require systematical inactivation of all other areas of the brain but the striatum. It

would also require preserving only the areas/functions necessary for the performance of the task. As we can see, this endeavor is technically challenging with the current technology. Alternatively, we can use a fully known artificial systems (i.e., simulations) to explore which assumptions are necessary to produce a behavior similar to the one produced by rodents. More particularly, we could assess whether this simulation manifests, in the SFI task, commonly known properties of interval timing such as mean accuracy and variance sensitivity to the FI [24]. If so, we can further know if this sensitivity follows the properties of scalar timing (i.e., fixed coefficient of variation of PST across FIs, linear relationship between mean/median PST and FI; [25]). Hence, through the simulation we could test whether the striatum is conceptually (i.e., in principle, given some constraints) sufficient to generate interval timing behavior.

Figure 3.1 illustrates how we generated simulation to perform under the SFI task constraints. The core of this simulation is composed of a set of temporal basis functions which were inspired by the diverse single neuron responses observed in our striatal data set as well as existing timing and learning models [26-28]. We used the method described in Ludvig *et al.* [29] to generate these temporal bases. Each function was used as a rate function for generating inhomogeneous poisson spike trains from which time was read out during task performance. Whenever this time readout passed a threshold, presses were produced at a fixed rate proportional to the reciprocal of the interval. In order to adapt to the changing FIs, we implemented a simple learning rule to update a temporal scale factor for the basis functions depending on the difference between expected time of reward and encoded time at the time of reward delivery. Lastly, to account for our observation that many striatal neurons multiplexed information about action and time, each press produced a response proportional to the product of the original time dependent rate function (at the time of the press) and a rate function (generated by the press itself). With these elements, we ran the simulation under the conditions contained in the SFI task.

Even though we observed mean accuracy sensitivity to the FI, variance sensitivity was only present when a pressing rate across FI changed as

function of reward rate, thus affecting the variability of the reward acquisition time. The resulting behavior of the simulation was strictly conformed to scalar timing property [25]. By contrast, accuracy and precision of animal performance violated scalar timing predictions, and reflected additional strategies to optimize reward rate over session.

This simulation exemplifies how rescaling temporal receptive fields, that multiplex information about action and time, might generate behavior and use error signals to adjust to environmental changes.

RESULTS

Rescaling of temporal receptive fields across population that tiled intervals of tens of seconds to one minute was robust to behavioral contributions

We ran a simple simulation to test whether scalable multiplexing activity of striatal population observed in Mello *et al.* [19] could be conceptually sufficient to produce adaptive behavior in the SFI task. Our simulation (Figure 3.1 left column) employed the method described by Ludvig [29] to generate a set of temporal basis functions which were contingent on one single scaling factor (the decay rate coefficient of the memory trace). These basis functions were designed to mimic the overall responses of neurons observed in our striatal data set (Figure 3.2A), as they were used as rate functions to derive the spiking activity of each of the 75 neuronal units in our model.

We used the maximum of the sum-log-likelihood distribution of the activity of these 75 units as our estimate of time. In order to generate behavior from this temporal estimate, an arbitrary threshold of time was established. Whenever the time readout from the unit population crossed the defined threshold, the model produced presses at a fixed rate. We also implemented a simple learning rule (Figure 3.1, path 1, purple dashed line) to update the temporal scaling factor of the basis functions contingent on the difference between expected time of reward and decoded time at the time of reward delivery. The resulting population activity can be observed in Figure 3.2B.

To account for our previous observation that many striatal neurons multiplexed information about action and time, each press produced a rate

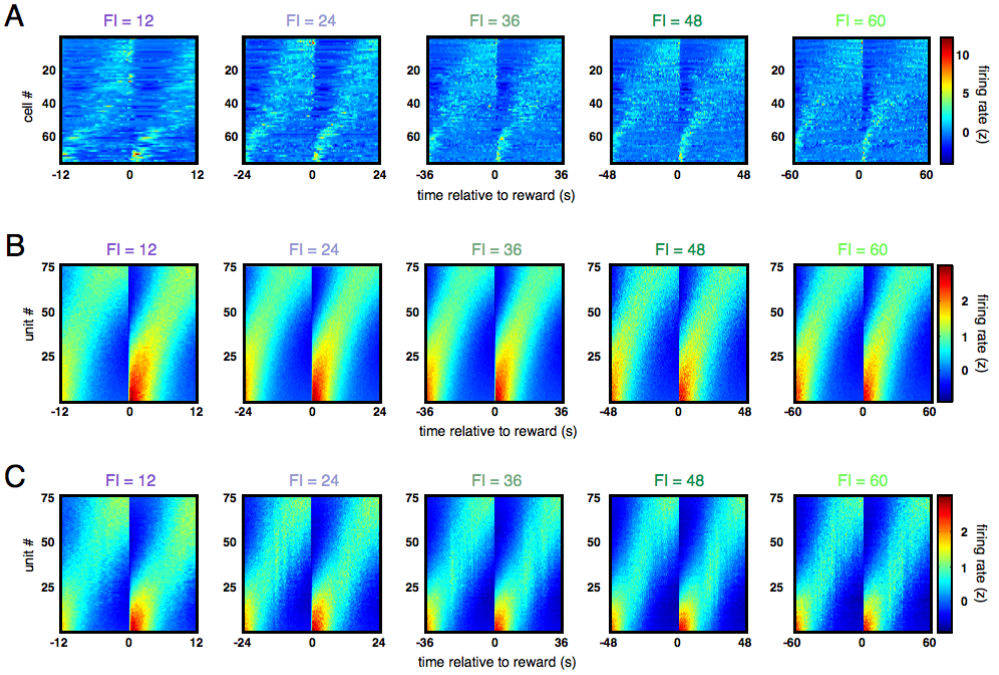

Figure 3.2 | Models's slow moving bump signal tiled tens of seconds to one minute as experimental data and was robust to behavioral locked contributions. (**A**) SDFs of striatal neurons that maintained their relative ordinal position in time within the population across all five FIs, aligned with reward. (**B**) SDFs of simulated units ordered by response profile within the population across all five FIs, and aligned with reward. (**C**) Same as (B) after adding press-locked contributions to each unit independently.

function response. The contribution of each press to the basis functions (i.e. rate function) was proportional to the product of the original time-dependent rate function at the time of the press and the rate function generated by the press itself (Figure 3.1, path 2, black dashed line). With these elements, we ran the simulation under the conditions contained in the SFI task.

Potentially, these press-locked contributions to the rate function could disrupt temporal representation, and consequently disrupt the simulation's capacity to perform the SFI task appropriately. Nonetheless, the result shows that the population activity in the simulation was robust to these behavioral contributions. Additionally, unit's activity reproduced the three main features that we observed in striatal neurons: temporal tuning, rescaling of neural

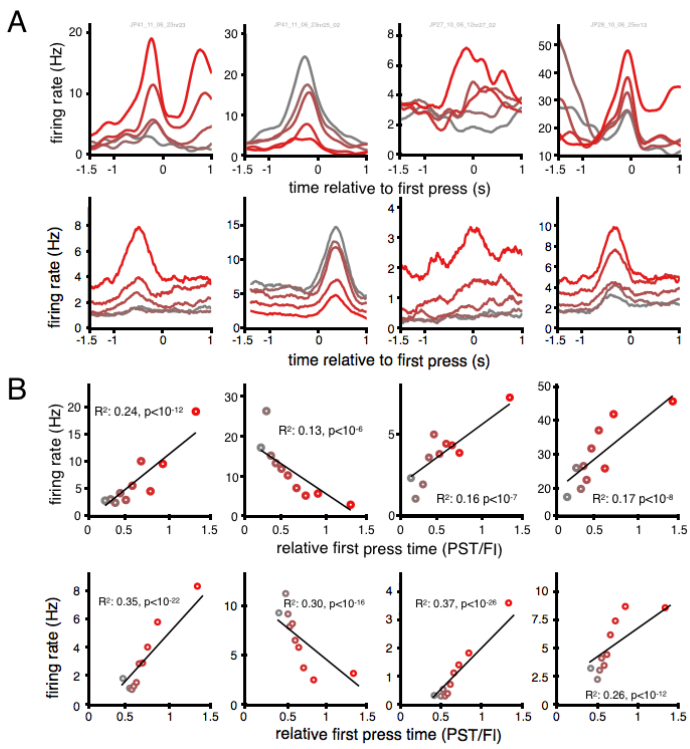

Figure 3.3 | Activity Profiles in Simulation's Units Multiplexed Time and Pressing Behaviors. (**A**,**B**) The graphs were generated with experimental data of animals in Mello et al. [19] and with simulation's data (bottom). (**A**) Four single unit peri-stimulus time histograms of 2.5 seconds aligned on pressing onset event. Trials were grouped by quintiles of pressing onset time relative to the FI. Here, the colors from grey to red represent the 1st to the 5th quintile, respectively. (**B**) Shows the correlation between the firing rate of the unit (in the same column of panel A), and the PST relative to the FI. Each datapoint is color coded from grey to red for the 1st to the 10th decile of the relative PST.

responses (Figure 3.2C), and multiplexing of information about action and time (Figures 3.3A bottom and 3B bottom) almost indistinguishable from experimental data (Figures 3.3A top and 3.3B top).

Simulated behavior in SFI exhibited block-wise median accuracy sensitivity to the FI but not variance sensitivity property.

Close inspection of the PSTs (Figure 3.4) produced by the simulation, in comparison to the rodents' PSTs, allowed us to compare them qualitatively. The major points of comparison were the PST median sensitivity to the FI shifts (median accuracy sensitivity), the gradual adjustment to these FI shifts, and the inverse relationship between PST precision and FI (variance sensitivity).

PSTs in both data sets presented gradual and systematic shifts following the transitions of FI (Figure 3.4B and 3.4C). These shifts were consistent with typical interval timing behavior in the SFI task [19]. The number of presses in average was higher in 60s trial than in trials within 12s because the pressing

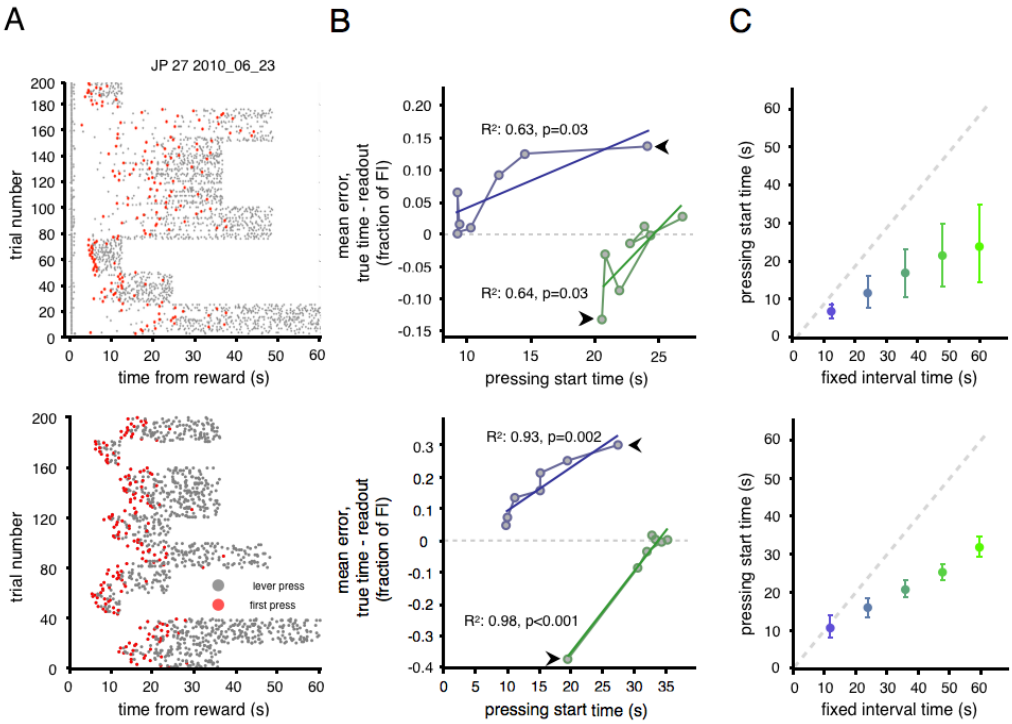

Figure 3.4 | Simulation displays mean accuracy sensitivity to the FI, but lacks variance sensitivity. (**A**) Example of the lever pressing behavior in one session of the SFI task. Grey markers indicate a lever press, red markers indicate the PST. Top panel is animals' behavior, bottom one represents the simulated behavior. (**B**) Mean error (average difference between true time and the decoded population estimate) on the first seven trials of the 12s (blue) and 60s (green) FI blocks for all sessions plotted against average PST. Contiguous trials are connected by solid lines to display the trajectory of the data over trials, and the first trial on each block is indicated by the black arrow. Dashed horizontal gray line represents zero error average decoding as compared to true time. (**C**) Median and interquartile range of PST for each of the five FIs colors coded by the length of the FI from blue to green for 12s to 60s FI respectively.

rate was the same in both conditions. Consequently, rate functions in the 60s FI were more influenced by the press-locked contributions. These contributions to the rate function seemed to produce a left shift to the average PST; while in the 12s the PST happened in average at 10 second (~0.8 of the interval), in the 60s FI the average PST was around 35s (~0.58 of the interval). Hence, it is likely that press-locked contributions to the rate function make time representations move faster during decoding.

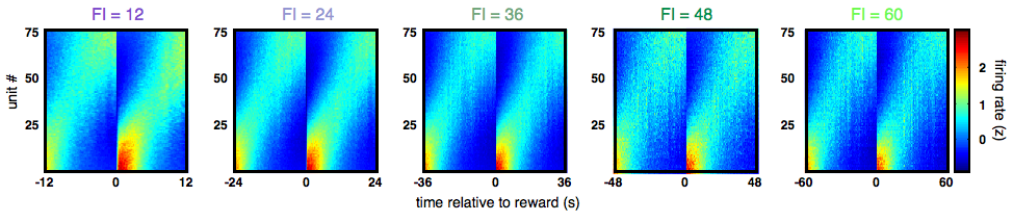

Figure 3.5 | Pressing rate sensitivity to reward rate increased dispersion In neural signal. SDFs of multiplexing scalable simulated units ordered by response profile within the population across all five FIs, and aligned with reward.

Regarding the PSTs variance, while experimental data exhibited clear inverse relationship between the FI length and precision (Figure 3.4C top), the simulation exhibited near-constant precision across all the FIs (Figure 3.4C bottom). The constant pressing rate after pressing onset in all FIs, established as a feature of the model, was probably the biggest source of PST variation for two reasons. Firstly, the random pressing introduced an irreducible difference between when the reward was expected and when it was acquired. This established a minimum reward prediction-error that affected precision trial-by-trial. Secondly, the simulation generates presses probabilistically starting from the moment it reaches the threshold. Consequently, reliability on which it starts pressing is also affected by the pressing rate.

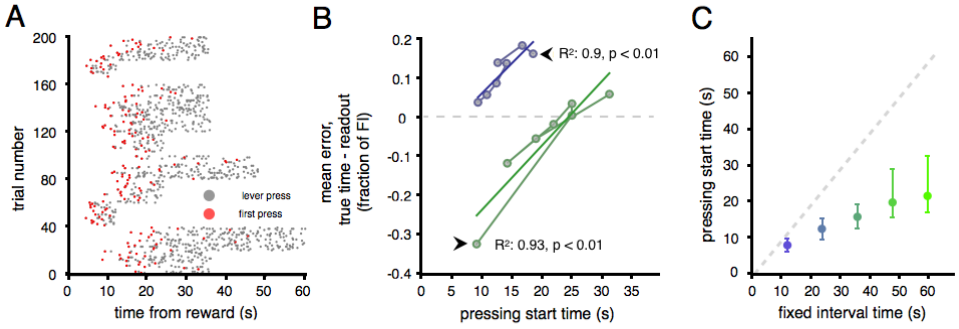

Figure 3.6 | Simulation's behavior was qualitatively similar to rat's behavior. (A) Example of simulated lever pressing behavior one session of the SFI task. Colors as in Figure 3.4A. **(B)** Mean-error plotted for the first seven trials after block switch, plotted against average PST. (see Figure 4B). **(C)** Median and interquartile range of PST for each of the five FIs colors as in Figure 3.4C.

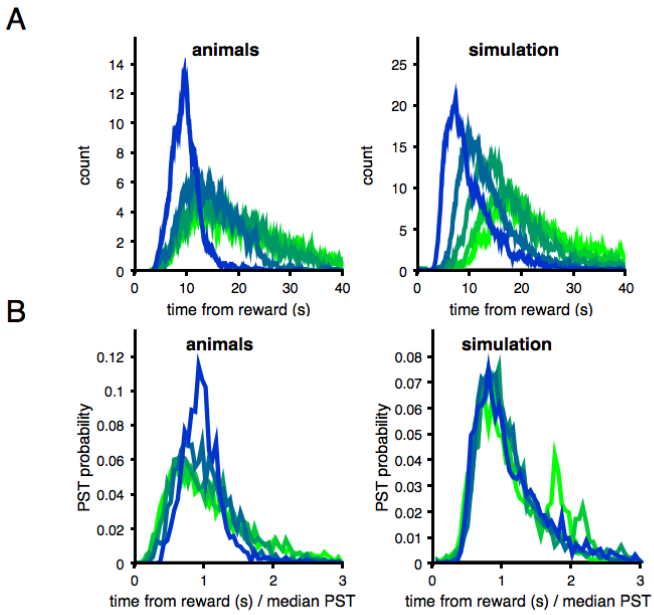

Figure 3.7 | Pressing start times distributions comparison between simulation and experimental data highlighted experimental data's violation of scalar timing. (**A**) Rats' (left) and model's (right) pressing start times distribution plotted against time since the reward delivery for all the five FIs. (**B**) Pressing start times distribution plotted against relative time (time from reward divided by the fixed interval) for all five FIs (colors as in Figure 3.4C).

Pressing start time variance sensitivity to the FI emerges from pressing rate sensitivity to the reward rate

In the experimental data of SFI performance, pressing rates were sensitive to the reward rate [19]. To mimic this feature we added a coefficient to modulate the pressing rate as a linear function of the reward rate (see methods), and ran the simulation once with a parameter picked arbitrarily (Figure 3.5 and 3.6).

The pressing rate, that depends on the reward rate, did affect the population activity (Figure 3.5) by increasing slightly the dispersion of the rate functions. Also, changes in pressing rate affected PST variance sensitivity to the interval. As intervals became longer and reward rate smaller, pressing rates decreased (Figure 3.6 A). Consequently, the variability of PSTs increased (Figure 3.6C) interfering with the adjustment of the PSTs to new FIs, especially to the longest FI (Figure 3.6B).

Simulation's median accuracy grows linearly with the FI

To compare quantitatively the simulation and experimental data, we optimized the parameters of the simulation session-by-session (see methods), so that simulation would act as close as possible to experimental data. We optimized two parameters, the pressing rate coefficient and the pressing onset threshold

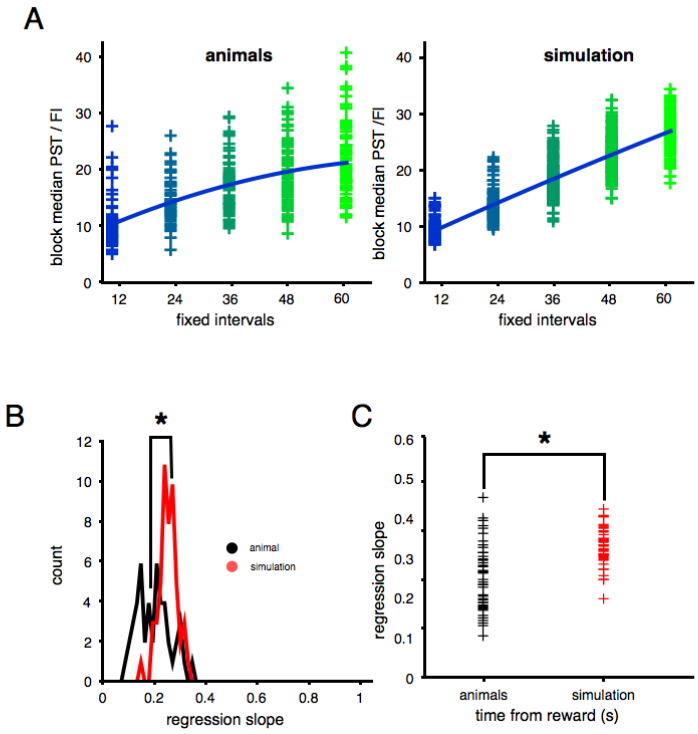

Figure 3.8 | Block-median PSTs in experimental data were biased toward the center of FIs distribution while simulations' block-median PSTs were a linear function of the FI. (**A**) Rats' (left) and simulation's (right) averages of pressing start times of each block in relative time separated by the fixed interval (colors as in Figure 3.4C); black line is the exponential decay regression. (**B,C**) Rats' (black) and simulation's distribution of PST over FIs linear regression slopes; star marks significant difference between the means (alpha =0.01, Fischer exact test : p=0.02).

relative to FI; both parameters were set to approach the average pressing rate and average relative PST within the respective session.

Distributions of simulation's PSTs where right skewed and shown progressively growing delays as FIs increases (Figure 3.7A). The PST probability densities normalized by the median PST exhibited almost complete overlap in simulation data but not in the experimental data (Figure 3.7B). Animals were visibly more precise during 12s FI than when estimating other intervals. Moreover, rats started to press relatively earlier and with less precision as FIs increased. These data suggest that animals' performance did not strictly comply with scalar timing.

Scalar timing behavior exhibits both, linear sensitivity of the mean/median accuracy to the FI, and scalar variance [24,25,30]. We looked for both features in the data. We tested for proportional PST accuracy sensitivity to the FI. We took the median PST for each block and regressed against its respective FI. Scalar timing predicted a linear relationship. Nonetheless, experimental PST data relationship with the FI was best described as a quadratic function of the FI (Figure 3.8A left), while the quadratic regression of the same relation for the simulation's data set revealed an almost perfect linear relationship (Figure 3.8A right). The nonlinear relationship demonstrated in the animals' data is one of the many known cases where timing behavior violates scalar timing [30,31], especially in tasks with multiple intervals such as the SFI.

Next, we used linear regressions for each session independently, for experimental and simulation data set. We asked whether the distribution of regression slopes for the different data set could have been sampled from the same underlying distribution (Figure 3.8B). The distributions were not significantly different (alpha = 0.01, p = 0.02, Fisher exact test) but barely. A more sensible interpretation driven by close examination of slope distributions shows that experimental data are more variable (Figure 3.8D) and slopes are typically less steep for experimental data than for simulation's data. Hence, experimental data had a lesser median-accuracy sensitivity of the to the FI with a bias towards the center of the distribution of FIs presented in the session. This result might reflect that rats retain knowledge about the overall distribution of intervals in the session, and consequently are using additional strategies to improve reward rate within the session, or that timing representations might be competing with each other in the same context.

Simulation's strict conformity with scalar variance property of interval timing highlights experimental data's violation to scalar variance property

Scalar variance, other classical feature of interval timing, posits that the relationship between mean and standard deviation, or between median and interquartile range, is linear. This is why the coefficient of variance (CV; standard deviation divided by average) is constant across all FIs. To test for scalar variance, we first performed a quadratic regression of the relationship

between block wise interquartile range and median (Figure 3.9A data points and 3.9B regression lines).

Experimental data relationship between median PST and interquartile were context (FI) dependent. In shorter FIs the relationship was almost constant, while as FIs got longer, the coefficient of the relationship increased. This result was a clear violation of the predictions derived from scalar timing theory, according to which, linear relationships were to be expected with a

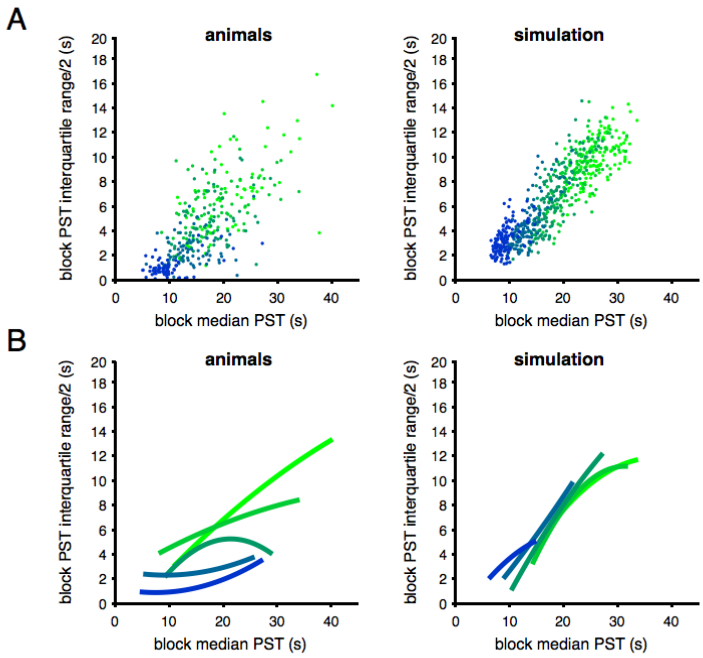

Figure 3.9 | Half-interquartile range had context (FI) dependent relationship with median PSTs in the experimental data set, while it was context independent for the simulation. (**A**) Rats' (left) and simulation's (right) standard deviation of pressing responses within each block as a function of average PST. (**B**) Colored lines represent the best quadratic fit to the data in panels A. Colors segregate different FIs (see Figure 3.4C)

constant coefficient across FIs (Figure 3.9B left). Simulation's behavior, in other hand, matched almost perfectly to scalar timing predictions.

The coefficients of variation across FIs grown with the FI in animals' data, while in simulation's they were held constant (Figure 3.10A). When we compared the distributions of CV between simulation and experimental data within each FI, we observed that experimental CVs (left) and the simulated ones (right) were significantly different in most of the FIs (Fischer exact

test, α =0.01; FI:12, p<0.01; FI:24, p=0.02; FI:36, p=0.26; FI:48, p<0.01; FI:60, p<0.01; Figure 3.10B). This result suggests that variance in the shortest and the longest intervals are respectively lower and higher than the variance expected by scalar timing, a violation typically observed in dynamic timing tasks such as SFI [24].

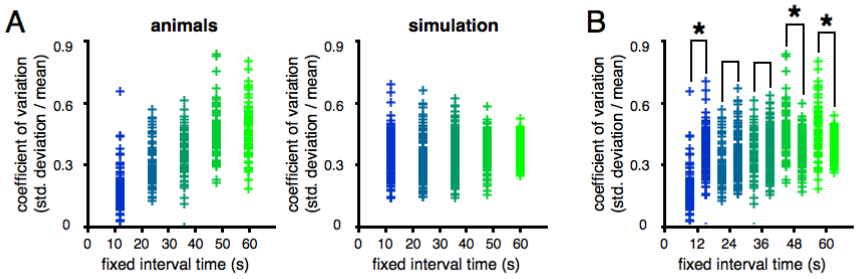

Figure 3.10 | Simulation's coefficient of variation (CV) displayed a constant trend which contrasted with animal's FI-dependent CV. (**A**) Coefficients of variation (standard deviation divided by mean) of PSTs from animal's (left) and simulation (right) data. Each cross is the CV of one block of trials, color segregated by FI (colors as in Figure 3.4C). (**B**) Same data as in A, but rearranged to facilitate the comparison between rats' and simulation data. For every FI (colors) there is a set of two columns of CVs. The stars mark significant differences between distributions (Fischer exact test, alpha = 0.01; FI:12, p<0.01; FI:24, p=0.02; FI:36, p=0.26; FI:48, p<0.01; FI: 60, p<0.01)

DISCUSSION

In this study we tested whether multiplexing scalable activity observed in the striatum is in principle sufficient to produce temporally adaptive behavior (i.e., proportional timing and scalar timing) and how the behavioral contributions to the timing signal might affect the time estimates. With these goals, we simulated the striatal activity using a model with only one free parameter, the decaying memory trace. This parameter was updated on every trial by the reward time prediction-error. The simulation also took into consideration the multiplexing feature of experimental data. To do so, it employed press-locked contributions to the spike rate functions, which subsequently affected the time signals. These contributions are the product of a fixed press-locked response with the current value of the rate function. Also, we reproduced the reward rate dependent pressing rate and assessed how similar the rats' behavior was to

the model's performance (when model's parameters were optimized to approach animals' behavior).

We found that behavioral contributions to timing signal did not disrupt temporal representations. Instead, it caused time estimations to move faster, as evidenced by the left-shift in PST in the longest FI relative to the shortest one (Figure 3.4B bottom and 3.6B). This result is consistent with temporal binding between action and event [20,21,32]. In this phenomenon, perception of event time is biased toward the time of the action. This process is considered to be important for the sense of agency, and ultimately, to how animals learn to control the environment through their actions. But regardless the slight temporal distortion, the simulation adjusted gradually its PST to the FIs in each block, therefore preserving mean PST accuracy sensitivity to the FI.

Against to what was expected (discussion in [19]), scalar variance property (Figure 3.4C, 3.7, 3.9 and 3.10) was not produced by the dispersion increase of the temporal receptive fields for longer times in the interval. The strict prediction of scalar timing is that the coefficient of variation is fixed for all estimated intervals, which would reflect in a perfect overlap between normalized PST probability distributions for all FIs. Instead, our simulation, in its first form, manifested a fixed precision for all FIs. The variance sensitivity property only emerged when pressing rate became proportional to the reward rate (i.e., inverse of memory trace decay rate). This result suggests that the scalar property emerges from trial-by-trial variations of reward acquisition time relative to the expected time. In our model trial-by-trial variation was introduced by behavior itself. Nonetheless, the same result could be obtained by introducing constant noise at every time step into the reward time expectation. The accumulation over time of small variations into the reward time expectation could increase the magnitude and variability of prediction-errors used to update the memory trace decay rate. Consequently, this would affect when the simulation tend to start pressing. Indeed, it has been suggested before that time-scale invariance can emerge from noise [33,34], which can be caused either by neural population noise or by trial-by-trial variations in the speed of the clock. Our model is more consistent with the latter source of variation.

The major difference between the model and the animal's behavior was how closely they conformed to the scalar variance. Our model strictly followed the scalar timing prediction, while rats' behavior manifested parametrical growth of the coefficient of variation following the duration of the FI. Such violations in scalar timing have been observed before [24,30,31,35], and they are especially frequent in dynamic timing tasks (i.e., tasks where animals estimate three or more FIs in a session; [36]), like the SFI task. But little has been discussed about the cause of these violations. The fast adjustment of PSTs to the new intervals might be the key to answer that question. Increases of PST variance in longer intervals provided a larger sampling space of reward times. This larger sampling space of times allows the animal to detect quickly new intervals on block switches. The same increase in variance during shorter intervals would only add effort without any sensible benefit to cease reward opportunities. Indeed, within the shortest interval, late PSTs save energy and facilitate detection of transitions to longer intervals. Therefore, the increase in PST variance was only beneficial in longer intervals while the reduction of variance was beneficial in the shorter intervals. We interpret this systematical increase in the coefficient of variation as part of exploratory strategies that reflected the animals' knowledge about the whole distributions of intervals in one session.

Some characteristics of our simulation raised interesting questions about how information is integrated in the striatum. In our model, multiplication was the mean by which temporal and behavioral information were combined. Multiplicative rules to connect neurons and integrate information have been reported in other brain areas [37] and explored in computational models [38-41] before. There are reasons to believe that the same multiplicative rules are also present in the striatum [42], and that they are mediated by dopamine [43]. Dopamine (DA) plays an important role in motor learning and timing [44]. It is possible that dopaminergic manipulations change the basic rules of multiplexing, and subsequently affect timing. Malapani *et al.* [44] demonstrated that parkinsonian patients (PKP) display poor temporal discrimination when tested off-medication. It is possible that lack of DA may disrupt the multiplication rule for multiplexing behavior and time, for instance by making

the contribution of behavior to the time fixed for all times. This might turn the temporal representation of two events more similar and therefore harder to discriminate by downstream neurons. Conversely, it should be expected a gain in separability between the estimation of two intervals in PKP trained off-medication and tested on-medication.

Also, it is known that when animals have to take an action upon an event, they tend to over-estimate the time when this event happened [20]; how exactly this happens, in the context of our model, is a possible direction for future research. For instance, if DA controls the gain of behavioral contributions to the time basis functions, a right-shift on time estimation is to be expected when training without DA and tested with DA. Moreover, the role of DA as the key agent for multiplexing has yet to be demonstrated. We could do that by manipulating DA in an organism performing the SFI, to attempt to eliminate or modulate the multiplicative feature of multiplexing while preserving the slow moving bump of activity.

Additionally, and perhaps more important, the stretch and contraction of temporal representations are directly dependent on the capacity of the system to learn using the prediction-errors. For long, DA has been considered to be a major teaching signal in the brain, and the activity of dopaminergic cells is consistent with the encoding of prediction-errors [2]. Hence, it is likely that non-pathological fluctuations of DA help to control the scale of striatal receptive fields.

Our simulation highlighted some variables that could be relevant to understand the timing strategies. As said before, behavior locked response magnitude covaried with time signal; it could be the case that some non-temporal features of behavior were affected by time. This influence of time estimation over behavioral features was observed before in humans. Droit-Volet and collaborators [23,45] have demonstrated that three-year-old children associate the strength of pressing with its duration, while five-and-half-year-old children can dissociate them. In the same fashion, it is possible that rodents press stronger for longer intervals and lighter for shorter ones, thus producing a time-dependent behavioral feature. This could explain some of the differences in magnitude of behavior-locked responses over time, but not

completely. Different from what was described by Droit-Volet's work, the behavior-locked contributions we observed did not grow monotonically with the interval. This suggests that the nature and genesis of the multiplexed signal are still open questions.

Finally, the mechanisms and parameters involved in setting the thresholds to start pressing remain elusive. As we described in the methods, we arbitrarily defined a fix relative point adequate to experimental data as the threshold. The striatum is also implicated in action selection and action initiation [46], and it is possible that the computations to implement this action initiation thresholds are performed within the striatum (perhaps even embedded in the signals we observed). But most likely, the computations performed to implement the threshold are implemented by the multiple feedback loops the striatum has with the downstream areas of the basal ganglia.

All things considered. This study not only exemplifies how organisms can use a series of progressively widening time receptive fields to implement behavior. It moves our understanding about interval timing further, by highlighting important components of the timing system and putting in evidence the complexity of the animal behavior while timing.

METHODS

Model description

We ran a simulation of timing behavior in the SFI task which took into account the temporal tuning, rescaling and multiplexing properties of striatal neurons recorded in Mello *et al.* [19]. The firing of striatal neurons was simulated using gaussian-shaped receptive fields for the height of a decaying memory trace of the reward (Figure 3.1 left top panel; [29]).

$$y_t = \gamma^{\tau}, \qquad (1)$$

The trace function y (Equation 1) was reset to the value of 1 at every reward delivery. Its exponential decay rate γ was always lower than 1, and on

every session it was initialized as 0.999. The trace function decayed over an arbitrary time unit τ, which varied from 0 to 10000. Also important for the model, the gaussian-shaped receptive fields f means μ were equidistant on the height of the trace function y, and their standard deviation σ was fixed at 0.1.

$$f(y, \mu, \sigma) = \frac{1}{\sqrt{2\pi}} exp\left(\frac{(y-\mu)^2}{2\sigma^2}\right), \tag{2}$$

Next, we generated 75 temporal basis functions. The basis functions were computed as follows:

$$b_t(i) = f\left(y_t, \frac{i}{m}, \sigma\right) y_t, \tag{3}$$

The level of the ith basis function b out of m total bases at time t, was determined by the product of the corresponding height of the trace function y_t and the receptive field f. The result was a set of temporal basis functions that became progressively wider, delayed and with a lower peak (Figure 3.1 left column second panel from top). Then, we generated spikes for each unit using these basis functions as rate functions in an inhomogeneous poisson spiking process. To compute internal estimates of time and simulate behavior, we counted the number of spikes in bins of 10 ms for each unit. At each time step, we multiplied the number of observed spikes per bin by the logarithm of its respective basis function (tuning curve for time). This produced the log-likelihood for time given the observed spikes for each unit. We summed the log-likelihood functions [47] of all units together. The maximum of the resulting likelihood function was our estimate of current-time relative to reward for each time bin.

Two thresholds were established to trigger changes in the simulated behavior. Crossing the first threshold, placed at three-eighths (3/8) of the maximally possible internal time estimate, triggered press initiation. The

second threshold, defined at twice the level of the pressing threshold, represented the expected reward time.

Once the decoded time crossed the pressing threshold, the simulation generated presses at a fixed rate until the delivery of the reward at the end of the FI. Then, the time of reward receipt was compared to the expected time of reward (the second threshold). The difference between the real and the expected time generated the prediction error. This prediction error was used to update the time constant γ of the exponential trace, which controlled scaling of the basis functions. The update proceeded as the equation below:

$$\gamma := \gamma + \alpha \left(\frac{1}{\gamma^{(t-t_r)}} \right) \left(\frac{(l(t_r) - \tau_r)}{max(l_\tau)} \right), \tag{4}$$

It was established that α was the learning rate set to 0.00007, t was the current time, and t_r was the time of the reward. The expected time of reward τ_r was fixed as three-fourths of the length of the τ vector (τ_r = ~7500) and $l(t_r)$ was the current estimation of time at the reward acquisition time. l_τ was the current estimation of time in internal representation unit.

Information about each press fed back to the temporal basis in the following manner. Each unit possessed a press-locked contribution to its rate function. This contribution to the firing was a gaussian-shaped rate function with a standard deviation of 200 ms, and a mean precedence relative to the press that was drawn from another gaussian distribution with a mean of -1500 ms and a SD of 300 ms. However, the contribution of each press to the firing of a given unit was computed as the product of the instantaneous, time dependent rate, and the press-locked contribution to firing.

This adjustment of the parameter γ in the trace function (Equation 1) led encoded time to change faster or slower, allowing the simulation to exhibit an adaptive timing of neural and behavioral responses that resembled the experimental data.

Finally, we included a coefficient that controlled the pressing rate in linear proportion to the reward rate (i.e., the reciprocal of γ) in order to replicate this

feature of the data observed in Mello *et al.* [19]. We opted for a linear relationship because it was the simplest assumption, after a constant pressing rate. Then, this pressing rate coefficient was optimized (see below), so that every simulated session had an average pressing rate for each FI as close as possible to the experimental data.

Model optimization

To quantify the differences between animal behavior and behavior generated from the model, we optimized the parameters of the model, so that model's and animals' performances were as close as possible. Firstly, we ran a series of simulations for every session in the experimental data set. These simulated sessions had the same sequence of FIs as the correspondent experimental session had. Secondly, we used a gradient descent method to iteratively minimize differences in performances between the model and animals, regarding two variables: the average pressing rate in each of the FIs, which controlled the pressing rate coefficient; and session average PST (in relative time), which adjusted the pressing start threshold for the whole session. Thus, for every session performed by an animal in our data set we generated one parallel simulation session with optimized parameters.

AUTHOR CONTRIBUTIONS

G.M. and J.J.P. designed experiments. G.M. and S.S. carried out experiments. G.M., S.S., and J.J.P. analyzed the data.

ACKNOWLEDGMENTS

We thank Bassam Atallah, Brian Lau, Kenway Louie, Christian Machens, Zachary Mainen, Thiago Gouvêa, Tiago Monteiro, Eric DeWitt, Alfonso Renart and Masayoshi Murakami for critical comments on versions of the manuscript and discussions. We thank the Histopathology and the Vivarium staff from the Champalimaud Scientific and Technological Platforms for the support. The work was supported by Champalimaud and Gulbenkian Foundations, and fellowships to G.M. and S.S from the Portuguese Foundation for Science and Technology.

REFERENCES

1. Montague, P. R., Dayan, P., & Sejnowski, T. J. (1996). A framework for mesencephalic dopamine systems based on predictive Hebbian learning. The Journal of Neuroscience, 16(5), 1936–1947. http://doi.org/10.1.1.156.635
2. Schultz, W., Dayan, P., & Montague, P. R. (1997). A neural substrate of prediction and reward. Science (New York, N.Y.), 275(5306), 1593–9. http://doi.org/10.1126/science.275.5306.1593
3. Sutton RS, Barto AG (1998) Reinforcement Learning: An Introduction (MIT Press, Cambridge, MA)
4. Doya, K. (1999). What are the computations of the cerebellum, the basal ganglia and the cerebral cortex? Neural Networks, 12(7-8), 961–974. http://doi.org/10.1016/S0893-6080(99)00046-5
5. Fee, M. S., & Goldberg, J. H. (2011). A hypothesis for basal ganglia-dependent reinforcement learning in the songbird. Neuroscience, 198, 152–170. http://doi.org/10.1016/j.neuroscience.2011.09.069
6. Joel, D., Niv, Y., & Ruppin, E. (2002). Actor-critic models of the basal ganglia: new anatomical and computational perspectives. Neural Networks, 15(4-6), 535–547. http://doi.org/10.1016/S0893-6080(02)00047-3
7. Lau, B., & Glimcher, P. W. (2007). Action and outcome encoding in the primate caudate nucleus. The Journal of Neuroscience : The Official Journal of the Society for Neuroscience, 27(52), 14502–14514. http://doi.org/10.1523/JNEUROSCI.3060-07.2007
8. Leblois, A., Wendel, B. J., & Perkel, D. J. (2010). Striatal dopamine modulates basal ganglia output and regulates social context-dependent behavioral variability through D1 receptors. The Journal of Neuroscience : The Official Journal of the Society for Neuroscience, 30(16), 5730–5743. http://doi.org/10.1523/JNEUROSCI.5974-09.2010
9. Ratcliff, R., & Frank, M. J. (2012). Reinforcement-Based Decision Making in Corticostriatal Circuits: Mutual Constraints by Neurocomputational and Diffusion Models. Neural Computation, 24(5), 1186–1229. http://doi.org/10.1162/NECO_a_00270
10. Redgrave, P., Coizet, V., Comoli, E., McHaffie, J. G., Leriche, M., Vautrelle, N., … Overton, P. (2010). Interactions between the Midbrain Superior Colliculus and the Basal Ganglia. Frontiers in Neuroanatomy, 4(September), 1–8. http://doi.org/10.3389/fnana.2010.00132
11. Meck, W. H. (2006). Neuroanatomical localization of an internal clock: A functional link between mesolimbic, nigrostriatal, and mesocortical dopaminergic systems. Brain Research, 1109(1), 93–107. http://doi.org/10.1016/j.brainres.2006.06.031

12. Malapani, C., Rakitin, B., Levy, R., Meck, W. H., Deweer, B., Dubois, B., & Gibbon, J. (1998). Coupled temporal memories in Parkinson's disease: a dopamine-related dysfunction. Journal of Cognitive Neuroscience, 10(3), 316–331. http://doi.org/10.1162/089892998562762

13. Rowe, K. C., Paulsen, J. S., Langbehn, D. R., Duff, K., Beglinger, L. J., Wang, C., … Moser, D. J. (2010). Self-paced timing detects and tracks change in prodromal Huntington disease. Neuropsychology, 24(4), 435–442. http://doi.org/10.1037/a0018905

14. Maricq, A. V., & Church, R. M. (1983). The differential effects of haloperidol and methamphetamine on time estimation in the rat. Psychopharmacology, 79(1), 10–15. http://doi.org/10.1007/BF00433008

15. Ward, R. D., Kellendonk, C., Simpson, E. H., Lipatova, O., Drew, M. R., Fairhurst, S., … Balsam, P. D. (2009). Impaired timing precision produced by striatal D2 receptor overexpression is mediated by cognitive and motivational deficits. Behavioral Neuroscience, 123(4), 720–730. http://doi.org/10.1037/a0016503

16. Hinton, S. C., & Meck, W. H. (2004). Frontal-striatal circuitry activated by human peak-interval timing in the supra-seconds range. Cognitive Brain Research, 21(2), 171–182. http://doi.org/10.1016/j.cogbrainres.2004.08.005

17. Tanaka, S. C., Doya, K., Okada, G., Ueda, K., Okamoto, Y., & Yamawaki, S. (2004). Prediction of immediate and future rewards differentially recruits cortico-basal ganglia loops. Nature Neuroscience, 7(8), 887–893. http://doi.org/10.1038/nn1279

18. Gershman, S. J., Moustafa, A. A, & Ludvig, E. a. (2014). Time representation in reinforcement learning models of the basal ganglia. Frontiers in Computational Neuroscience, 7(January), 194. http://doi.org/10.3389/fncom.2013.00194

19. Mello, G. B. M., Soares, S., & Paton, J. J. (2015). A Scalable Population Code for Time in the Striatum. Current Biology, 25(9), 1113–1122. http://doi.org/10.1016/j.cub.2015.02.036

20. Yabe, Y., & Goodale, M. a. (2015). Time Flies When We Intend to Act: Temporal Distortion in a Go/No-Go Task. Journal of Neuroscience, 35(12), 5023–5029. http://doi.org/10.1523/JNEUROSCI.4386-14.2015

21. Press, C., Berlot, E., Bird, G., Ivry, R., & Cook, R. (2014). Moving time: The influence of action on duration perception moving time. Journal of Experimental Psychology: General, 143(5), 1787–1793. http://doi.org/10.1037/a0037650

22. Droit-volet, S., & Wearden, J. (2002). Speeding up an internal clock in children? Effects of visual flicker on subjective duration. The Quarterly Journal of Experimental Psychology, 55B, 193–211. http://doi.org/10.1080/0272499014300025

23. Droit-Volet, S. (1998). Time estimation in young children: an initial force rule governing time production. Journal of Experimental Child Psychology, 68(3), 236–249. http://doi.org/10.1006/jecp.1997.2430

24. Lejeune, H., & Wearden, J. H. (2006). Review article Scalar properties in animal timing : Conformity and violations. Quarterly Journal of Experimental Psychology, 59(908038074), 1875 –1908. http://doi.org/10.1080/17470210600784649

25. Gibbon, J. (1977). Scalar expectancy theory and Weber's law in animal timing. Psychological Review, 84(3), 279–325. http://doi.org/10.1037/0033-295X.84.3.279

26. Grossberg, S., & Schmajuk, N. A. (1989). Neural dynamics of adaptive timing and temporal discrimination during associative learning. Neural Networks, 2(2), 79–102. http://doi.org/10.1016/0893-6080(89)90026-9

27. Suri, R. E., & Schultz, W. (1999). A neural network model with dopamine-like reinforcement signal that learns a spatial delayed response task. Neuroscience, 91(3), 871–890. http://doi.org/10.1016/S0306-4522(98)00697-6

28. Howard, M. W., MacDonald, C. J., Tiganj, Z., Shankar, K. H., Du, Q., Hasselmo, M. E., & Eichenbaum, H. (2014). A Unified Mathematical Framework for Coding Time, Space, and Sequences in the Hippocampal Region. Journal of Neuroscience, 34(13), 4692–4707. http://doi.org/10.1523/JNEUROSCI.5808-12.2014

29. Ludvig, E. a, Sutton, R. S., & Kehoe, E. J. (2008). Stimulus representation and the timing of reward-prediction errors in models of the dopamine system. Neural Computation, 20(12), 3034–3054. http://doi.org/10.1162/neco.2008.11-07-654

30. Staddon, J. E., & Higa, J. J. (1999). Time and memory: towards a pacemaker-free theory of interval timing. Journal of the Experimental Analysis of Behavior, 71(2), 215–251. http://doi.org/10.1901/jeab.1999.71-215

31. Zeiler, M. D., & Powell, D. G. (1994). Temporal control in fixed-interval schedules. Journal of the Experimental Analysis of Behavior, 61(1), 1–9.

32. Haggard, P., & Chambon, V. (2012). Sense of agency. Current Biology : CB, 22(10), R390–2. http://doi.org/10.1016/j.cub.2012.02.040

33. Gallistel, C. R., King, A., & McDonald, R. (2004). Sources of variability and systematic error in mouse timing behavior. Journal of Experimental Psychology. Animal Behavior Processes, 30(1), 3–16. http://doi.org/10.1037/0097-7403.30.1.3

34. Oprisan, S. a, & Buhusi, C. V. (2014). What is all the noise about in interval timing? Philosophical Transactions of the Royal Society of London. Series B, Biological Sciences, 369(1637), 20120459. http://doi.org/10.1098/rstb.2012.0459

35. Gibbon, J., Malapani, C., Dale, C. L., & Gallistel, C. R. (1997). Toward a neurobiology of temporal cognition: advances and challenges. … Opinion in Neurobiology, 7, 170–184. Retrieved from http://www.sciencedirect.com/science/article/pii/S0959438897800050

36. Ludvig, E. a, & Staddon, J. E. R. (2005). The effects of interval duration on temporal tracking and alternation learning. Journal of the Experimental Analysis of Behavior, 83(3), 243–262. http://doi.org/10.1901/jeab.2005.88-04

37. Fischer, B. J., Peña, J. L., & Konishi, M. (2007). Emergence of multiplicative auditory responses in the midbrain of the barn owl. Journal of Neurophysiology, 98(3), 1181–1193. http://doi.org/10.1152/jn.00370.2007

38. Fischer, B. J., Anderson, C. H., & Peña, J. L. (2009). Multiplicative auditory spatial receptive fields created by a hierarchy of population codes. PLoS ONE, 4(11), 24–26. http://doi.org/10.1371/journal.pone.0008015

39. Nezis, P., & van Rossum, M. C. W. (2011). Accurate multiplication with noisy spiking neurons. Journal of Neural Engineering, 8(3), 034005. http://doi.org/10.1088/1741-2560/8/3/034005

40. Bejjanki, V. R., Beck, J. M., Lu, Z.-L., & Pouget, A. (2011). Perceptual learning as improved probabilistic inference in early sensory areas. Nature Neuroscience, 14(5), 642–648. http://doi.org/10.1038/nn.2796

41. Zhang, D., Li, Y., Rasch, M. J., & Wu, S. (2013). Nonlinear multiplicative dendritic integration in neuron and network models. Frontiers in Computational Neuroscience, 7(May), 56. http://doi.org/10.3389/fncom.2013.00056

42. Thivierge, J. P., Rivest, F., & Monchi, O. (2007). Spiking neurons, dopamine, and plasticity: timing is everything, but concentration also matters. Synapse, 61(6), 375–390. http://doi.org/10.1002/syn.20378

43. Fino, E. (2005). Bidirectional Activity-Dependent Plasticity at Corticostriatal Synapses. Journal of Neuroscience, 25(49), 11279–11287. http://doi.org/10.1523/JNEUROSCI.4476-05.2005

44. Malapani, C., Deweer, B., & Gibbon, J. (2002). Separating storage from retrieval dysfunction of temporal memory in Parkinson's disease. Journal of Cognitive Neuroscience, 14(2), 311–322. http://doi.org/10.1162/089892902317236920

45. Gautier, T., & Droit-Volet, S. (2002). Attention and time estimation in 5- and 8-year-old children: A dual-task procedure. Behavioural Processes, 58(1-2), 57–66. http://doi.org/10.1016/S0376-6357(02)00002-5

46. Jin, X., & Costa, R. M. (2010). Start/stop signals emerge in nigrostriatal circuits during sequence learning. Nature, 466(7305), 457–462. http://doi.org/10.1038/nature09263

47. Jazayeri, M., & Movshon, J. A. (2006). Optimal representation of sensory information by neural populations. Nature Neuroscience, 9(5), 690–696. http://doi.org/10.1038/nn1691

CHAPTER 4: Decoding time from ongoing behavior

SUMMARY

To separate the temporal signal from other variables that covary with time is one of the most difficult problems faced in the electrophysiological study of interval timing. Behavior is the most concerning among these variables because it is the mean by which animals report their estimates of time. Additionally, defenders of the embodied cognition perspective posit that animals can use the structure of their own behavior to purposefully encode information about the environment. Nonetheless, researches that attempt to extract environmental information from the structure of the ongoing behavior are almost inexistent. We wanted to know if animals' ongoing behavior during the serial fixed interval timing (SFI) task embedded information about the passage of time. We tested this hypothesis by using a maximum likelihood decoder onto high speed videos of rats performing the SFI task. In comparison to the behavioral events from the operant chamber, we could predict almost perfectly what behavior the animals were engaging using data from the video. We observed that although the decoder was sensitive to temporal estimates across trials and FI-blocks, it was very poorly sensitive to the passage of time within each FI. Consequently, we could not prove that animals use embodied-cognition-based strategies to perceive the passage of time. Nonetheless, this work represents a methodological step toward the understanding on how animals might use their behavior to interact with a complex environment.

INTRODUCTION

Interval timing is the ability to estimate lapses of time between events in the range of seconds to minutes. This ability enables animals to identify patterns and regularities from the ever-changing environment, and generate anticipatory adaptive behaviors [1]. Hence, understanding of how animals represent time can shine light on how the brain represents reality, interact with the world and can ultimately help us to develop intelligent artificial agents. But regardless the great effort to comprehend interval timing, and the progress made to unveil how time is perceived, the biological mechanisms that underlie interval timing remain elusive.

The question of how timing is implemented has motivated a quest for the internal clock. Many models about how neural structures could implement this internal clock have been proposed. Some of these models use many mechanisms such as coincidence detection among oscillations of varying frequencies [2-4], integration of the noisy firing of neural populations [5] and variable firing dynamics within a population of neurons [6-8]. Nonetheless, other class of models bases its assumptions on the widely replicated observation that structured behavioral chains emerge in temporally structured reinforcement contingencies [9-15]. Indeed, these models posit that time is represented as a trajectory progressing through a sequence of behavioral states [16,17].

Supporting the idea that interval timing is driven by behavioral states, the embodied cognition theory posits that animals can leverage the idiosyncrasies of their sensors and effectors [18,19] to encode relevant environmental information in the structure of their behavior [20,21]. For instance, one can fold three fingers and keep them folded to hold information about the number of objects in a room, and then retrieve the information later by counting the number of folded fingers. To encode time, animals could generate action sequences as the temporal representations, and decide correctly about how much time has elapsed based on their current sensorimotor state [22].

Recently, Gouvêa *et al.* [23] provided evidence that rats might develop embodied strategies to represent the passage of time. In a two-alternative forced choice task (TAFC) they trained rats to discriminate the durations of the interval between the onset and the offset of sound cues. Rats had to press a

lever on the left or on the right for intervals that were shorter or longer than 1.5s respectively. They observed that some rats displayed a stereotypical sequence of behaviors starting at the onset cue. Depending on how long the interval was, the offset cue interrupted the animals at different points of their behavioral sequences. These rodents seemed to use their sensory-motor state (i.e., where they were in this sequence), at the moment of the offset cue, as their decision criteria for time. If they were in the earlier steps of the sequence they chose left, and right otherwise. Consequently, Gouvêa and colleagues could predict the animal's decision from its behavior at the moment of the offset cue.

The striatum has been implicated in interval timing [24,25], and its activity might provide biological plausibility to the embodied cognition's argument. Beyond its role in decision making [26], reinforcement learning [24,27-29] and timing [25,30], the dorsolateral striatum contributes to habitual learning (i.e., procedural memory; [31,32]). Habitual learning consists in chaining individual behaviors into sequences which are resistant to extinction and devaluation [33]. Hence, the striatum is especially suitable to generate sequences of actions, take decisions based on sensorimotor states and learn from these sequences.

Despite this scenario, very few studies addressed how variations in chains of behaviors should correlate with variations in time estimation [23]. Thus the amount of information stored in the structure of behavior remains unknown in most of interval timing research.

In the TAFC tasks, such as the one used by Gouvêa *et al.* [23], there is a necessary spatial element that animals can exploit (e.g., pressing left or right). However, it is not clear whether this behavioral strategy to time would emerge in tasks where the responses to different intervals are the same but at different times. In particular, we would like to know if rats were performing sequences of actions during the serial fixed interval (SFI; [30]; see Chapter 2) task which could be used to support timing.

In this work we analyzed the ongoing behavior captured using high speed videos. We used recent advances in computing power and computer vision algorithms to automate the analysis of the behaviors from these videos. Briefly,

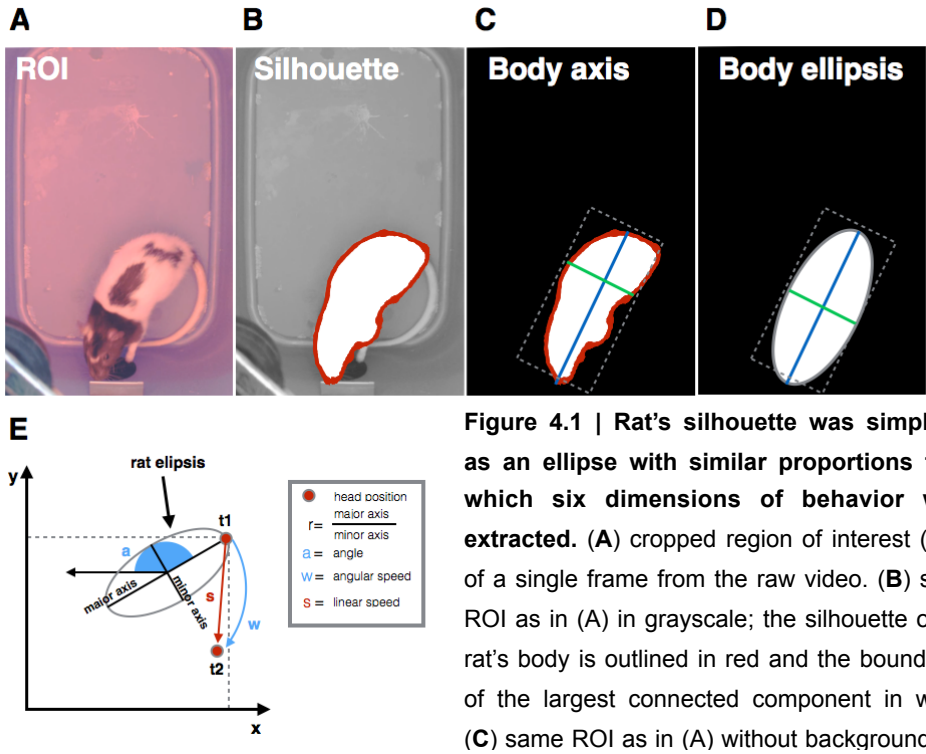

Figure 4.1 | Rat's silhouette was simplified as an ellipse with similar proportions from which six dimensions of behavior were extracted. (**A**) cropped region of interest (ROI) of a single frame from the raw video. (**B**) same ROI as in (A) in grayscale; the silhouette of the rat's body is outlined in red and the boundaries of the largest connected component in white. (**C**) same ROI as in (A) without background; the major and the minor axes of the connected component; dashed gray lines outline the boundaries of the largest connected component. (**D**) Ellipse (gray solid line) created using the major axis (blue line), minor axis (green line), angle of the major axis and boundaries (gray dashed line) of the major and minor axes as its parameters. (**E**) Schematics of the behavioral dimensions. The first two dimensions were the position of the head extracted in horizontal (x) and vertical (y) dimensions of every video frame (red circles with gray outline; here we exemplify two points in time, t1 and t2). The third dimension was the angle between the head edge of the major axis and the horizontal axis, represented here in blue shaded area and letter "a". The fourth dimension was the ratio between the major and the minor axes lengths. The fifth and the sixth dimensions were the linear (depicted by red line and letter "s") and angular (depicted by blue line and letter "w") speeds calculated at every frame from the difference between the current head position and the head position in the previous frame.

we adopted the following approach: we first reduced the dimensionality of the behavior represented in the video by describing the animal's body as an ellipsis (Figure 4.1A-D). Next, we extracted six continuous behavioral descriptors from the elliptical representation of the animal's body (Figure 4.1E; e.g., horizontal and vertical head positions, head linear and angular speeds, body angle, major-minor axis ratio). Then, we used these six variables, extracted from

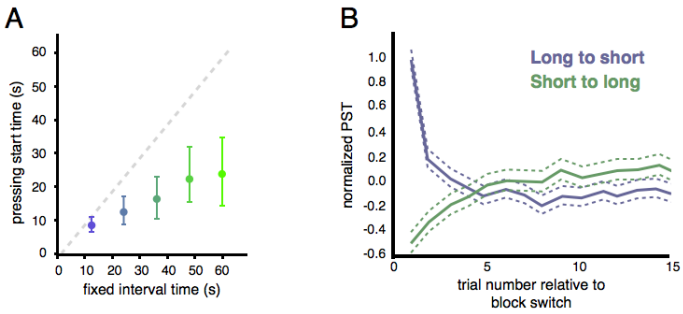

Figure 4.2 | PST adjusts to the new FI in less than 7 trials. (A) Median and interquartile range of PST for each of the five FIs (from 12s as blue to 60s as green). **(B)** Normalized PST for the first 15 trials after block switch. Solid blue trace represents block switches from any FI to the 12s FI block (long to short). The solid green trace represents block switches from any FI to the 60s FI (short to long). Dashed lines show the SEM. PSTs were normalized by subtracting the mean within-FI PST, and dividing by the within-FI standard deviation, across all sessions.

stable timing trials (8th trial onward from FI-block transition) to train a maximum likelihood decoder. Finally, we ran the decoder on every trial to generate time estimates, and observed how well these estimates corresponded to real time.

The decoder revealed sensitivity to interval transitions across early trials of the shortest and the longest blocks, evidenced by direction and systematic reduction of error across trials. Thus, it validates the approach to the problem at hand. Nevertheless, temporal estimates derived from behavior within trials shown little sensitivity to the passage of time, being almost constant during the early seconds of each interval, where the animal was retrieving the reward. These results suggest that animals do not organize their behavior in a stereotyped trajectory across a chain of actions as in Gouvêa *et al.* [23] (e.g., trajectory), but in a sequence of behavioral states between which the transition probabilities are affected by the fixed interval.

This work, for the first time, validates the use of the established decoding approach to answer embodied cognition questions (e.g., what information about the environment is embedded in the structure of the behavior), leveraging modern computer vision techniques. Further refinement in this approach can allow decoders to become sensitive to finer movements and provide higher standards to analyze behavioral data.

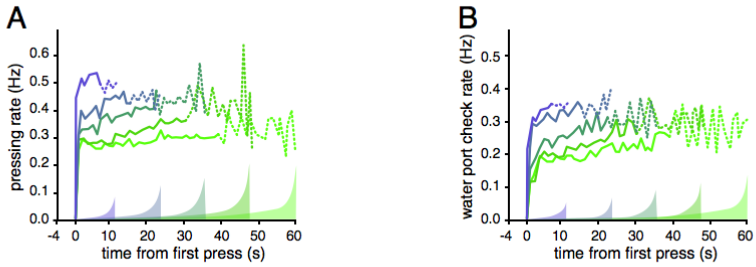

Figure 4.3 | Rats' pressing and licking behavior is constant after pressing onset. Normalized PST for the first 15 trials after block switch. Solid blue trace represents block switches from any FI to the 12s FI block (long to short). The solid green trace represents block switches from any FI to the 60s FI (short to long). Dashed lines show the SEM. PSTs were normalized by subtracting the mean within-FI PST, and dividing by the within-FI standard deviation, across all sessions.

RESULTS

Rats manifest typical behavior under serial fixed interval of reinforcement

Two male rats adjusted their pressing start times (PST) gradually to new intervals in the SFI task (Figure 4.2), taking up to 7 trials to reach average performance under the new criteria. As in the original experiment [30] pressing rate was proportional to reward rate and relatively constant along the FI (Figure 4.3A). Rates of head entries to the water port following the PST were lower than pressing rates and, as theses rates, also differ across FI to the other but were constant along each FI (Figure 4.3B).

Behavioral events estimates derived from video closely map the behavior observed by sensors in the operant chamber

We attempted to derive estimates of which behavior the animal was doing on every trial using the video data. Visual inspection of the behavior could classify behaviors in four distinct classes, namely: lick before PST, lick after PST, pressing and undefined. These behaviors could be easily identified by using the operant chamber's data. When a behavior was emitted in a video frame that was away three frames from any one of the other classes of behavior, we marked it as an undefined behavior. For every trial we trained the decoder using data from all but the current trial. For every behavioral class (i.e., lick before PST, lick after PST, pressing, undefined) we generated a distribution of

behavioral descriptors (6 dimensions) using the data from the three video frames surrounding each behavioral event. Then, at every frame of the current trial, we extracted the current behavioral descriptors. With both information from the distribution of behavior in other trials and the current behavior, we asked which one of the four behavioral classes was the most likely, given the current behavioral descriptors. We used the most likely (i.e. mode) behavior as our estimation of the current behavior and use that estimation to label the frame (Figure 4.4 shows a single session comparison between real data, left, and estimated data, right). By repeating this process for all sessions, we could generate the posterior Figure 4.5.

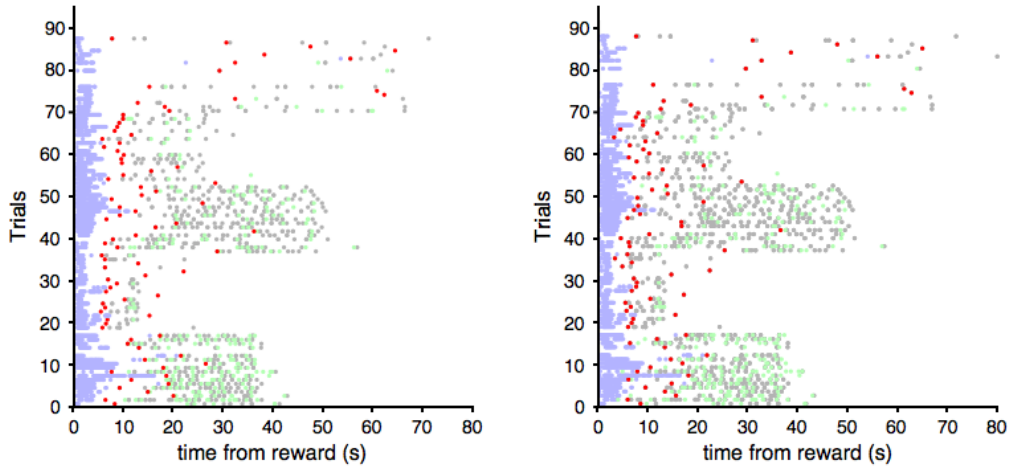

Figure 4.4 | Comparison between experimental behavioral data and behavior estimated from video data. Example of lever pressing behavior (gray), PST (red), pre-PST water port entries (blue) and post-PST water port entries (green) in a single session of the SFI task. On the left, experimental data, and on the right the estimated behavior derived from video data.

In most of the time, the decoder could estimate which behavior the animal was doing. The decoder performed especially well in face of highly stereotypical and distinct behaviors such as retrieving water. Conversely, when the animal was in an undefined behavior frame, chances of detecting pressing and water port checks were higher than when the animal was engaged in a particular behavior in the frame (Figure 4.5).

In order to be detected by the operant chamber, the behavior must be strong enough to activate the sensors. An animal that stands and touches the

lever without pressing it, or puts its head in the head-port without breaking the infra-red bean would probably have a very similar behavior, in the camera's perspective, as the fully executed behavior. But this difference in magnitude, although potentially irrelevant to the camera, is the difference that makes the operant chamber detects a behavior or not. Hence, it is possible that the rats were indeed emitting the behaviors estimated by the decoder but with lower magnitude.

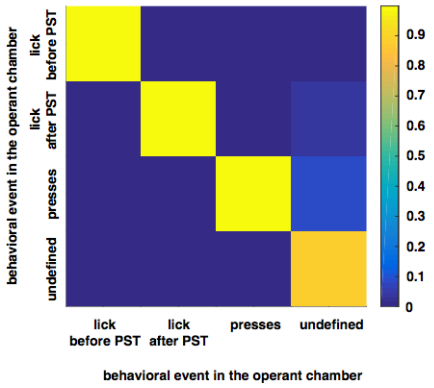

Figure 4.5 | Behavioral event estimates from video given the behavior observed in the operant chamber.

Single trial decoding captures behavioral systematic temporal error across trials on block switches

To explore the possibility that the temporal relationship between PST and FI might emerge from a chain of behaviors sequentially organized, we asked two questions. Firstly, we inquired whether errors in estimated time systematically followed the changes in the behavioral report of time at block transitions. Secondly, we asked whether the elapsed time estimates decoded from the video covaried with true time within the FI. We applied a decoding approach [35] to the data collected from single trials near to the block transitions, wherein animals systematically changed their pressing start times. We constructed a maximum likelihood decoder to derive an estimate of elapsed time from reward on single trials given behavioral features (e.g., head position, head linear and angular speed, body angle) extracted from the high-speed video. We limited our analysis to the first trials of the 12s and the 60s FI blocks because these blocks were the shortest and longest FIs employed, respectively. Transitions to these blocks were unidirectional (preceding blocks were always of longer FIs for 12s and of shorter FIs for 60s); animals reliably started to press later in the 12s FI and earlier in the 60s FI relative to the average PST in the 8th trial onward in the block. Hence, rats over- and underestimated the amount of time remaining until reward as they entered the 12s and the 60s blocks.

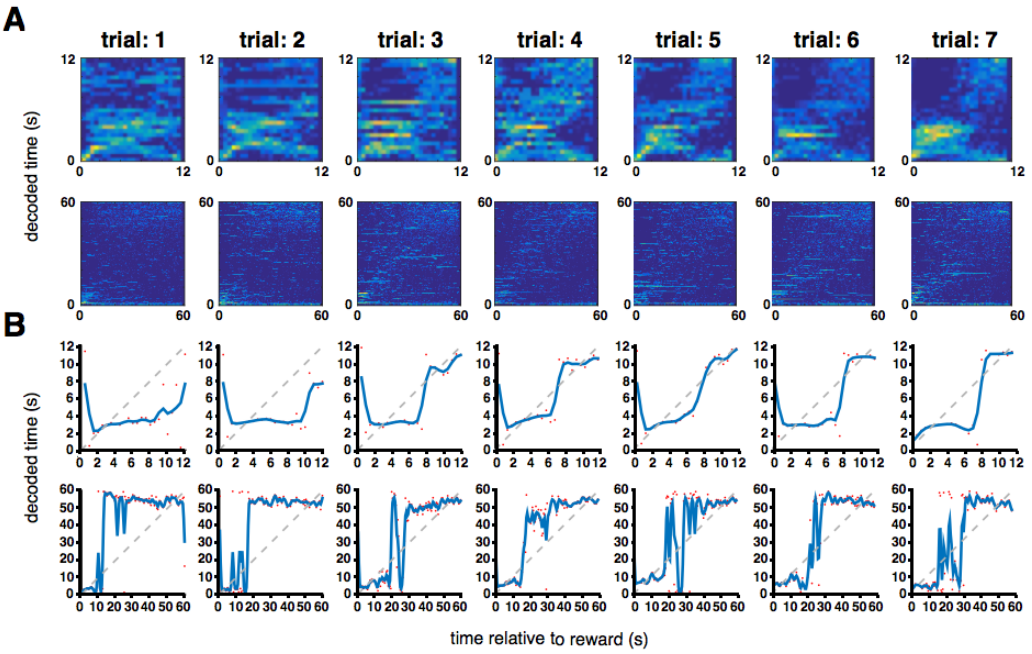

Figure 4.6 | Single trial estimates of elapsed time decoded from ongoing behavior during initial trials of 12s and 60s FI blocks. (**A**) Confusion matrix of video decoded estimates of elapsed time from reward on single trials, for the first seven trials of the 12s FI block (top) and 60s FI block (bottom) plotted against true time (bin size = 0.5s). (**B**) Circular average estimate (red dots) and running average (blue line) of video decoded estimate of elapsed time from reward on single trials, for the first seven trials of the 12s FI block (top) and 60s FI block (bottom) plotted against true time (bin size = 0.5s).

Briefly, our decoder was constructed as follows: On each of the first seven trials of a block, we generated a frequency histogram of the behavior where each dimension was a different behavioral parameter. Then we asked how likely we were to have observed that behavior at each video frame (time) given the observed distributions of behaviors on trials eight and onward of the corresponding block. This generated a likelihood function for current time given an observed behavior in each video frame. We projected this function onto a polar coordinate system, so that one revolution represents a full interval. By doing this we prevented estimation biases toward the center of the interval when the distribution was skewed toward the edges of the interval and multimodal. Then we took the circular average of the posterior function as our estimate for current time. The distribution of estimated times for each time point

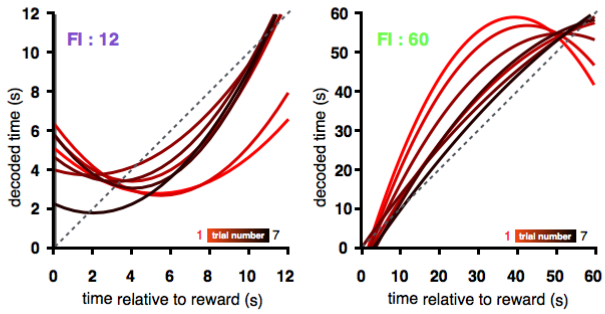

Figure 4.7 | Elapsed time estimates decoded from video correlate with true time during initial trials of 12s and 60s FI blocks. Decoded estimates of elapsed time for the first seven trials of the 12s (left) and 60s (right) FI block plotted in the same axis. Curves are quadratic fits to the circular mean of the likelihood function of each individual trial (red dots in Figure 4.3B). Red curves represent early trials and black curves represent later trials.

can be observed in the confusion matrices in Figures 4.6A for the seven first trials (columns) in the 12s (top row) and 60s (bottom row) FIs.

Systematic errors between estimates and true time were present in the first few trials of the 12s and 60s FI blocks (Figure 4.6B). We could observe this feature by plotting the estimates derived from multiple trials on the same axes (Figure 4.7, quadratic fits). Initial estimates were relatively slow and fast on the first trials of the 12s and 60s FI blocks respectively, and became more accurate after the first few trials.

The question that follows from these systematic errors is whether the errors in decoded time estimates over the first trials of each block were correlated with timing behavior. We found that the mean PST was significantly correlated with the errors in time estimates derived from the population over the first seven trials of the 12s and the 60s FI blocks (Figure 4.8, FI = 12, $R2 = 0.9$, $p < 0.01$, FI = 60, $R2 = 0.81$, $p < 0.01$). On the initial trials of the 12s FI block, rats began pressing late in comparison to subsequent trials, and likewise the decoded estimate of time relative to reward ran slow (Figures 4.7 left and 4.8 blue trace). Conversely, in the first trials of the 60s FI block the decoded estimate ran quickly on early trials, and rats were early to press (Figures 4.7 right and 4.8 green trace), displaying a similar relationship, yet opposite in direction.

Multimodal estimates of time within trial might suggest repetitive behavior within trials that lack sequential trajectory structure

Some features of the data suggest that animals engaged in repetitive behaviors within the FI. At the trial start the distribution of time estimates tended to be multimodal (Figure 4.6A). Consequently, the behavioral decoder did not distinguish well between the start and the end of the trial (Figure 4.6B). Also, time estimates were usually flat during the interval from ~0.5s to ~8s, most likely because during this time the rats were engaged in the repetitive behavior to acquire the reinforcer from the water port (i.e., licking; Figure 4.9). Additionally, the multimodality of decoded times in individual trials can be used as argument against the hypothesis that animals employed a stereotyped sequence of actions that develops over time within the FI. On the contrary, it suggests that animals performed many repetitive ballistic transitions between few behavioral states across the interval (i.e., pressing, checking the water port).

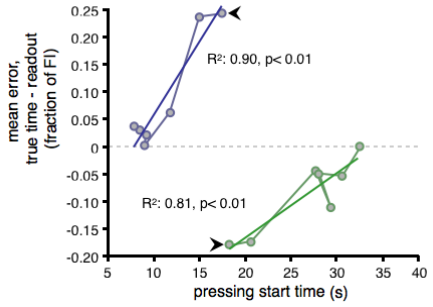

Figure 4.8 | Errors in decoded time predicted timing behavior. Mean error between true time and the video decoded estimate on the first seven trials of the 12s (blue) and 60s (green) FI blocks. Contiguous trials are connected by solid lines to display the trajectory of the data over trials, and the first trial on each block is indicated by the black arrow. Dashed horizontal gray line represents zero error average decoding as compared to true time.

A further visual inspection of the behavior suggests that animals alternate between four classes of behavioral states, namely: licking, press-checking, holding still and exploring. The latter two states were very infrequent (3 out of 100 trials inspected, 20 trials per FI) and only happened in the longest FI.

DISCUSSION

In this work we entertained the hypothesis that animals might have used cues of their sensorimotor state, in a highly structured sequences of actions that covaries with time, to produce judgements about time. To test this hypothesis we decoded time estimates from high speed videos of rats performing the SFI task. We used computer vision algorithms to reduce the dimensionality of the

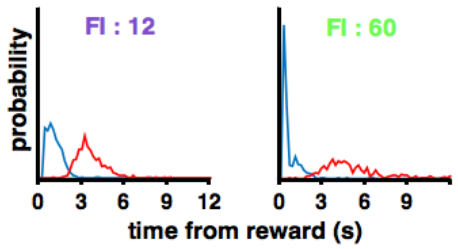

Figure 4.9 | Stereotyped reward acquisition behavior around the port might explain poor decoding performance within a fixed interval until ~7 seconds. Probability of licking sequence onset (blue) and licking sequence offset (red) in the first 12s of all five FIs for all the sessions of the two rats.

video into six behavioral descriptors, and then used these six variables to train a maximum likelihood decoder to estimate the current time.

Although the decoder could capture systematic changes in time estimated across trials from the start of the fixed interval transitions, we found that the temporal estimates decoded from ongoing behavior within the fixed interval correlated poorly with true time. The decoder sensitivity to the passage of time was especially poor when the behavior of the animal was highly invariant and repetitive (i.e., licking, pressing). These invariant behaviors clustered together at different moments of the interval, thus forming different “behavioral state modes”. Because the probability of the animal emitting any given behavioral state mode changed over time within the FI, the running average of the decoded time could capture this probability change across trials.

Although our approach represents a methodological step towards the understanding of how animals use sensorimotor states to encode information about the environment, there were some known limitations. Firstly, concerning the method, due to the process we used to reduce the video dimensionality, our approach could only capture broad movements and postures. This limited the decoder's ability to capture patterns that could emerge from fine movements. This issue might be especially problematic if we consider time as the encoded variable. But because it is well known that time perception is affected by general behavioral features such as motion flow [36,37] and movement [38], we are confident that this methodological limitation was not a major flaw. Secondly, there are some parameters of behavior that could be used to encode information that are not easily accessible from the video. For instance, a previous research from Droit-Volet [39] has shown that parameters of movements, such as the strength, were correlated with timing in pre-

arithmetical kids. Our approach completely ignored this dimension of behavior. Nonetheless, it is possible that these behavioral parameters have characteristic signatures in the behavior that might be observable in the video. If that was the case, deeper analysis of the video can provide more information about the behavior and associates processes.

We could not find any evidence to support the fact that the striatum encodes sequence of actions as a mean to time intervals. In fact, time estimates decoded from ongoing behavior were worse during the earlier seconds of each FI. This result conflicts directly with the data from Mello *et al.* [30], that shows that time estimates decoded from striatal population are best during the same earlier seconds of each FI. To support the claim that striatum is encoding time as a sequential action pattern, one could expect behavior to be more predictive of ongoing time in the same periods when striatal activity encodes it best. Thus this study provided arguments to support the claim stated in Mello *et al.* [30] that striatal activity has a temporal component which, although interacts with behavior, cannot be fully explained by it.

This work validates the decoder's sensitivity to behavior, by showing that it can identify behavioral events and the temporal features of the SFI task which could also be extracted through the operant chamber. We believe that future advancements in behavior tracking technology will open the possibility to probe into finer behavioral structures and extract patterns that may help us to understand how the brain represents the environment and implements behavior.

As it is, this work assessed the consistency with previous data in SFI task. It also demonstrates an alternative method, that leverages current technology, to assess different ways in which animals can encode environmental information, as depicted by the embodied cognition theory.

METHODS

All experiments were approved by the Champalimaud Foundation Bioethics Committee and the Portuguese *"Direção Geral Veterinária"*.

Behavioral set-up

Operant chambers consisted of a plastic bucket (rats, IKEA, Alfragide, Portugal) containing one operant lever (Med Associates ENV-110M) and one custom made acrylic nose port (Island Motion). The lever and the nose port were aligned horizontally on the middle of one of the smallest walls of the box; the nose port was placed vertically close to the ground level and the lever positioned vertically higher so rats had to stand to press. The nose port contained one infra-red beam/sensor pair for detecting muzzle entries in the port and one visible (white light) LED. In addition, a rubber tube connected a 30 mL syringe filled with water (reward), a solenoid valve (Lee) and the nose port together. These valves were calibrated to deliver ~15 μL of water per reward event. Stripes of LEDs illuminated the operant chamber with red light. Rats are irresponsive to red light spectrum due to lack of specific red sensitive opsin in the eye [41,42].

Except for the video camera, all sensors and effectors in the behavioral box were read and controlled by an Arduino Mega 2560 microprocessor (additional information and free software available at http://www.arduino.cc/) via a custom circuit board. The microprocessor implemented the behavioral task, and outputted data to a desktop computer through serial communication. A custom software based on Python's pySerial module (freely available at http://pyserial.sourceforge.net/) performed the data acquisition.

Behavior and subjects

Two male Long-Evans hooded rats (*Rattus novergicus*) were trained in the Serial Fixed Interval (SFI; see methods in Mello *et al.*[30]) timing task, where the Fixed Intervals varied randomly in blocks of >18 trials among five intervals ranging in multiples of 12s from 12s to 60s. A custom Arduino state machine software controlled the task and outputted the raw data to the custom data acquisition software developed in Python.

Video acquisition and tracking

We acquired top view videos of the rats performing the SFI task with a high speed camera (Flea3FL3-U3-13S2C-CS, PointGrey Research Inc., Richmond, Canada) at 120 frames/s with a resolution of 1280 × 960 pixels in grayscale at

8 bits. Video acquisition and online tracking were performed using the in-house developed software Bonsai (freely available at http://bitbucket.org/horizongir/bonsai/downloads). Each frame of the video was background subtracted (absolute difference of a frame with the image of the empty box), smoothed with a 21 pixels kernel and then thresholded. Standard computer vision procedures of erode and dilate were used to eliminate noise and to assure that the animal's body appeared as the largest distinct blob in each frame. Once parameters were set for each video, the largest connected component (i.e., largest blob of pixels) was automatically tracked, and its properties used for further analysis.

We used a standard procedure to simplify the rat's shape [43]. By taking the major and the minor axes of the connected component, we could represent the body of the rat as an ellipse (see Figure 4.1). The major axis matched the rostral to caudal axis of the rat's body and the minor axis the perpendicular dimension, or the width of its body (Figure 4.1C). The center of this ellipse was the center of the major axis in x (horizontal) and y (vertical) dimensions. We assumed that information about fine movements (e.g., pinna, whiskers bauds) or body bent was completely removed from the data set after this simplification process.

Since our simplification of rat's body had no information about the head position, we established the following heuristics to identify it. On every water port visit, we defined that extreme of the major axis nearest (euclidean distance) to the water port was the head position. We considered this edge of the major axis to be the head position in x and y for all tracking purposes until the next visit to the water port. We also obtained the linear speed of the head movement by calculating the euclidean distance of the head position in two consecutive frames.

The angle of the major axis, as representative of the direction to which the rat is facing. The angular difference in two consecutive frames was considered the angular speed.

Finally, we performed a visual inspection of the video using ellipse properties to help us to identify behavioral patterns. The ratio between the lengths of the major and the minor axis seemed to correlate with the rearing

and grooming behaviors. The closer the major/minor axis ratio was to one, the higher the animal stood or the more curled it was over its own body (data not shown). Due to its high face validity, we decided to include the major to minor axis ratio as one of the behavioral measures.

Video maximum likelihood decoder

We decoded the current time from the ongoing behavior of the animals recorded in high speed videos (120 fps). The head position (x,y), linear head speed (s), major-minor axis ratio (r), angular position of the body (a) and angular speed (w) were the behavioral descriptors we extracted from the video data to implement our decoding (Figure 4.1E; see Video Acquisition and Tracking in methods section).

Once we had the six dimensions of the behavior for each video frame, we generated the prior probability for any particular behavior *P(x,y,s,r,a,w)* by generating a probability distribution histogram for each behavioral variable independently, except for head position that was calculated as the joint probability of x and y. All the dimensions had their values normalized by the amplitude (i.e., x = (x-min(X))/(max(X)-min(X)) of values in that dimension, so that all dimensions had values from 0 to 1. Each dimension was discretized with 40 bins of even sizes. Then, we convolved these histograms with a standard gaussian kernel ($\mu = 0$ $\sigma = 1$), or a bidimensional gaussian in the case of head position. The prior was calculated independently using the data from all trials that had the same FI, excluding data from the first seven trials of each block.

Next, we estimated the distribution of behaviors in a particular frame (time), relative to the start of the trial (reward). We used a similar process to the one used to generate the prior, but with one difference. We generated the behavior distribution histograms using frames that had the same delays relative to the start of the trial (in bins of 0.5s). This allowed us to estimate the distribution of behavior in a particular time relative to the reward. We calculated their probability independently for each delay from block start. Because timing behavior was stable in the 8th trial or higher from the block start, only frames belonging these trials were used to train our decoder.

To decode time from ongoing behavior *P(t|x,y,s,r,a,w)*, we used an iterative bayesian inference process. We started by extracting the current behavioral state for every time (frame) in the current trial, and then calculating the probability of time given the behavioral parameter by seeing how likely this particular behavior was for all times divided by the prior. Since we assumed independence among behavioral variables we calculated the time estimate probability separately for each behavioral parameter, and then we multiplied all the posteriors by each other. Since FI transitions to the shortest and longest FIs (12s and 60s respectively) were unidirectional, we only used trials from these FIs, and from these trials, only the first seven trials from the block start were included.

To get our time estimate, we circularized time by linking the end of the interval to its beginning. We did this by representing the resulting posterior distribution of time given behavior in a polar space using time as the angular dimension; one revolution was equal to one interval. Then we extracted the circular average. This process was especially important to prevent errors in multimodal distributions (which composed 2% of the trials). Next, we reconverted the average vector back to polar space, and finally restored the original time series unit. Thus, the average angle provided the time estimate.

Each estimate was then used to generate the confusion matrix (Figures 4.6A). Finally, due to the high skewness and multimodality of the distribution of decoded times for each frame in the confusion matrix, we used the circular mean of time estimates to visualize the decoding trend (Figures 4.6B).

ACKNOWLEDGEMENTS

We thank Gonçalo Lopes and Ricardo Ribeiro for creative and critical input about the video tracking system. We thank Tiago Monteiro and Thiago Gouvêa for the help constructing the behavioral set-up. We thank the histopathology and the vivarium staff from the Champalimaud Scientific and Technological Platforms for the support. We thank Gonçalo Lopes and Tiago Monteiro for the help reviewing this article. The work was supported by Champalimaud and Gulbenkian Foundations and fellowships to G.M. from the Portuguese Foundation for Science and Technology.

REFERENCES

1. Buhusi, C. V, & Meck, W. H. (2005). What makes us tick? Functional and neural mechanisms of interval timing. Nature Reviews. Neuroscience, 6(10), 755–765. http://doi.org/10.1038/nrn1764
2. Miall, C. (1989). The Storage of Time Intervals Using Oscillating Neurons. Neural Computation, 1(3), 359–371. http://doi.org/10.1162/neco.1989.1.3.359
3. Matell, M. S., & Meck, W. H. (2004). Cortico-striatal circuits and interval timing: Coincidence detection of oscillatory processes. Cognitive Brain Research, 21(2), 139–170. http://doi.org/10.1016/j.cogbrainres.2004.06.012
4. Matell, M. S., & Meck, W. H. (2000). Neuropsychological mechanisms of interval timing behavior. BioEssays, 22(1):94-103. http://doi:10.1002/(SICI)1521-1878(200001)22:1<94::AID-BIES14>3.0.CO;2-E
5. Simen, P., Balci, F., de Souza, L., Cohen, J. D., & Holmes, P. (2011). A model of interval timing by neural integration. The Journal of Neuroscience : The Official Journal of the Society for Neuroscience, 31(25), 9238–9253. http://doi.org/10.1523/JNEUROSCI.3121-10.2011
6. Grossberg, S., & Schmajuk, N. A. (1989). Neural dynamics of adaptive timing and temporal discrimination during associative learning. Neural Networks, 2(2), 79–102. http://doi.org/10.1016/0893-6080(89)90026-9
7. Buonomano, D. V, & Merzenich, M. M. (1995). Temporal information transformed into a spatial code by a neural network with realistic properties. Science (New York, N.Y.), 267(5200), 1028–1030. http://doi.org/10.1126/science.7863330
8. Shinomoto, S., Omi, T., Mita, A., Mushiake, H., Shima, K., Matsuzaka, Y., & Tanji, J. (2011). Deciphering elapsed time and predicting action timing from neuronal population signals. Frontiers in Computational Neuroscience, 5(June), 29. http://doi.org/10.3389/fncom.2011.00029
9. Skinner, B. F. (1948). Superstition in the pigeon. Journal of Experimental Psychology, 38(2), 168–172. http://doi.org/10.1037/h0055873
10. Hodos, W., Ross, G. S., & Brady, J. V. (1962). Complex response patterns during temporally spaced responding. Journal of the Experimental Analysis of Behavior, 5, 473–479. http://doi.org/10.1901/jeab.1962.5-473
11. Anderson, M. C., & Shettleworth, S. J. (1977). Behavioral adaptation to fixed-interval and fixed-time food delivery in golden hamsters. Journal of the Experimental Analysis of Behavior, 27(1), 33–49. http://doi.org/10.1901/jeab.1977.27-33
12. Haight, P. a., & Killeen, P. R. (1991). Adjunctive behavior in multiple schedules of reinforcement. Animal Learning & Behavior, 19(3), 257–263. http://doi.org/10.3758/BF03197884

13. Machado, A., & Keen, R. (2003). Temporal discrimination in a long operant chamber. Behavioural Processes, 62(1-3), 157–182. http://doi.org/10.1016/S0376-6357(03)00023-8

14. Balci, F., Papachristos, E. B., Gallistel, C. R., Brunner, D., Gibson, J., & Shumyatsky, G. P. (2008). Interval timing in genetically modified mice: A simple paradigm. Genes, Brain and Behavior, 7(3), 373–384. http://doi.org/10.1111/j.1601-183X.2007.00348.x

15. Ölveczky, B. P. (2011). Motoring ahead with rodents. Current Opinion in Neurobiology, 21(4), 571–578. http://doi.org/10.1016/j.conb.2011.05.002

16. Killeen, P. R., & Fetterman, J. G. (1988). A behavioral theory of timing. Psychological Review, 95(2), 274–295. http://doi.org/10.1037/0033-295X.95.2.274

17. Machado, a. (1997). Learning the temporal dynamics of behavior. Psychological Review, 104(2), 241–265. http://doi.org/10.1037/0033-295X.104.2.241

18. Brooks, R. a. (1990). Elephants don't play chess. Robotics and Autonomous Systems, 6(1-2), 3–15. http://doi.org/10.1016/S0921-8890(05)80025-9

19. Critchley, H. D., & Harrison, N. a. (2013). Visceral Influences on Brain and Behavior. Neuron, 77(4), 624–638. http://doi.org/10.1016/j.neuron.2013.02.008

20. Wilson, M. (2002). Six views of embodied cognition. Psychonomic Bulletin & Review, 9(4), 625–636. http://doi.org/10.3758/BF03196322

21. Wilson, A. D., & Golonka, S. (2013). Embodied Cognition is Not What you Think it is. Frontiers in Psychology, 4(February), 58. http://doi.org/10.3389/fpsyg.2013.00058

22. Wolpert, D. M., & Landy, M. S. (2012). Motor control is decision-making. Current Opinion in Neurobiology, 1–8. http://doi.org/10.1016/j.conb.2012.05.003

23. Gouvêa, T. S., Monteiro, T., Soares, S., Atallah, B. V., & Paton, J. J. (2014). Ongoing behavior predicts perceptual report of interval duration. Frontiers in Neurorobotics, 8(MAR), 10. http://doi.org/10.3389/fnbot.2014.00010

24. Drew, M. R., Simpson, E. H., Kellendonk, C., Herzberg, W. G., Lipatova, O., Fairhurst, S., … Balsam, P. D. (2007). Transient overexpression of striatal D2 receptors impairs operant motivation and interval timing. The Journal of Neuroscience : The Official Journal of the Society for Neuroscience, 27(29), 7731–7739. http://doi.org/10.1523/JNEUROSCI.1736-07.2007

25. Meck, W. H. (2006). Neuroanatomical localization of an internal clock: A functional link between mesolimbic, nigrostriatal, and mesocortical dopaminergic systems. Brain Research, 1109(1), 93–107. http://doi.org/10.1016/j.brainres.2006.06.031

26. Kim, H., Sul, J. H., Huh, N., Lee, D., & Jung, M. W. (2009). Role of striatum in updating values of chosen actions. The Journal of Neuroscience : The Official Journal of the Society for Neuroscience, 29(47), 14701–14712. doi:10.1523/JNEUROSCI.2728-09.2009

27. Eunjeong Lee, X., Seo, M., Dal Monte, O., & Averbeck, B. B. (2015). Injection of a Dopamine Type 2 Receptor Antagonist into the Dorsal Striatum Disrupts Choices Driven by Previous Outcomes, But Not Perceptual Inference. Journal of Neuroscience 35(16), 6298–6306. http://doi.org/10.1523/JNEUROSCI.4561-14.2015

28. Klein-Flügge, M. C., Hunt, L. T., Bach, D. R., Dolan, R. J., & Behrens, T. E. J. (2011). Dissociable Reward and Timing Signals in Human Midbrain and Ventral Striatum. Neuron, 72(4), 654–664. http://doi.org/10.1016/j.neuron.2011.08.024

29. Seo, M., Lee, E., & Averbeck, B. B. (2012). Action Selection and Action Value in Frontal-Striatal Circuits. Neuron, 74(5), 947–960. http://doi.org/10.1016/j.neuron.2012.03.037

30. Mello, G. B. M., Soares, S., & Paton, J. J. (2015). A Scalable Population Code for Time in the Striatum. Current Biology, 25(9), 1113–1122. http://doi.org/10.1016/j.cub.2015.02.036

31. Mandali, A., Rengaswamy, M., Chakravarthy, V. S., & Moustafa, A. A. (2015). A spiking Basal Ganglia model of synchrony, exploration and decision making. Frontiers in Neuroscience, 9(May), 1–21. http://doi.org/10.3389/fnins.2015.00191

32. Sadeh, T., Shohamy, D., Levy, D. R., Reggev, N., & Maril, A. (2011). Cooperation between the hippocampus and the striatum during episodic encoding. Journal of Cognitive Neuroscience, 23(7), 1597–1608. http://doi.org/10.1162/jocn.2010.21549

33. Kandel, E. R., Schwartz, J. H., Jessell, T. M., Siegelbaum, S., & Hudspeth, A. J. (2012). Principles of Neural Science. Neurology (Vol. 1). http://doi.org/10.1036/0838577016

34. Ohayon, S., Avni, O., Taylor, A. L., Perona, P., & Roian Egnor, S. E. (2013). Automated multi-day tracking of marked mice for the analysis of social behaviour. Journal of Neuroscience Methods, 219(1), 10–19. doi:10.1016/j.jneumeth.2013.05.013

35. Quian Quiroga, R., & Panzeri, S. (2009). Extracting information from neuronal populations: information theory and decoding approaches. Nature Reviews. Neuroscience, 10(3), 173–185. http://doi.org/10.1038/nrn2578

36. Eagleman, D. M. (2005). Distortions of time during rapid eye movements. Nature Neuroscience. http://doi.org/10.1038/nn0705-850

37. Brown, S. W. (1995). Time, change, and motion: the effects of stimulus movement on temporal perception. Perception & psychophysics (Vol. 57). http://doi.org/10.3758/BF03211853

38. Yabe, Y., & Goodale, M. A. (2015). Time Flies When We Intend to Act: Temporal Distortion in a Go/No-Go Task. Journal of Neuroscience, 35(12), 5023–5029. http://doi.org/10.1523/JNEUROSCI.4386-14.2015

39. Droit-Volet, S. (1998). Time estimation in young children: an initial force rule governing time production. Journal of Experimental Child Psychology, 68(3), 236–249. http://doi.org/10.1006/jecp.1997.2430

40. Lopes, G., Bonacchi, N., Frazão, J., Neto, J. P., Atallah, B. V., Soares, S., … Kampff, A. R. (2014). Bonsai: An event-based framework for processing and controlling data streams. bioRxiv (Vol. 9). Retrieved from http://www.biorxiv.org/content/biorxiv/early/2014/07/02/006791.full.pdf

41. Szél, A., & Röhlich, P. (1992). Two cone types of rat retina detected by anti-visual pigment antibodies. Experimental Eye Research, 55(1), 47–52. http://doi.org/10.1016/0014-4835(92)90090-F

42. Radlwimmer, F. B., & Yokoyama, S. (1998). Genetic analyses of the green visual pigments of rabbit (Oryctolagus cuniculus) and rat (Rattus norvegicus). Gene, 218(1-2), 103–109. http://doi.org/10.1016/S0378-1119(98)00359-X

43. Ohayon, S., Avni, O., Taylor, A. L., Perona, P., & Roian Egnor, S. E. (2013). Automated multi-day tracking of marked mice for the analysis of social behaviour. Journal of Neuroscience Methods, 219(1), 10–19. doi: 10.1016/j.jneumeth.2013.05.013

CHAPTER 5: Conclusion and Discussion

Overview of the empirical findings

In this thesis we investigated the role of striatal activity in representing time in the range of seconds to one minute. We were especially interested in investigating three questions: what were the dynamics of striatal population activity under interval timing conditions, how these dynamics could account for timing and what was the nature of the information contained in these dynamics.

We addressed these questions by combining experimental and computational approaches. Firstly, we recorded neurons in the striatum while the animals were performing the SFI timing task. We observed responses that resembled a moving bump of activity across the population. This pattern of activity possessed three striking features: different neurons responded at different delays spanning the whole timed intervals, most of these responses held their relative position in time to each other when the interval to be timed changed, suggesting relative coding for time, and responses multiplexed information about time and behavior.

Secondly, because the striatal population activity continuously evolved in a non-repeating manner, it could serve as a representation of time. Indeed, we could decode time estimates from these striatal population activity. These estimates correlated with the animals' report of perceived time.

Thirdly, we tested whether the activity we observed in the striatum could be used to generate temporally adaptive behavior. To do so, we built a model to simulate animals' performance during the SFI task. Temporally adaptive behavior conforming to the mean accuracy sensitivity to the interval could be derived from the simulation. Interestingly, mean accuracy was also sensitive to the press-locked contributions. Time estimates in longer intervals, where animals pressed more times, had a left shift of their PST relative to the FI when compared to the shortest interval. Regarding the precision sensitivity to the interval, the dispersion of the PSTs was mainly affected by trial-by-trial variations in when the animals acquired the reward relative to the expected time. Ultimately, this variation was caused by the rate of pressing. Additionally,

we shown that PST precision sensitivity emerges from variations in pressing rates. Under the SFI schedule of reinforcement animals' pressing rate correlated with the FI. To approach the simulation's behavior to the FI correlated pressing rate displayed by the rodents, we tied the pressing rate to the reward rate (inverse of memory trace decay rate); in this condition, the precision sensitivity to the interval emerged from the simulation. We demonstrated that although the simulation conformed strictly to the criteria for scalar timing, by displaying a linear relationship between accuracy/precision to the interval, experimental data didn't.

Finally, we tested the embodied cognition hypothesis, which states that during an interval, the animal would display a structured and non-repeating sequence of actions in time that could be used as a representation for time. This hypothesis, suggests that the FI dependent dynamics observed in the striatal population encode behavioral information over time rather than time *per se*. Consequently, this hypothesis represents a major point of concern in interval timing research. To test it, we ran a bayesian decoder on behavioral data extracted from videos of animals performing the SFI task. We validated the decoder by showing that temporal estimates, derived from the video, captured the sign and magnitude of the temporal adjustment, as revealed in the behavioral data acquired through the operant chamber. Although the decoder captured shifts in temporal estimation across trials, our results failed to demonstrate clear temporally structured behavior within trial. Hence, we did not find evidence, in the SFI task, that could support the hypothesis that animals use chains of behaviors as their representation of time.

Mechanisms of interval timing and action selection

Our results have direct implications to the understanding of action selection mechanisms. Choosing how to act in order to maximize outcome and minimize effort or cost is the problem that RL [1] seeks to solve. To perform RL, animals have to establish a causal link between context, behavior and outcome. In naturalistic conditions, actions might be separated from their outcomes by long delays, or outcomes might depend on a series of actions instead of a single behavior (e.g., game of chess, ambushing a prey, or navigating through a

labyrinth). Consequently, it is much harder to distinguish the behavior that is critical to produce the desired outcome. To identify the critical behavior in a naturalistic situation, animals must take into account multiple variables (e.g., the value of the outcome, its conditional probability, its expected value) in function of time. For this reason, most RL models use some sort of representation of time [1,2]. The temporal representation within the striatum we found — as a series of progressively widening receptive fields for delays — resembled the temporal basis functions of some existing learning models. These basis functions are considered to be more biologically plausible, and to represent time more efficiently [3-5]. Such representation (as a set of basis functions) can incorporate a time-sensitive action selection mechanism into RL models [6]. Therefore, the sequential neural states, which we described in the striatum during timing behavior, could provide a unifying view of the BG's role in timing and RL. This claim is further supported by a dominant view about the BG that sustains its critical role to implement some aspects of RL [7-12]. Also, multiple loops within BG nuclei, and with other structures of the brain, can generate signals that propagate phasic inputs about environmental or behavioral events over time [13]. It is plausible that RL and interval timing may indeed be implemented by the same signal within the striatum, and our data support this hypothesis.

Experimental and theoretical studies suggest that different neural mechanisms might underlie interval timing, including: monotonically ramping neurons that integrate activity from a pacemaker or tonic input [14,15]; neurons that detect the beats of a population of oscillators that fire at different frequencies [16,17]; or a population clock [18], where the population of active neurons dynamically changes time progresses. Because these models are already accurate to predict the behavioral data [19-22], much of their attractiveness derives either from their simplicity (for engineering implementations) or from their potential to generate predictions about the biological underpinnings of the interval timing system, rather than from their predictive accuracy. Our data is most consistent with a population clock in which a sequential chain of active neurons encodes time.

What are the neural mechanisms driving this sequential state pattern? Data from other timing systems in the brain, that share some properties with the striatum, might help us to elucidate the matter. In the millisecond timing scales, temporal information is represented by an activity that lasts for the duration of the whole interval. This lasting activity allegedly arises from the dynamics within local recurrent circuits [23,24]. Striatal MSNs are GABAergic (i.e., inhibitory) neurons. Consequently, these neurons cannot sequentially drive each other in absence of external input. It is unlikely that the dynamics necessary to elicit the temporal code in our data are a product of local computations occurring within the striatum. One possibility is that this inhibitory feedback within the BG could generate a population clock in response to tonic input from the cortex. This scenario has been contemplated in cerebellar models of timing in which the negative feedback of the Golgi cells generates a time-varying neural trajectory in response to tonic input [25]. Nonetheless, this model has been used to explain data from trace conditioning experiments, where PFC provided this tonic input to the cerebellum during the interval between the conditioned and unconditioned stimuli over timescales that are around and below one second [26-29].

Could the striatum, or more generally the BG, generate a time-varying neural trajectory in response to tonic excitatory input from the cortex using negative feedback? At least two requirements must be fulfilled for that to happen. The first requirement to propagate a signal in time is an excitatory input or feedback that could drive and sustain the signal during the whole interval [13]. The striatum has three main sources of excitatory inputs that could fulfill this requirement, namely the CTX, thalamus and STN. Multiple sources of evidence [30-36] have established the critical role of PFC to interval timing. During the retention interval of delayed response tasks, the PFC manifests sustained patterns of activity that are thought to contribute to learning by providing a way to link one action to the next and allow reward signals to be combined over time. This persistent activity is often informative about the passage of time [35,37]. Nonetheless, in timing tasks, sustained activity in the PFC has only been observed to last for up to 5 s [37-39], or up to ~10 s in phasic activity around reward time [40]; certainly a duration much

smaller than the 60s necessary in the longest interval of the SFI. Although other cortical areas also carry temporal signals, evidence demonstrating the necessary role of these areas for interval timing is yet to be shown [35,41]. Thus, the source of excitation to drive the temporal representations in the striatum is likely to arise from the PFC or from other subcortical inputs. Consistent with the time-varying neural trajectory supported by negative feedback hypothesis, the PFC should provide continuous input to the striatum for the whole length of the interval. Therefore, if the PFC is the source of the excitatory drive to time signals in the striatum, future recordings of the PFC under the SFI condition should reveal sustained activity during the length of the interval of the FI. The second requirement is that striatum should have some sort of negative feedback process similar to the one implemented by Golgi cells in the cerebellum. Lateral inhibition between MSNs was once thought to have a winner-take-all function of the striatum [4], useful to select between possible actions. It has been noted that the reciprocal connections necessary for this interpretation are too few and their relative strength is weak [42-44]. But a simulation study made by Ponzi and Wickens [45] points otherwise. In this study, they have shown that ensembles of striatal neurons fired in sequential coherent episodes in the timescales of hundreds of milliseconds even when cortical excitation is simply constant or fluctuating noisily; the model used physiologically realistic assumptions of sparse random connectivity, weak inhibitory synapses, and sufficient cortical excitation to drive firing in some cells. Thus, at least for hundreds of milliseconds, the striatum seems to have all the requirements needed to generate time-varying neural trajectory.

It is also thought that the striatum might be reproducing a dimensionally reduced version of the cortical activity. As far as it is known, the BG segregates topographically the cortical inputs by their functions (e.g., associative, limbic, motor). This segregation is preserved across the multiple nuclei of the BG. As information transverses the BG, it has to be represented with a progressively smaller number of neurons. Because the same information is repeatedly represented in progressively smaller groups of neurons, we have reasons to believe that the information is either compressed or filtered somehow. If that was the case, it might be that we can find in the cortical activity series of

progressively widening peaks of activity tiling the whole interval, like the ones in the striatum. Previous research addressing the cortical input to the striatum has reported scaling effect on cortical (i.e., prefrontal, primary motor and parietal) population activity that is time sensitive [35,46,47]. But regardless efforts, Matell *et al.* [48] did not find peak activity in CTX that resemble the peaked activity in the striatum. Temporally sensitive activity in the CTX seems to be either too brief to account for striatal activity or in areas that do not seem to have causal interaction with time estimates [35].

The output pathways of the striatum pass through the BG output nuclei, through the thalamus and return to the same cortical regions that innervated the striatal neurons in question [49], thereby making up cortico-basal ganglio-thalamo-cortical loops. This form or architecture implies that the striatum can potentially modify its own inputs dynamically. This is an important feature if we consider that continuous cortical input is required to implement temporal representations in the inhibitory striatal network, as discussed before. In every iteration of the cortico-basal ganglia-thalamic loop, delays could be potentially integrated to propagate the signal even further in time. Goldman [50] advocated that a feedforward mechanism can perform this integration. In this mechanism, activity is passed sequentially through a chain of network stages. In each stage of the network, delays are integrated resulting in signals that can propagate information over 15 s. Because each synapse in such kind network acts as a linear filter adding a time constant, the activity of the neurons in each network stage resembles the progressively widening receptive fields we observed in the striatum.

It has been proposed by Matell *et al.* [48] that, striatal neurons are either at the decision stage output (of an interval time) or downstream from it. This proposition is based on the empirical observation that the majority of striatal neurons showing a difference in firing rate as a function of time had peak-shaped activity patterns. This claim assumes that striatal neurons are detecting synchrony in cortical oscillations. Hence, striatal activity would implement the mechanism to derive temporal estimates in the SBF model. Nonetheless, Matell did not provided evidence for these oscillations in the cortex during the timing task. On the contrary, Matell points out that cortical oscillations in the

appropriate range to support SBF model are most frequently found during inactivity or rest states [51,52], rather than when the animal is actively behaving. Thus, it is not clear if striatal neurons are detecting synchronies in oscillations or that they reflect decisions about time. Although we cannot exclude entirely the possibility that oscillation based mechanisms play a significant role in timing, our data suggest that the series of peaked activity in the striatum represent the passage of time as a fixed sequence of states. In this framework, to represent different intervals, the transition probability between states should be able to change in accordance with the interval to be timed. This transition probability is likely to be controlled by factors external to the striatum such as DA. This is consistent with part of what is known about the temporal effects of DA and PFC input modulations to the striatum [53,54]. The temporal effects of thalamic inputs to the striatum is yet an unexplored territory.

This sequence of states also embedded information about action events, which might reflect aspects of an action selection mechanism. In our task, some neurons displayed press-locked activity. Interestingly, in most of these neurons, press-locked activity was also modulated by when the press happened within the interval. This modulation was complex. Some neurons increased their firing as the pressing onset happened later in the interval, others decreased their firing, and there were those that seemed to fire maximally at a particular moment in the interval. This result is consistent with predictions from the LET model. According to LET, operant responses would be associated with underlying sequential states through differential reinforcement [21]. Operant responses (allegedly encoded by the cortex) and underlying sequential behavioral states (in the striatum) could be associated through differential reinforcement to generate time-sensitive-action-value representations. This scenario offers important implications for the future study of interval timing and action selection in the BG. LET presumes that, by strengthening the association between one operant behavior and its underlying sequential state, competing operands in the same context are weakened. If press-locked contributions to the time signals are reflecting action value in time, future experiments in tasks where competing behaviors are investigated

over time (e.g., dual bisection task) should be able to capture changes in the representation of one behavior in opposition to the competing ones.

Relevance and mechanism of multiplexing action and time

The multiplexing of behavioral and temporal information might cause temporal distortions that are relevant for implementing learning. Behavior locked contributions from the cortex could provide an extra excitatory input to the striatal activity. This extra input could affect how quickly the striatal population transverse the temporal receptive fields. In this way, behavioral activity of the subject would influence the contraction and dilation of temporal representations.

The temporal binding of stimuli to action is the widely reported phenomenon that describes the time perception bias of sensorial events toward the closest action [55-60]. Experimental data suggest that if an action precedes a timing cue (with some interval between them), the time when the cue has happened is usually underestimated [61]. Conversely, this time tend to be overestimated if the cue elicits or evokes a behavior [62]. This temporal binding of sensorial events to action is allegedly important for the ability to assign credit of an outcome to one's action [57,59,63] (a critical component of the sense of agency) because it can improve learning. Warping the timing of events in a direction that always brings action and environmental cue together might reduce the effect of intervenient processes, such as the temporal discounting (the rate by which time reduces the perceived value of an action or outcome) and improve the chances of the associative learning to take place.

These temporal distortions derived from behavior have specific characteristics that might help us to dissect its underpinnings in future studies. Haggard and colleagues [55,61] suggested that perception of the event time should be biased toward the behavior related to the event, not away from it. Also, there is a clear asymmetry between conditions in which the action precedes in time the environmental event, and in which the action follows in time the environmental event. How these different conditions affect the way behavioral contributions are integrated in the computations of time, might be a relevant part of the timing puzzle. For instance, in the particular case of the SFI

task, there is only one timing cue. Given that this cue marks the beginning and the end of the trial, how do the animals use the timing cue? Do they respond towards the upcoming reward or do they act in response to the previous reward? Haggard's studies suggest that this difference matters because it might cause different perception biases in each condition. Perhaps, this temporal bias towards behavior, might help to explain the fact that animals pressed relatively late in shorter FIs and relatively early in longer FIs.

Although the data in our study demonstrate how behavior interacts with temporal representation, nothing can be really concluded about how sensorial or cognitive contributions can affect the temporal perception. Given that the striatum is also implicated in limbic and associative [64-66] processes, and that these processes can cause temporal distortions [67-70], it might be the case that these other functions (e.g., limbic, associative or mnemonic) affect temporal representations in the striatum in a similar manner in which behavior does.

Another interesting question evoked by our data is how behavioral and temporal information are integrated in the striatum. To approach the activity profile observed in the multiplexing cells of the striatum, we multiplied the fixed press-locked contribution to firing rate by the instantaneous time dependent firing rate. Multiplicative rules to connect neurons and integrate information have been reported before in the striatum [71] and they are allegedly mediated by DA [72]. DA plays an important, but yet poorly understood, role in interval timing. To the extent of what is known, DA (or the absence of it) causes distortions in the perception of time. In the experiment conducted by Malapani and collaborators [73], parkinsonian patients were trained to reproduce two intervals (i.e., 6 s and 17 s) by pressing a button. Additionally, participants differed on conditions in which they were on- or off-medication, during training or testing. Compared to the groups that were on-medication in both training and testing phases, individuals that were trained off-medication reproduced the interval with larger delays. Participants that were tested off-medication suffered a much more drastic effect. They overestimated the shortest interval and underestimated the longest one. Scalar timing was also violated in participants tested off-medication [73,74]. Is multiplexing a possible mechanism through

which DA manifests such effects on timing? One possibility is that without DA, the multiplication rule for multiplexing behavior and time information might be disrupted. Possible consequences of this disruption are the increase of noise and/or complete disarray of the temporal representation. Future studies could show evidence for this multiplicative rule or assess how this rule changes as DA is manipulated. Given Malapani's results, it is fair to assume that DA has distinct roles in encoding and decoding processes. Hence, multiplexing might be critical in one of the processes and not in the other.

In our simulation, the precision sensitivity to the FI emerged from the trial-by-trial variation derived from the probabilistic pressing, and not from any particular feature of the temporal receptive fields of striatal neurons. When the pressing rate was proportional to the reward rate, scalar property emerged. DA might be a key component to control the mapping between pressing and reward rates. As it is now established, unexpected outcomes strongly activate midbrain dopaminergic neurons, and the magnitude of this activity is proportional to the discrepancies between actual and expected outcomes [75]. DA neurons exert a dichotomous and opposite effect on the canonical pathways of the BG [76]. DA positively modulates MSNs of the direct pathway, which can drive movement when excited. On the other hand, MSNs in the indirect pathway are negatively modulated by dopamine. It has been proposed that the indirect pathway inhibits undesirable muscular movement [77]. Thus, at least hypothetically, DA might be able to adjust the amount of movement output as a function of information about reward.

Interactions between ongoing behavior and time perception

As with all electrophysiological investigations in behaving animals, it is important to be able to dissociate the "cognitive" variable of interest from the motor activity that is circumstantial to the task performance. Because animals' behaviors evolve as time progresses, a major criticism to any electrophysiological study of time is that the neural activity recorded might be simply related to the sensory-motor aspects of the task and not in the temporal aspects [20].

In this work, much effort was directed to control motor artifacts in our data. Firstly, we looked for moments in which behavior was invariable, but neural activity could still account for the passage of time. In our task, this moment was right after reward delivery. At this moment, animals spent a significant amount of time (~5s) engaged in one repeated behavior (i.e., licking water from the port). If brain activity in the striatum was locked to time, decoding the passage of time from the population activity should display a constant estimation for as long as the licking behavior lasted. That was not the case. Secondly, we inactivated the striatum using the GABA receptor agonist muscimol. Infusions of muscimol produced relative insensitivity of PSTs to the lengths of the interval without altering session-average pressing rate. If pressing itself was exclusively encoded in the striatum, pressing behavior should be disrupted. Thirdly, we used a bayesian decoder to extract temporal information about the task from the ongoing behavior captured in high speed video. The striatal population signal was very reliable from trial-to-trial. Behavior should demonstrate similar reliability from trial-to-trial to be used as a source of temporal information. Were this the case, temporal estimates decoded from within the trial should be smooth, unimodal and very similar to the estimates derived from striatal neurons. Temporal decoding from video was actually very consistent with the behavior acquired in the operant box across trials, but substantially different from neuronal estimates. Estimates were close to constant for the first ~5 s (time spent licking water from the port), and very noisy otherwise. The increase in noise was a direct consequence of the animals' tendency to repeat the same actions (e.g., pressing and checking) across the interval. Hence, while temporal estimates derived from neural activity progressed smoothly within the interval; temporal estimates derived from video within interval progressed in steps. This suggests that as time elapsed, animals engaged in a sequence of three behavioral states (i.e., licking, waiting, press-checking).

This view, that temporal representation should be independent of behavior, reflects in part the overwhelming influence that information processing models have on the interval timing literature so far. Alternative views about interval timing admit structured behavior as a valid source for

temporal information. BeT and LeT models are examples of these views. These models assume an underlying sequential chain of behavioral states, a set of operant responses (i.e., overt behaviors) and a vector of associative links connecting operant responses to the underlying behavioral states. The transitions between states are probabilistic and depend on the rate of reinforcement, so that increases in reinforcement rate lead to quick state transitions. The succession of underlying states takes on the role of a clock process, each state acting as a discriminative stimuli to perform at a different temporal criteria. Subjects can act at the right time by identifying their current state. The sequence of underlying behavioral states predicted by BeT and LeT models maps very closely the chain of progressively widening temporal receptive fields we found in the striatum. We believe that these temporal receptive fields might represent transitions in underlying behavioral states, which makes our data most consistent with the sequential state family of timing models.

One can argue that we could not show ongoing structured behavior because we discarded the relevant information from the videos we used. Indeed, when we simplified the shape of the animals, we discarded substantial information about the fine behavior of the animals. How much this fine behaviors are relevant to timing is open to debate. Allegorical evidence from everyday life experience suggest we use subtle actions (e.g., tapping, folding fingers, subvocal verbal counting) to represent the passage of time. And because animals might use their behavior in the same way we do, we tend to agree with this argument. Nonetheless, there is evidence that weakens this argument. A recent study, which identified such structured behaviors as predictive of temporal judgments [78], showed that neural activity predicts earlier (300 ms) and better what decision the animal will take than any prediction derived from the ongoing behavior. This result suggests that neuronal temporal representations are more relevant to drive behavior, than the behavior being a major source of temporal information to the striatum.

Derived from the criticism above is the argument that some components of the behavior, although measurable, cannot be captured in the video. Previous research from Droit-Volet [79] has shown that features of movements

such as strength were correlated with timing in pre-arithmetical kids. In other words, together with pressing rate, pressing strength would also be affected by the reward rate. In our data set, if modulation of behavioral locked contributions were derived from strength, and not from time as we said, the relationship of the modulation should be linear with time or with the reward rate. Nonetheless, the behavior locked contributions revealed rich diversity of relationships with the passage of time, sometimes ramping up as time passed, sometimes ramping down and in some cases with more complex relationships.

Knowing how to extract relevant information from the increasingly dense dataset becomes progressively more relevant as new technologies allow us to extract richer data sets. Part of this work was to provide a proof of principle for how we could use the same decoding approach, widely used in electrophysiological studies, to address embodied cognition questions. Although we could not find any particular pattern of behavior within the interval, we could categorize the behavior of the animal from the video and make correct estimations about the overall behavior across trials. We consider these results as a positive validation of the approach. Additionally, the major benefits of the video-based decoding approach were the speed and the reliability of the behavior analysis. Our algorithm could perform, in few hours, the analysis that would take days to do manually. We hope that as technology advances and tracking algorithms become more sophisticated, this kind of approach becomes more popular.

Future directions: the source of timing signal in the striatum

Although we could identify temporal signals in the striatum that were necessary for interval timing behavior, it is not clear how these signals are used in broader contexts (e.g., in relationship to other brain areas, in other behavioral contingencies). The interval timing literature points out that the striatum, cerebellum [80,81] and hippocampus [82,83] interact to produce the estimation of intervals in the range of seconds to minutes. The three structures have remarkable functional similarities regarding how they generate signals with the required properties to generate reliable representation of intervals. The three

are able to produce reliable non-repeating signals that propagate in time, starting from an event inputs [13]. Why have three systems to generate temporal representations? There are many possible answers. The brain might have developed redundant mechanisms to preserve critical functions, such as timing, in face of eventual brain damage [84]. An alternative answer is that different regions differ regarding their reliability to reproduce signals in specific ranges or contexts. For instance, although striatum and cerebellum can manifest temporal representations in the range of 1 s to 5 s, the cerebellum might be a more reliable source of information in the lower end of this range than the striatum. Also, differences in the behavioral demand imposed by the task might determinate the preference for encoding time in one area in opposition to other. For example, both striatum and hippocampus are deeply involved in memory processes. The former is involved in implicit [85-89] and the latter in explicit memory [89-91]. To generate a temporal estimation, most of retrospective timing tasks require from the subject to recall events in the past and reconstruct its history until the present moment. In this context, temporal processing would be more likely to engage the hippocampus than the striatum [92]. Because it would be very hard to perform this task without episodic memory. Further investigations to delineate the functional boundaries of brain area engagement in interval timing can provide a valuable source of information. This knowledge can help to organize the data from the field and lead to more inclusive, general and comprehensive models.

Our future studies should concentrate on identifying the mechanism that generated the striatal dynamics we observed and on clarifying that striatal population response is best explained as a sequence of active neurons. About 32% of the neurons we recorded did not maintain their ordinal position over the different intervals. How these neurons might contribute or interfere to time processing remains unknown. Most likely these neurons are processing other cortical information (e.g., associative, limbic, sensorial, motor), but because we lack information about input areas (downstream and upstream) to the striatum, we cannot make any conclusive statement about it. Thus, the next step should be to record activity from relevant input areas. Good candidates are the PFC

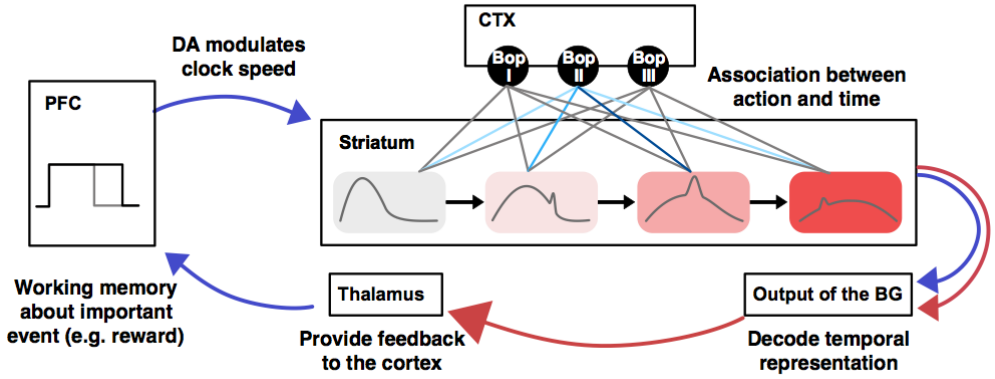

Figure 5.1 | Schematic of temporal information flow in the striatum. Prefrontal cortex (PFC) sends persistent input (a memory trace; gray line) to the striatum through cortical-striatal projections which weights are modulated by dopaminergic inputs. The negative feedback network within the striatum transforms the input in a temporal receptive fields (gray curves). The downstream nuclei of the BG operate on striatal information to implement decision about which action sequence to execute. The information that leaves the BG is than sent as a feedback to the cortex through the thalamus. This feedback, when excitatory can extend the memory trace (black line). Bop I, II and III stand for behavior: operand. Cortical representation of multiple behaviors might be differentially reinforced (by Hebbian plasticity) with striatal neurons that represent particular delays from the reward. This process would result in a representation of action value over time.

given its know relevance to interval timing, and the GPe or STN given their direct and indirect feedback loops with the striatum.

Alternatively, another possible direction of research would be to explore how striatal population reorganizes its activity across timing tasks with different behavioral demands. By chronically recordings neural activity in animals that were trained to perform in different tasks, we could observe whether the sequential chain of temporal receptive fields is a fixed universal mediator of all timing behavior or if these cells reassemble their dynamics depending on the context.

This study has contributed to the field by being the first one to demonstrate evidence for a relative code for time in the striatum in the scale of seconds to minutes. We demonstrated that these signals were relevant for the animals to derive their estimates of times and we have shown that these signals do not derive exclusively from motor programs. Our data is consistent with a subset of theoretical timing models, the sequential state models. Hence, our data provide to these models a possible biological substrate. In addition, our study gave rise to relevant and tangible research hypothesis regarding

what signals should be found in the areas that send projections to the striatum. Also, we proposed some ideas about the mechanism by which these signals are generated within the striatum. More specifically, we posit (Figure 5.1) that in order to generate activity that resemble a temporal receptive field, the striatum needs persistent input from thalamic and/or cortical areas, among which the PFC is the most likely region, given the reasons already discussed. This perseverant input should be transformed into a signal resembling a receptive field for few hundreds of milliseconds in the inhibitory network of the striatum. This temporal representation could feedback to PFC, extending in time its input to the BG, and allowing the striatum to generate multiple receptive fields that tile the whole interval. The strength of cortico-striatal connections between the PFC and the associative striatum, which is highly modulated by DA, is likely to control how narrow or wide these receptive fields are. Together with temporal representations, as a series of progressively widening receptive fields, the striatum would also receive input from other motor, limbic and sensorial areas. Hebbian plasticity could guarantee strengthening of sensory-motor input that is concomitant with a currently active temporal receptive field. The strength of the connection between behavior and temporal receptive field would encode value of the behavior in time. Finally, since this behavior-time association can change how striatal neurons represent time without changing the rules by which they are decoded by downstream neurons, this associative process could cause behaviorally driven changes in temporal estimation.

REFERENCES

1. Sutton, R. S., & Barto, a. G. (1998). Reinforcement Learning: An Introduction. IEEE Transactions on Neural Networks, 9(5), 1054–1054. http://doi.org/10.1109/TNN.1998.712192
2. Niv, Y., & Montague, P. R. (2008). Theoretical and Empirical Studies of Learning. Learning, 329–350. http://doi.org/10.1016/B978-0-12-374176-9.00022-1
3. Grossberg, S., & Schmajuk, N. (1988). Neural dynamics of adaptive timing and temporal discrimination during associative learning. Neural Networks, 1(1 SUPPL), 98. http://doi.org/10.1016/0893-6080(88)90137-2

4. Suri, R. E., & Schultz, W. (1999). A neural network model with dopamine-like reinforcement signal that learns a spatial delayed response task. Neuroscience, 91(3), 871–890. http://doi.org/10.1016/S0306-4522(98)00697-6

5. Ludvig, E. a, Sutton, R. S., & Kehoe, E. J. (2008). Stimulus representation and the timing of reward-prediction errors in models of the dopamine system. Neural Computation, 20(12), 3034–54. http://doi.org/10.1162/neco.2008.11-07-654

6. Gershman, S. J., Moustafa, A. a, & Ludvig, E. a. (2014). Time representation in reinforcement learning models of the basal ganglia. Frontiers in Computational Neuroscience, 7(January), 194. http://doi.org/10.3389/fncom.2013.00194

7. Schultz, W., Dayan, P., & Montague, P. R. (1997). A neural substrate of prediction and reward. Science (New York, N.Y.), 275(5306), 1593–1599. http://doi.org/10.1126/science.275.5306.1593

8. Kim, H., Sul, J. H., Huh, N., Lee, D., & Jung, M. W. (2009). Role of striatum in updating values of chosen actions. The Journal of Neuroscience : The Official Journal of the Society for Neuroscience, 29(47), 14701–14712. http://doi.org/10.1523/JNEUROSCI.2728-09.2009

9. Doya, K. (1999). What are the computations of the cerebellum, the basal ganglia and the cerebral cortex? Neural Networks, 12(7-8), 961–974. http://doi.org/10.1016/S0893-6080(99)00046-5

10. Lauwereyns, J., Watanabe, K., Coe, B., & Hikosaka, O. (2002). A neural correlate of response bias in monkey caudate nucleus. Nature, 418(6896), 413–417. http://doi.org/10.1038/nature00892

11. Samejima, K., Ueda, Y., Doya, K., & Kimura, M. (2005). Representation of action-specific reward values in the striatum. Science (New York, N.Y.), 310(5752), 1337–1340. http://doi.org/10.1126/science.1115270

12. Lau, B., & Glimcher, P. W. (2008). Value Representations in the Primate Striatum during??Matching Behavior. Neuron, 58(3), 451–463. http://doi.org/10.1016/j.neuron.2008.02.021

13. Anastasio, T (2010) Tutorial on Neural Systems Modeling. ISBN: 978-0-87893-339-6

14. Durstewitz, D. (2003). Self-organizing neural integrator predicts interval times through climbing activity. The Journal of Neuroscience : The Official Journal of the Society for Neuroscience, 23(12), 5342–5353. http://doi.org/23/12/5342 [pii]

15. Simen, P., Balci, F., de Souza, L., Cohen, J. D., & Holmes, P. (2011). A model of interval timing by neural integration. The Journal of Neuroscience : The Official Journal of the Society for Neuroscience, 31(25), 9238–9253. http://doi.org/10.1523/JNEUROSCI.3121-10.2011

16. Miall, C. (1989). The Storage of Time Intervals Using Oscillating Neurons. Neural Computation, 1(3), 359–371. http://doi.org/10.1162/neco.1989.1.3.359

17. Matell, M. S., & Meck, W. H. (2004). Cortico-striatal circuits and interval timing: Coincidence detection of oscillatory processes. Cognitive Brain Research, 21(2), 139–170. http://doi.org/10.1016/j.cogbrainres.2004.06.012

18. Mauk, M. D., & Buonomano, D. V. (2004). The neural basis of temporal processing. Annual Review of Neuroscience, 27, 307–340. http://doi.org/10.1146/annurev.neuro.27.070203.144247

19. Gibbon, J. (1977). Scalar expectancy theory and Weber's law in animal timing. Psychological Review. http://doi.org/10.1037/0033-295X.84.3.279

20. Fetterman, J.G., Killeen, P. R., & Hall, S. (1998). Watching the clock. Behavioural Processes, 44(2), 211–224. http://doi.org/10.1016/S0376-6357(98)00050-3

21. Machado, A. (1997). Learning the temporal dynamics of behavior. Psychological Review, 104(2), 241–265. http://doi.org/10.1037/0033-295X.104.2.241

22. Staddon, J. E., & Higa, J. J. (1999). Time and memory: towards a pacemaker-free theory of interval timing. Journal of the Experimental Analysis of Behavior, 71(2), 215–251. http://doi.org/10.1901/jeab.1999.71-215

23. Long, M. A., Jin, D. Z., & Fee, M. S. (2010). Support for a synaptic chain model of neuronal sequence generation. Nature, 468(7322), 394–9. http://doi.org/10.1038/nature09514

24. Liu, J. K., & Buonomano, D. V. (2009). Embedding multiple trajectories in simulated recurrent neural networks in a self-organizing manner. The Journal of Neuroscience : The Official Journal of the Society for Neuroscience, 29(42), 13172–13181. http://doi.org/10.1523/JNEUROSCI.2358-09.2009

25. Mauk, M. D., & Donegan, N. H. (1997). A model of Pavlovian eyelid conditioning based on the synaptic organization of the cerebellum. Learning & Memory (Cold Spring Harbor, N.Y.), 4(1), 130–158. http://doi.org/10.1101/lm.4.1.130

26. Kalmbach, B. E., Ohyama, T., Kreider, J. C., Riusech, F., & Mauk, M. D. (2009). Interactions between prefrontal cortex and cerebellum revealed by trace eyelid conditioning. Learning & Memory (Cold Spring Harbor, N.Y.), 16(1), 86–95. http://doi.org/10.1101/lm.1178309

27. Kalmbach, B. E., Ohyama, T., & Mauk, M. D. (2010). Temporal patterns of inputs to cerebellum necessary and sufficient for trace eyelid conditioning. Journal of Neurophysiology, 104(2), 627–40. http://doi.org/10.1152/jn.00169.2010

28. Siegel, J. J., Kalmbach, B., Chitwood, R. a, & Mauk, M. D. (2012). Persistent activity in a cortical-to-subcortical circuit: bridging the temporal gap in trace eyelid conditioning. Journal of Neurophysiology, 107(1), 50–64. http://doi.org/10.1152/jn.00689.2011

29. Siegel, J. J., & Mauk, M. D. (2013). Persistent activity in prefrontal cortex during trace eyelid conditioning: dissociating responses that reflect cerebellar output from those that do not. The Journal of Neuroscience : The Official Journal of the Society for Neuroscience, 33(38), 15272–84. http://doi.org/10.1523/JNEUROSCI.1238-13.2013

30. Narayanan, N. S., Land, B. B., Solder, J. E., Deisseroth, K., & DiLeone, R. J. (2012). Prefrontal D1 dopamine signaling is required for temporal control. Proceedings of the National Academy of Sciences of the United States of America, 109(50), 20726–31. http://doi.org/10.1073/pnas.1211258109

31. Kim, J., Jung, A. H., Byun, J., Jo, S., & Jung, M. W. (2009). Inactivation of medial prefrontal cortex impairs time interval discrimination in rats. Frontiers in Behavioral Neuroscience, 3(November), 38. http://doi.org/10.3389/neuro.08.038.2009

32. Li, Y.-C., Kellendonk, C., Simpson, E. H., Kandel, E. R., & Gao, W.-J. (2011). D2 receptor overexpression in the striatum leads to a deficit in inhibitory transmission and dopamine sensitivity in mouse prefrontal cortex. Proceedings of the National Academy of Sciences of the United States of America, 108(29), 12107–12112. http://doi.org/10.1073/pnas.1109718108

33. Chiba, a., Oshio, K. -i., & Inase, M. (2015). Neuronal representation of duration discrimination in the monkey striatum. Physiological Reports, 3(2), e12283–e12283. http://doi.org/10.14814/phy2.12283

34. Hinton, S. C., & Meck, W. H. (2004). Frontal-striatal circuitry activated by human peak-interval timing in the supra-seconds range. Cognitive Brain Research, 21(2), 171–182. http://doi.org/10.1016/j.cogbrainres.2004.08.005

35. Xu, M., Zhang, S., Dan, Y., & Poo, M. (2014). Representation of interval timing by temporally scalable firing patterns in rat prefrontal cortex. Proceedings of the National Academy of Sciences of the United States of America, 111(1), 480–5. http://doi.org/10.1073/pnas.1321314111

36. Standage, D., You, H., Wang, D. H., & Dorris, M. C. (2013). Trading Speed and Accuracy by Coding Time: A Coupled-circuit Cortical Model. PLoS Computational Biology, 9(4), e1003021. http://doi.org/10.1371/journal.pcbi.1003021

37. Kim, J., Ghim, J.-W., Lee, J. H., & Jung, M. W. (2013). Neural correlates of interval timing in rodent prefrontal cortex. The Journal of Neuroscience: The Official Journal of the Society for Neuroscience, 33(34), 13834–47. http://doi.org/10.1523/JNEUROSCI.1443-13.2013

38. Histed, M. H., Pasupathy, A., & Miller, E. K. (2009). Learning substrates in the primate prefrontal cortex and striatum: sustained activity related to successful actions. Neuron, 63(2), 244–53. http://doi.org/10.1016/j.neuron.2009.06.019

39. Horst, N. K., & Laubach, M. (2012). Working with memory: evidence for a role for the medial prefrontal cortex in performance monitoring during spatial delayed alternation. Journal of Neurophysiology, 108(12), 3276–3288. http://doi.org/10.1152/jn.01192.2011

40. Matell, M.S., Meck, W.H., Nicolelis, M.A.L., (2003). Integration of behavior and timing: anatomically separate systems or distributed processing? In: Meck, WH, (ed.) Functional and neural mechanisms of interval timing. (Vol. 19), 371–392. http://doi.org/10.1201/9780203009574

41. Jaldow, E. J., Oakley, D. a., & Davey, G. C. L. (1989). Performance of Decorticated Rats on Fixed Interval and Fixed Time Schedules. Eurpoean Journal of Neuroscience, 1(5), 461–470.

42. Czubayko, U., & Plenz, D. (2002). Fast synaptic transmission between striatal spiny projection neurons. Proceedings of the National Academy of Sciences of the United States of America, 99(24), 15764–15769. http://doi.org/10.1073/pnas.242428599

43. Tunstall, M. J., Oorschot, D. E., Kean, A., & Wickens, J. R. (2002). Inhibitory interactions between spiny projection neurons in the rat striatum. Journal of Neurophysiology, 88(3), 1263–1269. http://doi.org/12205147

44. Koos, T., Tepper, J. M., & Wilson, C. J. (2004). Comparison of IPSCs evoked by spiny and fast-spiking neurons in the neostriatum. The Journal of Neuroscience : The Official Journal of the Society for Neuroscience, 24(36), 7916–7922. http://doi.org/10.1523/JNEUROSCI.2163-04.2004

45. Ponzi, A., & Wickens, J. (2010). Sequentially switching cell assemblies in random inhibitory networks of spiking neurons in the striatum. The Journal of Neuroscience : The Official Journal of the Society for Neuroscience, 30(17), 5894–5911. http://doi.org/10.1523/JNEUROSCI.5540-09.2010

46. Renoult, L., Roux, S., & Riehle, A. (2006). Time is a rubberband: Neuronal activity in monkey motor cortex in relation to time estimation. European Journal of Neuroscience, 23(11), 3098–3108. http://doi.org/10.1111/j.1460-9568.2006.04824.x

47. Schneider, B. a., & Ghose, G. M. (2012). Temporal Production Signals in Parietal Cortex. PLoS Biology, 10(10), e1001413. http://doi.org/10.1371/journal.pbio.1001413

48. Matell, M. S., Meck, W. H., & Nicolelis, M. a L. (2003). Interval timing and the encoding of signal duration by ensembles of cortical and striatal neurons. Behavioral Neuroscience, 117(4), 760–773. http://doi.org/10.1037/0735-7044.117.4.760

49. Strick, P.L., Dum, R.P. & Picard, N. Macro-organization of the circuits connecting the basal ganglia with the cortical motor areas, in: Models of information Processing in the Basal Ganglia, Houk J.C., Davis, J.L., and Beiser, D.G., Eds., MIT Press, Cambridge, 1995, pp. 117-130.

50. Goldman, M. S. (2009). Memory without Feedback in a Neural Network. Neuron, 61(4), 621–634. http://doi.org/10.1016/j.neuron.2008.12.012

51. Ahissar, E., & Vaadia, E. (1990). Oscillatory activity of single units in a somatosensory cortex of an awake monkey and their possible role in texture analysis. Proceedings of the National Academy of Sciences of the United States of America, 87(22), 8935–8939.

52. Steriade, M. (1997). Synchronized activities of coupled oscillators in the cerebral cortex and thalamus at different levels of vigilance. Cerebral Cortex, 7(6), 583–588. http://doi.org/10.1093/cercor/7.6.583

53. Rivest, F., Kalaska, J. F., & Bengio, Y. (2010). Alternative time representation in dopamine models. Journal of Computational Neuroscience, 28(1), 107–130. http://doi.org/10.1007/s10827-009-0191-1

54. Schultz, W. (2013). Updating dopamine reward signals. Current Opinion in Neurobiology, 23(2), 229–238. http://doi.org/10.1016/j.conb.2012.11.012

55. Haggard, P., & Clark, S. (2003). Intentional action: Conscious experience and neural prediction. Consciousness and Cognition, 12(4), 695–707. http://doi.org/10.1016/S1053-8100(03)00052-7

56. Hughes, G., Desantis, A., & Waszak, F. (2012). Mechanisms of Intentional Binding and Sensory Attenuation: The Role of Temporal Prediction, Temporal Control, Identity Prediction, and Motor Prediction. Psychological Bulletin, 139(1), 133–151. http://doi.org/10.1037/a0028566

57. Moore, J. W., & Obhi, S. S. (2012). Intentional binding and the sense of agency: A review. Consciousness and Cognition, 21(1), 546–561. http://doi.org/10.1016/j.concog.2011.12.002

58. Wohlschläger, A., Haggard, P., Gesierich, B., & Prinz, W. (2003). The perceived onset time of self- and other-generated actions. Psychological Science : A Journal of the American Psychological Society / APS, 14(6), 586–91. http://doi.org/10.1046/j.0956-7976.2003.psci

59. Kawabe, T., Roseboom, W., & Nishida, S. (2013). The sense of agency is action-effect causality perception based on cross-modal grouping. Proceedings. Biological Sciences / The Royal Society, 280(1763), 20130991. http://doi.org/10.1098/rspb.2013.0991

60. Buehner, M. J., & Humphreys, G. R. (2009). Causal binding of actions to their effects: Research article. Psychological Science, 20(10), 1221–1228. http://doi.org/10.1111/j.1467-9280.2009.02435.x

61. Haggard, P., & Chambon, V. (2012). Sense of agency. Current Biology : CB, 22(10), R390–2. http://doi.org/10.1016/j.cub.2012.02.040

62. Yabe, Y., & Goodale, M. a. (2015). Time Flies When We Intend to Act: Temporal Distortion in a Go/No-Go Task. Journal of Neuroscience, 35(12), 5023–5029. http://doi.org/10.1523/JNEUROSCI.4386-14.2015

63. Tanaka, S. C., Doya, K., Okada, G., Ueda, K., Okamoto, Y., & Yamawaki, S. (2004). Prediction of immediate and future rewards differentially recruits cortico-basal ganglia loops. Nature Neuroscience, 7(8), 887–893. http://doi.org/10.1038/nn1279

64. Floresco, S. B. (2007). Dopaminergic regulation of limbic-striatal interplay. J Psychiatry Neurosci, 32(6), 400–411. Retrieved from http://www.ncbi.nlm.nih.gov/entrez/query.fcgi?cmd=Retrieve&db=PubMed&dopt=Citation&list_uids=18043763

65. Karreman, M., & Moghaddam, B. (1996). The prefrontal cortex regulates the basal release of dopamine in the limbic striatum: an effect mediated by ventral tegmental area. Journal of Neurochemistry, 66, 589–598. http://doi.org/10.1046/j.1471

66. Goll, Y., Atlan, G., & Citri, A. (2015). Attention: the claustrum. Trends in Neurosciences, 38(8), 486–495. http://doi.org/10.1016/j.tins.2015.05.006

67. Balci, F., Papachristos, E. B., Gallistel, C. R., Brunner, D., Gibson, J., & Shumyatsky, G. P. (2008). Interval timing in genetically modified mice: A simple paradigm. Genes, Brain and Behavior, 7(3), 373–384. http://doi.org/10.1111/j.1601-183X.2007.00348.x

68. Droit-Volet, S., & Meck, W. H. (2007). How emotions colour our perception of time. Trends in Cognitive Sciences, 11(12), 504–513. http://doi.org/10.1016/j.tics.2007.09.008

69. Merchant, H., Harrington, D. L., & Meck, W. H. (2013). Neural basis of the perception and estimation of time. Annual Review of Neuroscience, 36(June), 313–36. http://doi.org/10.1146/annurev-neuro-062012-170349

70. Tamm, M., Uusberg, A., Allik, J., & Kreegipuu, K. (2014). Emotional modulation of attention affects time perception: Evidence from event-related potentials. Acta Psychologica, 149, 148–156. http://doi.org/10.1016/j.actpsy.2014.02.008

71. Thivierge, J.-P., Rivest, F., & Monchi, O. (2007). Spiking Neurons, Dopamine, and Plasticity: Timing Is Everything, but Concentration Also Matters. Synapse (New York, N.Y.), 61(9), 375–390.

72. Fino, E., Glowinski, J., & Venance, L. (2005). Bidirectional activity-dependent plasticity at corticostriatal synapses. The Journal of Neuroscience : The Official Journal of the Society for Neuroscience, 25(49), 11279–11287. doi:10.1523/JNEUROSCI.4476-05.2005

73. Malapani, C., Deweer, B., & Gibbon, J. (2002). Separating storage from retrieval dysfunction of temporal memory in Parkinson's disease. Journal of Cognitive Neuroscience, 14(2), 311–322. doi:10.1162/089892902317236920

74. Shea-Brown, E., Rinzel, J., Rakitin, B. C., & Malapani, C. (2006). A firing rate model of Parkinsonian deficits in interval timing. Brain Research, 1070(1), 189–201. http://doi.org/10.1016/j.brainres.2005.10.070

75. Steinberg, E. E., Keiflin, R., Boivin, J. R., Witten, I. B., Deisseroth, K., & Janak, P. H. (2013). A causal link between prediction errors, dopamine neurons and learning. Nature Neuroscience, 16(7), 966–973. http://doi.org/10.1038/nn.3413

76. Shen, W., Flajolet, M., Greengard, P., & Surmeier, D. J. (2008). Dichotomous dopaminergic control of striatal synaptic plasticity. Science (New York, N.Y.), 321(5890), 848–51. http://doi.org/10.1126/science.1160575

77. Nambu, A. (2004). A new dynamic model of the cortico-basal ganglia loop. Progress in Brain Research, 143, 461–6. http://doi.org/10.1016/S0079-6123(03)43043-4

78. Gouvêa, T. S., Monteiro, T., Motiwala, A., Soares, S., Machens, C. K., & Paton, J. J. (2015). Striatal dynamics explain duration judgments. Retrieved from http://biorxiv.org/lookup/doi/10.1101/020883

79. Droit-Volet, S. (1998). Time estimation in young children: an initial force rule governing time production. Journal of Experimental Child Psychology, 68(3), 236–249. doi:10.1006/jecp.1997.2430

80. Gooch, C. M., Wiener, M., Wencil, E. B., & Coslett, H. B. (2010). Interval timing disruptions in subjects with cerebellar lesions. Neuropsychologia, 48(4), 1022–1031. http://doi.org/10.1016/j.neuropsychologia.2009.11.028

81. Teki, S., Grube, M., Kumar, S., & Griffiths, T. D. (2011). Distinct neural substrates of duration-based and beat-based auditory timing. The Journal of Neuroscience : The Official Journal of the Society for Neuroscience, 31(10), 3805–3812. http://doi.org/10.1523/JNEUROSCI.5561-10.2011

82. Kraus, B., Robinson, R., White, J., Eichenbaum, H., & Hasselmo, M. (2013). Hippocampal “Time Cells”: Time versus Path Integration. Neuron, 78(6), 1090–1101. http://doi.org/10.1016/j.neuron.2013.04.015

83. Eichenbaum, H. (2013). Memory on time. Trends in Cognitive Sciences, 17(2), 88. http://doi.org/10.1016/j.tics.2012.12.007

84. Glassman, R. B. (1987). An hypothesis about redundancy and reliability in the brains of higher species: Analogies with genes, internal organs, and engineering systems. Neuroscience & Biobehavioral Reviews, 11(3), 275–285. http://doi.org/10.1016/S0149-7634(87)80014-3

85. Roediger, H. L. (1990). Implicit memory. Retention without remembering. The American Psychologist, 45(9), 1043–1056. http://doi.org/10.1037/0003-066X.45.9.1043

86. Schacter, D. L. (1987). Implicit Memory: History and Current Status. Journal of Experimental Psychology: Learning, Memory, and Cognition, 13(3), 501–518. http://doi.org/10.1037/0278-7393.13.3.501

87. Schacter, D. L., Chiu, C. Y., & Ochsner, K. N. (1993). Implicit memory: a selective review. Annual Review of Neuroscience, 16, 159–182. http://doi.org/10.1146/annurev.ne.16.030193.001111

88. Watkins, P. C. (2002). Implicit memory bias in depression. Cognition & Emotion, 16(915540789), 381–402. http://doi.org/10.1080/02699930143000536

89. Rugg, M. D., Mark, R. E., Walla, P., Schloerscheidt, A. M., Birch, C. S., & Allan, K. (1998). Dissociation of the neural correlates of implicit and explicit memory. Nature, 392(6676), 595–598. http://doi.org/Doi 10.1038/33396

90. Hoffman, Y., Bein, O., & Maril, A. (2011). Explicit Memory for Unattended Words. Psychological Science, 22(12), 1490–1493. http://doi.org/10.1177/0956797611419674

91. Rose, M., Haider, H., & Büchel, C. (2010). The emergence of explicit memory during learning. Cerebral Cortex (New York, N.Y. : 1991), 20(12), 2787–97. http://doi.org/10.1093/cercor/bhq025

92. Wiener, M., Turkeltaub, P., & Coslett, H. B. (2010). The image of time: A voxel-wise meta-analysis. NeuroImage, 49(2), 1728–1740. http://doi.org/10.1016/j.neuroimage.2009.09.064

ITQB-UNL | Av. da República, 2780-157 Oeiras, Portugal
Tel (+351) 214 469 100 | Fax (+351) 214 411 277

www.itqb.unl.pt